THE ASTROPHYSICAL JOURNAL, 544:993–1015, 2000 December 1

COMPLETE *RXTE* SPECTRAL OBSERVATIONS OF THE BLACK HOLE X-RAY NOVA XTE J1550−564

GREGORY J. SOBCZAK,[1] JEFFREY E. MCCLINTOCK,[2] RONALD A. REMILLARD,[3] WEI CUI,[3] ALAN M. LEVINE,[3] EDWARD H. MORGAN,[3] JEROME A. OROSZ,[4] AND CHARLES D. BAILYN[5]

Received 2000 January 14; accepted 2000 July 17

ABSTRACT

We report on the X-ray spectral behavior of XTE J1550−564 during its 1998–1999 outburst. XTE J1550−564 is an exceptionally bright X-ray nova and is also the third Galactic black hole candidate known to exhibit quasi-periodic X-ray oscillations above 50 Hz. Our study is based on 209 pointed observations using the PCA and HEXTE instruments on board the *Rossi X-Ray Timing Explorer* (*RXTE*) spanning 250 days and covering the entire double-peaked eruption that occurred from 1998 September until 1999 May. The spectra are fitted to a model including multicolor blackbody disk and power-law components. The spectra from the first half of the outburst are dominated by the power-law component, whereas the spectra from the second half are dominated by the disk component. The source is observed in the very high and high/soft outburst states of black hole X-ray novae. During the very high state, when the power-law component dominated the spectrum, the inner disk radius is observed to vary by more than an order of magnitude; the radius decreased by a factor of 16 in one day during a 6.8 crab flare. If the larger of these observed radii is taken to be the last stable orbit, then the smaller observed radius would imply that the inner edge of the disk is inside the event horizon! However, we conclude that the apparent variations of the inner disk radius observed during periods of increased power-law emission are probably caused by the failure of the multicolor disk/power-law model; the actual physical radius of the inner disk may remain fairly constant. This interpretation is supported by the fact that the observed inner disk radius remains approximately constant over 120 days in the high state, when the power-law component is weak, even though the disk flux and total flux vary by an order of magnitude. The mass of the black hole inferred by equating the approximately constant inner disk radius observed in the high/soft state with the last stable orbit for a Schwarzschild black hole is $M_{\rm BH} = 7.4\ M_{\odot}(D/6\ {\rm kpc})(\cos i)^{-1/2}$.

Subject headings: black hole physics — stars: individual (XTE J1550−564) — X-rays: stars

On-line material: machine-readable tables

1. INTRODUCTION

The X-ray nova and black hole candidate XTE J1550−564 was discovered with the All Sky Monitor (ASM; Levine et al. 1996) on board the *Rossi X-Ray Timing Explorer* (*RXTE*) just after the outburst began on 1998 September 6 (Smith et al. 1998). The source exhibited a flare on 1998 September 19–20 that reached 6.8 crab (or 1.6×10^{-7} ergs s^{-1} cm^{-2}) at 2–10 keV. The discovery of XTE J1550−564 prompted a series of almost daily pointed *RXTE* observations with the Proportional Counter Array (PCA; Jahoda et al. 1996) and the High-Energy X-Ray Timing Experiment (HEXTE; Rothschild et al. 1998) instruments. The first 14 *RXTE* observations were part of a guest observer program with results reported by Cui et al. (1999). They found that during the initial X-ray rise (0.7–2.4 crab at 2–10 keV), the source exhibited very strong quasi-periodic X-ray oscillations (QPOs) in the range 0.08–8 Hz. The spectral and timing analysis of 60 additional *RXTE* observations, reported in Sobczak et al. (1999a) and Remillard et al. (1999a), revealed the presence of canonical outburst states characteristic of black hole X-ray novae (see Tanaka & Lewin 1995) and X-ray QPOs at a few Hz and ∼200 Hz. XTE J1550−564 is one of only a few Galactic black hole candidates known to exhibit QPOs above 50 Hz (Remillard et al. 1999a; Homan, Wijnands, & van der Klis 1999); the others are 4U 1630−47 (Remillard & Morgan 1999) and the microquasars GRS 1915+105 (Morgan, Remillard, & Greiner 1997) and GRO J1655−40 (Remillard et al. 1999b).

The X-ray light curve of XTE J1550−564 from the ASM aboard *RXTE* is shown in Figure 1. The outburst exhibits a "double-peaked" profile, with the first half generally dominated by power-law emission, and the second half generally dominated by emission from the accretion disk (see § 3). The double-peaked profile of the outburst is different from the outbursts of classical X-ray novae like A0620−00 (see Chen, Shrader, & Livio 1997) but is similar to the outburst behavior of the microquasar GRO J1655−40 (Sobczak et al. 1999b).

The optical (Orosz, Bailyn, & Jain 1998) and radio (Campbell-Wilson et al. 1998) counterparts of XTE J1550−564 were identified shortly after the source was discovered. The presence of an optical counterpart, with $B \sim 22$ mag in quiescence (Jain et al. 1999), is especially important since this will allow radial velocity studies of the companion star during quiescence that could confirm the black hole nature of the primary.

Herein we present spectral results for 209 X-ray observations spanning the entire 250 days of the 1998–1999 out-

[1] Harvard University, Astronomy Department, 60 Garden Street, MS-10, Cambridge, MA 02138; gsobczak@cfa.harvard.edu.

[2] Harvard-Smithsonian Center for Astrophysics, 60 Garden Street, MS-3, Cambridge, MA 02138; jem@cfa.harvard.edu.

[3] Center for Space Research, MIT, Cambridge, MA 02139; rr@space.mit.edu, cui@space.mit.edu, aml@space.mit.edu, ehm@space.mit.edu.

[4] Sterrekundig Instituut, Universiteit Utrecht, Postbus 80.000, 3508 TA Utrecht, The Netherlands; J. A. Orosz@astro.uu.nl.

[5] Department of Astronomy, Yale University, P.O. Box 208101, New Haven, CT 06520; bailyn@astro.yale.edu.

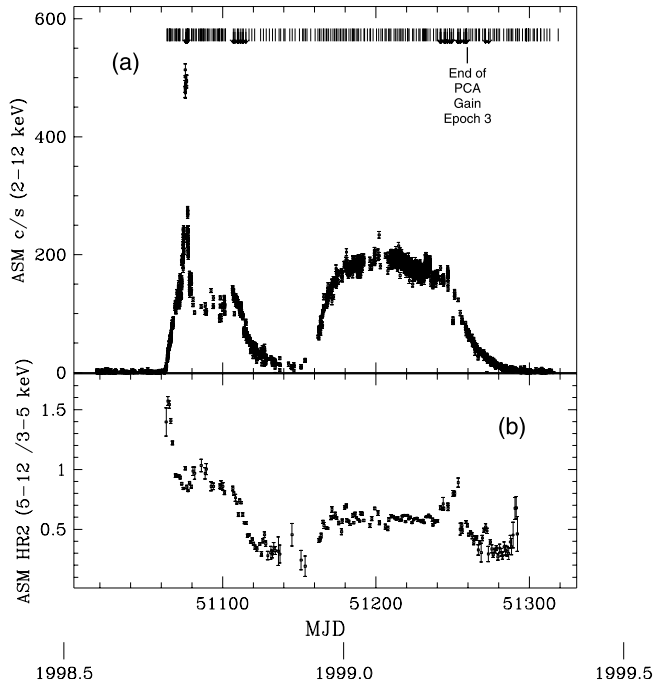

FIG. 1.—(*Upper panel*) The 2–12 keV ASM light curve and (*lower panel*) the ratio of the ASM count rates (5–12 keV)/(3–5 keV) for XTE J1550−564. The small, solid vertical lines in the top panel indicate the times of pointed *RXTE* observations; the downward arrows indicate the observations during which high-frequency 161–283 Hz QPOs are present.

burst of XTE J1550−564. These observations include the rising phase observations with results first reported by Cui et al. (1999) (*RXTE* program P30188−06), all of our *RXTE* guest observer program (P30191), and all of the public observations of this source (P30435 and P40401). The spectral analysis of PCA observations 15–75 (see Table 1) was first reported by Sobczak et al. (1999a). A timing study based on those same *RXTE* observations is presented in Remillard et al. (1999a) and observations of the optical counterpart are presented in Jain et al. (1999). Low-frequency QPOs (0.08–18 Hz) were observed during 74 of the 209 observations reported in the present paper. The frequencies, amplitudes, and coherence factors (Q) of these QPOs can be found in Table 1 of Sobczak et al. (2000).

2. OBSERVATIONS AND ANALYSIS

We present spectral results for 209 observations of XTE J1550−564 (see Fig. 1) obtained using the PCA and HEXTE instruments on board *RXTE*. The PCA consists of five xenon-filled detector units (PCUs) with a total effective area of ~ 6200 cm^{-2} at 5 keV. The PCA is sensitive in the range 2–60 keV, the energy resolution is $\sim 17\%$ at 5 keV, and the time resolution capability is 1 μs. The HEXTE consists of two clusters of 4 NaI/CsI phoswich scintillation detectors, each with an effective area of 800 cm^2, covering the energy range 15 to 250 keV with an energy resolution of 9 keV at 60 keV. A journal of the PCA/HEXTE observations of XTE J1550−564 is given in Table 1, including exposure times, count rates, etc.

The PCA and HEXTE pulse height spectra were not fitted simultaneously because of uncertainty in the cross-calibration of the instruments. This uncertainty is apparent when fitting the spectrum of the Crab. Fitting the Crab spectrum (e.g. 1997 December 15 and 1999 March 24) to a power law using either PCA or HEXTE data alone yields $\chi^2_\nu \sim 1$ for each detector; however, fitting PCA and HEXTE data simultaneously, even while floating the relative normalization of the detectors, results in $\chi^2_\nu \sim 4$. For this reason, we present separate fits to the PCA and HEXTE spectra.

2.1. *PCA*

The PCA data were taken in the "Standard 2" format, which consists of 129 channel spectra accumulated for each PCU every 16 s. The data span PCA gain epochs 3 & 4 (epoch 4, which covers observations 170–209, began when the PCA gain was lowered on 1999 March 22 at 16:30 UT). The epoch 3 response matrix for each PCU was obtained from the 1998 January distribution of response files, and the response matrix for epoch 4 was obtained from the *RXTE* GOF website and dated 1999 March 31. We tested the latest epoch 4 response matrices released with FTOOLS v5.0 and found that there are no significant changes in the fits. The pulse height spectrum from each PCU was fit over the energy range 2.5–20 keV for epoch 3, using a systematic error in the count rates of 1%. For epoch 4, the pulse height spectrum from each PCU was fit over the energy range 3–20 keV, using a systematic error in the count rates of 2%. The lower limit of the energy range was raised to 3 keV for epoch 4 because the sensitivity of the detectors at low energy decreased when the gain was lowered, and a systematic error of 2% was adopted in order to maintain $\chi^2_\nu \sim 1$ for the Crab nebula. All of the spectra were corrected for background using the standard bright source background models appropriate for each epoch. We began using the epoch 4 faint source background model beginning on 1999 April 27, when the source count rate dropped below 40 counts s^{-1} per PCU. Only PCUs 0 & 1 were used for the spectral fitting reported here and the spectra from both PCUs were fitted simultaneously using XSPEC (Sobczak et al. 1999a, 1999b).

The PCA spectral data were fitted to the widely used model consisting of a multicolor blackbody accretion disk plus power law (Tanaka & Lewin 1995; Mitsuda et al. 1984; Makishima et al. 1986). The fits were significantly improved by including a smeared Fe absorption edge near 8 keV (Ebisawa et al. 1994; Inoue 1991) and a weak Fe emission line; the best-fit line had a central energy around 6.5 keV, a width held fixed at 1.2 keV (FWHM), and an equivalent width $\lesssim 100$ eV. Interstellar absorption was modeled using the Wisconsin cross sections (Morrison & McCammon 1983). All of the observations were first fit with a floating hydrogen column density ($N_{\rm H}$), which was generally in the range 1.5–2.5 $\times$ 10^{22} cm^{-2} (Jain et al. 1999 estimated $N_{\rm H} = 0.9 \times 10^{22}$ cm^{-2} from optical reddening). The fits were insensitive to $N_{\rm H}$ differences in this small range, and in the final analysis presented here, $N_{\rm H}$ was fixed at 2.0×10^{22} cm^{-2}. There are a total of eight free parameters: the apparent temperature ($T_{\rm in}$) and radius ($R_{\rm in}$) of the inner accretion disk, the power-law photon index (Γ) and normalization (K), the edge energy and optical depth ($\tau_{\rm Fe}$) of the Fe absorption feature, and the central energy and normalization of the Fe emission line.

The addition of the Fe emission and absorption components is motivated in Figures 2*a* and 2*b*, which show the ratio of a typical spectrum to the best-fit model without and with the Fe emission and absorption. The addition of the Fe

TABLE 1

PCA Observations of XTE J1550−564

Observation Number	Date (UT) (yymmdd)	MJD[a]	Exposure (s)	Count Rate[b] (counts s^{-1} per PCU)	HR[c]
1	980907	51063.697	1808	950	0.622
2	980908	51064.006	5744	995	0.553
3	980909	51065.068	3568	1788	0.485
4	980909	51065.342	2144	1760	0.471
5	980910	51066.067	2880	2143	0.419
6	980910	51066.345	2656	2291	0.398
7	980911	51067.271	3200	2797	0.365
8	980912	51068.345	2560	3096	0.317
9	980913	51069.275	2880	3504	0.288
10	980914	51070.131	3760	3482	0.291
11	980914	51070.274	2896	3513	0.290
12	980915	51071.200	3552	3928	0.279
13	980915	51071.996	1136	3277	0.309
14	980916	51072.345	2624	4022	0.269
15	980918	51074.140	2020	5151	0.242
16	980919	51075.987	2975	13195	0.220
17	980920	51076.802	5000	6360	0.232
18	980920	51076.953	4930	7153	0.200
19	980921	51077.143	3680	7970	0.213
20	980921	51077.211	9710	6866	0.223
21	980921	51077.869	10450	5557	0.236
22	980922	51078.132	4100	4779	0.245
23	980923	51079.794	2700	3963	0.250
24	980924	51080.078	3130	3807	0.252
25	980925	51081.062	4430	3345	0.297
26	980926	51082.002	7170	3266	0.300
27	980927	51083.002	3860	3172	0.306
28	980928	51084.342	4750	3120	0.310
29	980929	51085.270	4500	3609	0.276
30	980929	51085.920	1800	3076	0.303
31	980929	51085.991	5060	3100	0.300
32	980930	51086.889	5630	3238	0.289
33	981001	51087.723	8390	3146	0.292
34	981002	51088.007	6050	3045	0.300
35	981003	51089.008	3030	2907	0.306
36	981004	51090.143	3160	3143	0.289
37	981004	51090.704	3500	2990	0.292
38	981005	51091.743	2830	3741	0.262
39	981007	51093.143	3030	4021	0.252
40	981008	51094.143	2970	3018	0.290
41	981008	51094.572	3850	3161	0.271
42	981009	51095.609	1300	2871	0.280
43	981010	51096.572	4050	3087	0.270
44	981011	51097.572	1480	2751	0.284
45	981011	51097.809	1050	2575	0.290
46	981012	51098.275	1710	2785	0.278
47	981013	51099.215	1480	2679	0.281
48	981013	51099.608	2620	2640	0.283
49	981014	51100.287	2700	3142	0.262
50	981015	51101.607	1630	3071	0.256
51	981015	51101.941	2080	3021	0.260
52	981020	51106.953	930	3755	0.219
53	981022	51108.076	9870	3548	0.224
54	981023	51109.737	1230	3272	0.223
55	981024	51110.270	3560	3013	0.200
56	981025	51111.602	850	2862	0.230
57	981026	51112.802	1720	2695	0.231
58	981027	51113.668	1050	2396	0.221
59	981029	51115.280	2070	1802	0.213
60	981031	51117.351	1950	1243	0.160
61	981102	51119.003	3680	1025	0.177
62	981104	51121.003	3750	760	0.074
63	981107	51124.727	2190	611	0.151
64	981109	51126.595	4680	649	0.204

TABLE 1—*Continued*

Observation Number	Date (UT) (yymmdd)	MJD[a]	Exposure (s)	Count Rate[b] (counts s^{-1} per PCU)	HR[c]
65	981111	51128.564	2520	504	0.203
66	981113	51130.457	4800	454	0.209
67	981115	51132.479	2980	386	0.180
68	981117	51134.436	5050	311	0.114
69	981119	51136.777	6500	261	0.172
70	981120	51137.923	4220	331	0.246
71	981122	51139.991	1600	322	0.358
72	981123	51140.706	2500	286	0.245
73	981126	51143.800	1880	258	0.224
74	981128	51145.476	5660	168	0.190
75	981130	51147.335	4600	220	0.221
76	981203	51150.073	2220	206	0.210
77	981205	51152.080	2360	230	0.034
78	981205	51152.866	4830	258	0.090
79	981207	51154.016	1650	314	0.000
80	981208	51155.067	3030	385	0.000
81	981210	51157.493	2410	635	0.000
82	981213	51160.276	2250	1031	0.000
83	981215	51162.202	2430	1422	0.000
84	981216	51163.205	870	1609	0.000
85	981217	51164.205	930	1907	0.003
86	981218	51165.590	3180	2327	0.003
87	981219	51166.011	1400	2423	0.000
88	981220	51167.418	1390	2811	0.032
89	981221	51168.010	1710	2861	0.000
90	981222	51169.009	4150	3127	0.000
91	981223	51170.520	1230	3359	0.006
92	981225	51172.065	2583	3506	0.000
93	981226	51172.990	3250	3568	0.002
94	981227	51173.990	3180	3641	0.005
95	981227	51174.722	3110	3769	0.006
96	981228	51175.796	5400	3852	0.010
97	981229	51176.847	3900	3871	0.012
98	981230	51177.846	4000	3965	0.010
99	981231	51178.846	4000	3911	0.011
100	990101	51179.919	3490	4183	0.030
101	990102	51180.845	4110	4546	0.073
102	990104	51182.337	4120	4163	0.009
103	990105	51183.540	2600	4258	0.007
104	990106	51184.711	5550	4250	0.008
105	990107	51185.126	1760	4266	0.022
106	990107	51185.846	8640	4233	0.007
107	990109	51187.126	4120	4259	0.009
108	990110	51188.194	4470	4263	0.006
109	990110	51188.731	1650	4240	0.003
110	990112	51190.054	1210	4307	0.007
111	990113	51191.485	4230	4382	0.007
112	990114	51192.187	4420	4491	0.006
113	990114	51192.593	1500	4341	0.009
114	990116	51194.500	2720	4513	0.008
115	990118	51196.051	4350	4607	0.007
116	990118	51196.522	2030	4443	0.008
117	990120	51198.051	4100	4638	0.008
118	990122	51200.383	3070	5031	0.070
119	990123	51201.783	2670	5443	0.106
120	990125	51203.249	4630	4780	0.015
121	990126	51204.248	1500	4771	0.010
122	990127	51205.850	2970	4809	0.011
123	990128	51206.781	2690	4714	0.009
124	990130	51208.179	1150	4884	0.029
125	990130	51208.845	3330	4751	0.013
126	990131	51209.711	2490	4707	0.014
127	990202	51211.709	2620	4584	0.011
128	990203	51212.775	3090	4573	0.012
129	990204	51213.774	3150	4556	0.013
130	990205	51214.975	3460	4734	0.049

TABLE 1—*Continued*

Observation Number	Date (UT) (yymmdd)	MJD[a]	Exposure (s)	Count Rate[b] (counts s^{-1} per PCU)	HR[c]
131	990206	51215.839	7140	4624	0.046
132	990207	51216.838	3610	4468	0.019
133	990208	51217.704	3100	4438	0.009
134	990210	51219.053	3920	4352	0.009
135	990211	51220.508	1890	4308	0.013
136	990211	51220.836	5200	4300	0.014
137	990212	51221.567	2300	4245	0.001
138	990214	51223.766	4500	4142	0.007
139	990215	51224.699	3530	4052	0.006
140	990217	51226.296	2320	4068	0.008
141	990218	51227.837	3020	3970	0.003
142	990219	51228.696	3615	3910	0.006
143	990221	51230.424	3480	3869	0.005
144	990222	51231.293	1300	3997	0.024
145	990222	51231.422	3150	3940	0.021
146	990223	51232.252	1540	4368	0.101
147	990223	51232.860	860	4442	0.114
148	990224	51233.835	3140	4362	0.110
149	990226	51235.199	5830	4390	0.125
150	990228	51237.619	4080	3642	0.034
151	990302	51239.081	5980	3788	0.087
152	990303	51240.063	2160	3912	0.101
153	990304	51241.828	3130	4171	0.166
154	990305	51242.507	1525	4023	0.174
155	990307	51244.496	685	4894	0.192
156	990308	51245.353	2790	4583	0.217
157	990309	51246.414	2820	4488	0.183
158	990310	51247.979	2830	4392	0.212
159	990311	51248.091	1365	4408	0.206
160	990312	51249.400	1275	4095	0.229
161	990313	51250.693	2920	2571	0.261
162	990316	51253.225	1170	3518	0.225
163	990317	51254.092	3190	3145	0.242
164	990318	51254.107	5170	2346	0.182
165	990320	51257.362	600	1892	0.167
166	990321	51258.088	900	1874	0.176
167	990321	51258.496	1090	1874	0.176
168	990321	51258.975	1835	1784	0.205
169	990322	51259.252	900	1745	0.204
170[d]	990323	51260.552	2310	1430	0.176
171	990324	51261.766	1960	1305	0.169
172	990326	51263.108	1445	1177	0.158
173	990327	51264.748	3560	944	0.166
174	990328	51265.613	2610	910	0.185
175	990329	51266.880	3220	725	0.122
176	990330	51267.612	2725	756	0.169
177	990401	51269.677	3580	683	0.170
178	990402	51270.742	3670	703	0.194
179	990403	51271.408	2000	676	0.206
180	990405	51273.541	5225	472	0.167
181	990406	51274.471	2610	413	0.154
182	990408	51276.278	1255	308	0.13
183	990409	51277.401	2370	290	0.11
184	990410	51278.686	1570	250	…
185	990411	51279.531	3800	223	…
186	990412	51280.544	2600	191	…
187	990415	51283.224	1300	205	…
188	990417	51285.197	2890	118	0.11
189	990418	51286.058	3055	114	0.20
190	990419	51287.257	1255	101	0.15
191	990420	51288.382	940	80.0	0.11
192	990421	51289.146	1360	109	…
193	990422	51290.984	685	108	0.11
194	990423	51291.183	5300	91.0	0.13
195	990424	51292.451	3925	41.4	…

TABLE 1—*Continued*

Observation Number	Date (UT) (yymmdd)	MJD[a]	Exposure (s)	Count Rate[b] (counts s^{-1} per PCU)	HR[c]
196	990425	51293.450	3870	54.1	...
197	990427	51295.520	4280	28.2	...
198	990429	51297.376	3820	14.1	...
199	990430	51298.052	5480	10.9	...
200	990501	51299.344	4840	8.4	...
201	990502	51300.458	2620	7.0	...
202	990504	51302.459	2510	5.3	...
203	990505	51303.391	2030	4.1	...
204	990507	51305.124	3530	9.1	...
205	990509	51307.322	3620	26.7	...
206	990511	51309.720	3740	11.9	...
207	990513	51311.519	1780	5.9	...
208	990515	51313.317	1770	6.0	...
209	990520	51318.768	2970	0.0	...

[a] Start of observation. MJD = JD − 2,400,000.5.
[b] 1 crab = 2500 counts s^{-1} per PCU.
[c] HR is the ratio of PCA source rate: 13–30 keV/6–13 keV.
[d] Start of PCA Gain Epoch 4.

emission and absorption components reduces the χ^2_ν from 7.9 to 0.9 in this example. The Fe line and edge energies also agree with the relation in Figure 17 of Nagase (1989) and indicate variations in the ionization state of Fe during the outburst.

The fitted temperature and radius of the inner accretion disk presented here ($T_{\rm in}$ and $R_{\rm in}$) are actually the color temperature and radius of the inner disk, which may be affected by spectral hardening due to electron scattering (Shakura & Sunyaev 1973; Shimura & Takahara 1995). The physical interpretation of these parameters remains uncertain and is discussed below. The reader should also note that the inner disk radius is obtained from the normalization of the multicolor disk model, $R_{\rm in}(\cos i)^{1/2}/(D/6\ {\rm kpc})$, which is a function of the distance D and inclination i of the system. We use $i = 0$ and $D = 6$ kpc for XTE J1550−564, but the actual distance and inclination are unknown. Six representative spectra are shown in Figures 3*a*–3*f*. The model parameters and component fluxes (see Tables 2 and 3) are plotted in Figures 4*a*–4*f*. All uncertainties are given at the 1 σ confidence level. Unless otherwise noted, the spectral parameters discussed in this paper are those derived using the PCA as opposed to the HEXTE spectra.

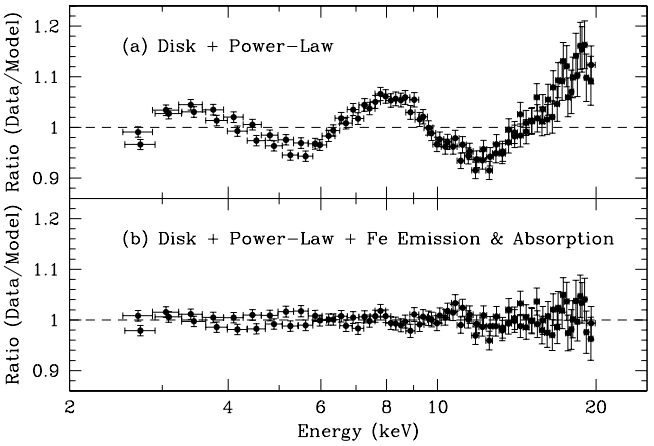

FIG. 2.—Ratio data/model for (*a*) the best-fit multicolor disk plus power-law model and (*b*) the multicolor disk plus power law plus Fe emission and absorption model for a representative high/soft state spectrum (MJD 51126, 1998 November 9). The addition of the Fe emission and absorption components improves the χ^2_ν from (*a*) 7.9 to (*b*) 0.9 in this example.

2.2. *HEXTE*

The standard HEXTE reduction software was used for the extraction of the HEXTE archive mode data. The HEXTE modules were alternatingly pointed every 32 s at source and background positions, allowing background subtraction with high sensitivity to time variations in the particle flux at different positions in the spacecraft orbit. Clusters A and B were fitted simultaneously and the normalization of each cluster was allowed to float independently, since there is a small systematic difference between the normalizations of the two clusters. We used the HEXTE response matrices released 1997 March 20. Only the data above 20 keV were used because of uncertainty in the response at lower energies.

The source was not detected in the HEXTE during all observations. For those observations in which the source was detected, the HEXTE spectra were fitted to a power-law model from 20 keV to the maximum energy at which the source was detected, which ranged from 50 to 200 keV. In a number of cases we found that the HEXTE spectra could not be adequately fit using a pure power-law model in the observed energy range (Figs. 5*a*–5*d*). In these instances, we used a power-law with a high-energy cutoff of the form (cf. Grove et al. 1998)

$$N(E) = KE^{-\Gamma} \text{ for } E \le E_{\rm cut}$$
$$= KE^{-\Gamma} \exp\left[(E_{\rm cut} - E)/E_{\rm fold}\right] \quad (1a)$$
$$\text{for } E \ge E_{\rm cut}\ . \quad (1b)$$

The addition of the high-energy cutoff improved the value of χ^2_ν from 4.9 to 0.7 for the observation on 1998 September 7 (Fig. 5) and gave similarly dramatic improvements for many other observations. A three-parameter cutoff model (the equivalent of $E_{\rm cut} = 0$) can also fit the data in some cases. Similarly, the "comptt" model in XSPEC v.10 (Titarchuk 1994) can be used to fit most of these data, but it tends to cutoff more rapidly than the data

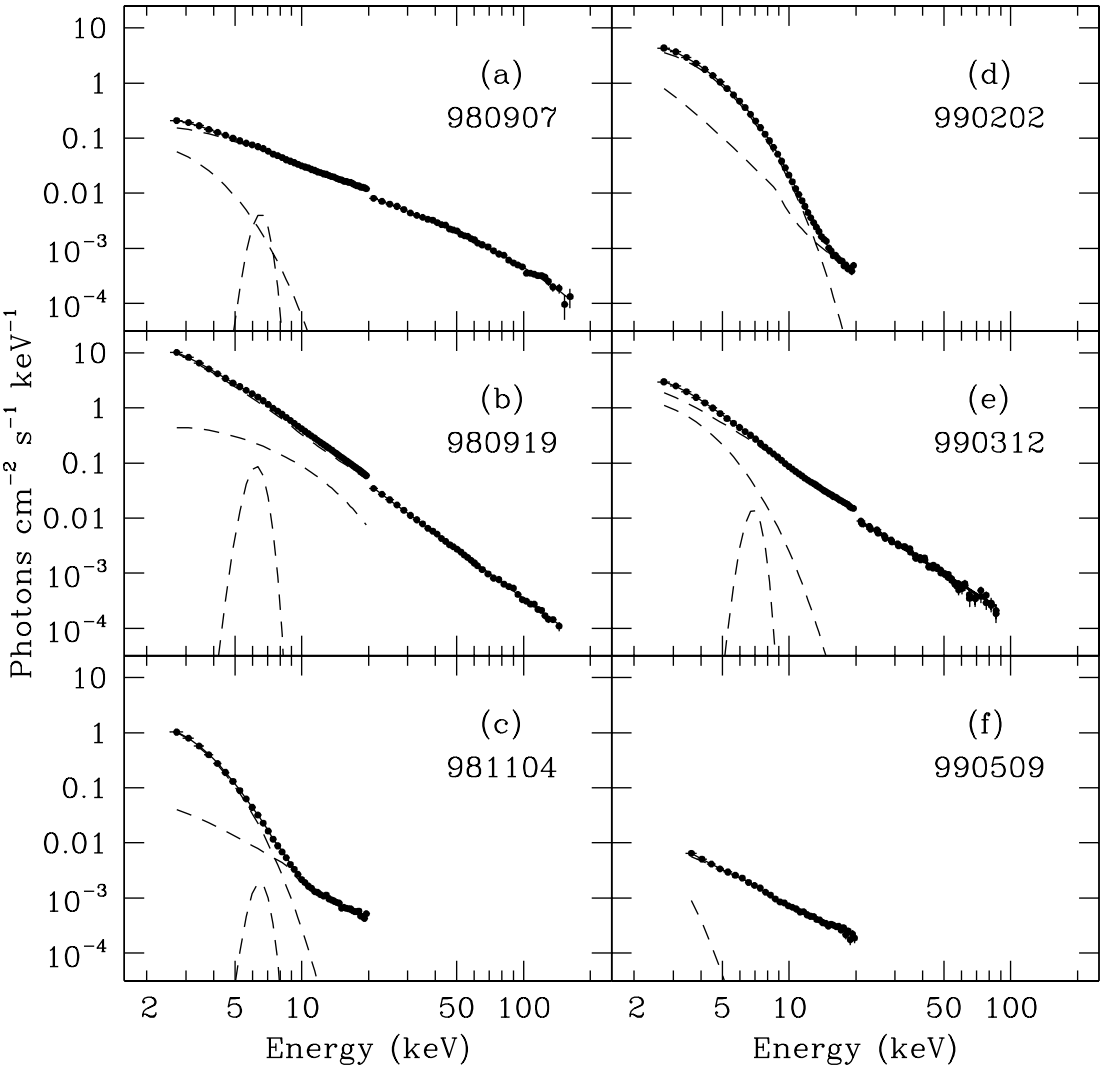

FIG. 3.—Sample PCA spectra from (*a*) the rising phase on MJD 51063 (1998 September 7), (*b*) the flare on MJD 51075 (1998 September 19), (*c*, *d*) the high/soft state on MJD 51121 and 51211 (1998 November 4 and 1999 February 2), (*e*) the power-law flare during the decline of the outburst (MJD 51249; 1999 March 12), and (*f*) one of the last observations on MJD 51307 (1999 May 9) during gain epoch 4. The individual components of the model are also shown (*dashed lines*). Although error bars are plotted for all the data, they are usually not large enough to be visible.

at high energy. These data can also be adequately fitted by a model including a pure power-law component plus a broad Gaussian or reflection component. The presence of a reflection component is possible, given the inclusion of Fe absorption when fitting the PCA spectra (see above). If a reflection component is present, the fitted parameters indicate that it would contribute as much as half of the 2–20 keV or 2–100 keV flux for the 1998 September 7 observation. Observations at higher energies are necessary to determine whether the high-energy cutoff seen in the 20–200 keV range is due to a physical cutoff in the power-law component or an underlying reflection feature.

The HEXTE model parameters are given in Table 4. The parameters of the high-energy cutoff are given only for those cases where the addition of the cutoff improved the value of χ^2_ν by more than 30%. The value of χ^2_ν for the pure power-law model is also given for comparison in these cases. Upper limits for the 20–100 keV HEXTE flux were determined by assuming a fixed power-law photon index of 2.5. The reader should also note that the normalization of the HEXTE instrument is systematically ~20%–30% lower than the PCA; we have not adjusted our spectral fits of the HEXTE data to correct for this discrepancy.

3. SPECTRAL RESULTS

Six representative spectra are shown in Figures 3*a*–3*f*. These spectra illustrate the range of X-ray spectra for XTE J1550−564, in which (*a*) a strong power law with high-energy cutoff dominates a warm disk (rising phase), (*b*) an intense power-law component dominates a hot disk (very high state flare), (*c*, *d*) the disk dominates a weak power law (high/soft state), (*e*) a strong power law dominates a warm disk, and (*f*) a weak power law dominates a cool disk.

As discussed in § 1, the outburst of XTE J1550−564 can be divided into two halves, which we now discuss in turn. We define the first half as extending from the start of the outburst on MJD 51062 (1998 September 6) to approximately MJD 51150 (1998 December 3). During the initial rise (MJD 51063−51072), the spectra are dominated by the power-law component with a photon index that gradually steepens from $\Gamma = 1.5$ to 2.5 (Fig. 4*c*, Table 2), and the

TABLE 2

SPECTRAL PARAMETERS FOR XTE J1550−564

Observation Number	Date (UT)	MJD[a]	T_{in} (keV)	R^{*}_{in}[b] (km)	Photon Index	Power-Law[c] Norm.	Fe Edge[d] (keV)	τ_{Fe}[d]	E_{line}[e] (keV)	$N_{line} \times 100$[e,f]	Line Equivalent Width (eV)	χ^2_ν (dof)
1	980907	51063.697	$0.892^{+0.057}_{-0.065}$	$7.46^{+1.16}_{-0.82}$	$1.47^{+0.02}_{-0.02}$	$1.00^{+0.05}_{-0.05}$	$8.28^{+0.33}_{-0.33}$	$0.40^{+0.08}_{-0.07}$	$6.52^{+0.10}_{-0.11}$	$0.56^{+0.11}_{-0.13}$	85^{+16}_{-19}	0.84(87)
2	980908	51064.006	$0.803^{+0.057}_{-0.069}$	$10.70^{+2.23}_{-1.41}$	$1.53^{+0.01}_{-0.01}$	$1.47^{+0.07}_{-0.06}$	$8.02^{+0.27}_{-0.27}$	$0.46^{+0.08}_{-0.07}$	$6.49^{+0.09}_{-0.09}$	$0.74^{+0.15}_{-0.17}$	87^{+17}_{-19}	0.33(87)
3	980909	51065.068	$0.552^{+0.072}_{-0.068}$	$30.79^{+15.89}_{-9.15}$	$1.72^{+0.01}_{-0.01}$	$3.99^{+0.08}_{-0.08}$	$7.85^{+0.18}_{-0.17}$	$0.40^{+0.05}_{-0.05}$	$6.61^{+0.09}_{-0.08}$	$1.30^{+0.24}_{-0.23}$	83^{+15}_{-14}	0.49(87)
4	980909	51065.342	$0.517^{+0.073}_{-0.067}$	$36.82^{+22.12}_{-12.15}$	$1.76^{+0.01}_{-0.01}$	$4.32^{+0.08}_{-0.09}$	$7.87^{+0.19}_{-0.18}$	$0.37^{+0.04}_{-0.05}$	$6.55^{+0.07}_{-0.07}$	$1.57^{+0.12}_{-0.23}$	98^{+7}_{-14}	0.59(87)
5	980910	51066.067	$0.352^{+0.060}_{-0.059}$	$160.33^{+228.79}_{-9.53}$	$1.91^{+0.00}_{-0.00}$	$7.32^{+0.08}_{-0.08}$	$7.98^{+0.09}_{-0.19}$	$0.25^{+0.04}_{-0.04}$	$6.61^{+0.06}_{-0.06}$	$2.31^{+0.22}_{-0.22}$	116^{+10}_{-11}	0.66(87)
6	980910	51066.345	$0.327^{+0.055}_{-0.039}$	$241.05^{+338.80}_{-121.24}$	$1.98^{+0.00}_{-0.00}$	$8.88^{+0.09}_{-0.09}$	$8.18^{+0.19}_{-0.20}$	$0.21^{+0.04}_{-0.04}$	$6.70^{+0.06}_{-0.06}$	$2.46^{+0.21}_{-0.21}$	118^{+10}_{-10}	0.69(87)
7	980911	51067.271	$0.345^{+0.041}_{-0.019}$	$265.64^{+159.88}_{-102.00}$	$2.12^{+0.00}_{-0.00}$	$13.97^{+0.13}_{-0.15}$	$8.24^{+0.22}_{-0.23}$	$0.17^{+0.04}_{-0.04}$	$6.66^{+0.06}_{-0.05}$	$3.19^{+0.25}_{-0.26}$	126^{+10}_{-10}	0.63(87)
8	980912	51068.345	$0.429^{+0.033}_{-0.033}$	$146.20^{+52.38}_{-35.18}$	$2.31^{+0.01}_{-0.01}$	$21.98^{+0.29}_{-0.31}$	$7.91^{+0.21}_{-0.22}$	$0.23^{+0.04}_{-0.04}$	$6.65^{+0.06}_{-0.06}$	$3.12^{+0.35}_{-0.34}$	112^{+12}_{-12}	0.93(87)
9	980913	51069.275	$0.525^{+0.034}_{-0.034}$	$88.84^{+20.98}_{-15.53}$	$2.46^{+0.01}_{-0.01}$	$32.27^{+0.65}_{-0.69}$	$7.75^{+0.22}_{-0.22}$	$0.32^{+0.05}_{-0.05}$	$6.58^{+0.08}_{-0.07}$	$2.90^{+0.49}_{-0.48}$	92^{+15}_{-15}	0.81(87)
10	980914	51070.131	$0.506^{+0.034}_{-0.035}$	$98.88^{+25.99}_{-18.19}$	$2.45^{+0.01}_{-0.01}$	$31.40^{+0.61}_{-0.62}$	$7.73^{+0.21}_{-0.22}$	$0.31^{+0.05}_{-0.05}$	$6.59^{+0.08}_{-0.07}$	$3.00^{+0.48}_{-0.47}$	96^{+15}_{-15}	0.81(87)
11	980914	51070.274	$0.503^{+0.034}_{-0.036}$	$98.25^{+27.17}_{-18.50}$	$2.45^{+0.01}_{-0.01}$	$31.63^{+0.60}_{-0.60}$	$7.81^{+0.21}_{-0.21}$	$0.31^{+0.05}_{-0.05}$	$6.61^{+0.08}_{-0.07}$	$2.98^{+0.46}_{-0.46}$	95^{+14}_{-14}	0.85(87)
12	980915	51071.200	$0.548^{+0.036}_{-0.037}$	$81.72^{+19.46}_{-13.71}$	$2.52^{+0.01}_{-0.01}$	$39.08^{+0.91}_{-0.92}$	$7.74^{+0.22}_{-0.22}$	$0.35^{+0.05}_{-0.05}$	$6.57^{+0.09}_{-0.08}$	$2.99^{+0.56}_{-0.56}$	87^{+16}_{-16}	0.69(87)
13	980915	51071.996	$0.429^{+0.030}_{-0.030}$	$162.98^{+51.94}_{-35.69}$	$2.36^{+0.01}_{-0.01}$	$25.59^{+0.37}_{-0.20}$	$7.96^{+0.11}_{-0.12}$	$0.23^{+0.04}_{-0.04}$	$6.64^{+0.06}_{-0.06}$	$3.29^{+0.38}_{-0.37}$	112^{+12}_{-12}	0.97(87)
14	980916	51072.345	$0.602^{+0.039}_{-0.043}$	$60.80^{+13.59}_{-9.20}$	$2.57^{+0.01}_{-0.01}$	$44.18^{+1.24}_{-1.20}$	$7.78^{+0.23}_{-0.23}$	$0.35^{+0.06}_{-0.06}$	$6.58^{+0.08}_{-0.08}$	$3.07^{+0.59}_{-0.62}$	86^{+16}_{-17}	0.81(87)
15	980918	51074.140	$0.793^{+0.035}_{-0.042}$	$33.20^{+3.32}_{-2.67}$	$2.70^{+0.01}_{-0.01}$	$71.24^{+3.22}_{-2.75}$	$7.99^{+0.26}_{-0.25}$	$0.37^{+0.08}_{-0.07}$	$6.57^{+0.10}_{-0.11}$	$3.23^{+0.70}_{-0.82}$	71^{+15}_{-18}	0.50(87)
16	980919	51075.987	$3.314^{+0.156}_{-0.164}$	$2.05^{+0.17}_{-0.14}$	$2.82^{+0.02}_{-0.01}$	$243.50^{+4.83}_{-4.46}$	$8.47^{+0.14}_{-0.14}$	$0.69^{+0.10}_{-0.09}$	$6.24^{+0.11}_{-0.11}$	$11.62^{+1.83}_{-1.85}$	71^{+11}_{-11}	0.34(87)
17	980920	51076.802	$0.884^{+0.032}_{-0.037}$	$26.96^{+2.30}_{-2.30}$	$2.77^{+0.01}_{-0.01}$	$98.24^{+4.57}_{-3.92}$	$8.08^{+0.24}_{-0.24}$	$0.38^{+0.08}_{-0.07}$	$6.54^{+0.13}_{-0.14}$	$3.08^{+0.81}_{-0.91}$	54^{+14}_{-16}	0.47(87)
18	980920	51076.953	$1.034^{+0.080}_{-0.068}$	$13.69^{+3.13}_{-4.32}$	$2.84^{+0.02}_{-0.01}$	$134.80^{+6.67}_{-5.93}$	$8.05^{+0.24}_{-0.24}$	$0.41^{+0.08}_{-0.08}$	$6.38^{+0.15}_{-0.18}$	$3.82^{+1.00}_{-1.13}$	52^{+13}_{-15}	0.72(87)
19	980921	51077.143	$1.294^{+0.138}_{-0.074}$	$9.45^{+2.43}_{-2.93}$	$2.86^{+0.01}_{-0.01}$	$149.40^{+6.25}_{-6.06}$	$8.07^{+0.31}_{-0.32}$	$0.38^{+0.08}_{-0.08}$	$6.35^{+0.18}_{-0.23}$	$3.87^{+1.10}_{-1.29}$	47^{+13}_{-15}	0.83(87)
20	980921	51077.211	$1.042^{+0.052}_{-0.043}$	$15.37^{+2.32}_{-3.10}$	$2.82^{+0.01}_{-0.01}$	$120.20^{+5.23}_{-4.36}$	$8.05^{+0.25}_{-0.26}$	$0.35^{+0.08}_{-0.06}$	6.5(fixed)	$3.31^{+0.91}_{-1.05}$	50^{+14}_{-16}	0.71(88)
21	980921	51077.869	$0.813^{+0.032}_{-0.040}$	$32.49^{+2.85}_{-2.41}$	$2.73^{+0.01}_{-0.01}$	$77.81^{+3.86}_{-3.11}$	$7.92^{+0.25}_{-0.25}$	$0.39^{+0.09}_{-0.08}$	$6.55^{+0.11}_{-0.12}$	$3.14^{+0.75}_{-0.90}$	65^{+15}_{-18}	0.54(87)
22	980922	51078.132	$0.737^{+0.037}_{-0.045}$	$39.49^{+5.04}_{-3.60}$	$2.69^{+0.01}_{-0.01}$	$64.38^{+2.84}_{-2.47}$	$7.81^{+0.23}_{-0.22}$	$0.43^{+0.09}_{-0.08}$	$6.55^{+0.10}_{-0.11}$	$2.83^{+0.73}_{-0.83}$	66^{+17}_{-19}	0.50(87)
23	980923	51079.794	$0.574^{+0.033}_{-0.035}$	$77.77^{+15.24}_{-10.89}$	$2.55^{+0.01}_{-0.01}$	$41.67^{+1.18}_{-1.14}$	$7.79^{+0.20}_{-0.19}$	$0.44^{+0.06}_{-0.06}$	$6.48^{+0.08}_{-0.08}$	$2.89^{+0.61}_{-0.64}$	81^{+17}_{-17}	0.69(87)
24	980924	51080.078	$0.570^{+0.035}_{-0.039}$	$74.49^{+16.70}_{-11.23}$	$2.55^{+0.01}_{-0.01}$	$40.65^{+1.07}_{-1.05}$	$7.74^{+0.18}_{-0.18}$	$0.44^{+0.06}_{-0.06}$	$6.54^{+0.09}_{-0.08}$	$2.76^{+0.58}_{-0.60}$	80^{+16}_{-17}	0.70(87)
25	980925	51081.062	$0.473^{+0.035}_{-0.033}$	$116.68^{+33.81}_{-24.50}$	$2.40^{+0.01}_{-0.01}$	$27.71^{+0.46}_{-0.50}$	$7.79^{+0.19}_{-0.19}$	$0.35^{+0.04}_{-0.04}$	$6.62^{+0.07}_{-0.07}$	$2.93^{+0.43}_{-0.41}$	98^{+14}_{-13}	0.86(87)
26	980926	51082.002	$0.462^{+0.034}_{-0.033}$	$122.51^{+37.55}_{-26.59}$	$2.38^{+0.01}_{-0.01}$	$26.33^{+0.41}_{-0.43}$	$7.80^{+0.18}_{-0.19}$	$0.32^{+0.04}_{-0.04}$	$6.61^{+0.07}_{-0.07}$	$3.01^{+0.41}_{-0.39}$	102^{+13}_{-13}	0.79(87)
27	980927	51083.002	$0.454^{+0.034}_{-0.032}$	$127.79^{+39.77}_{-28.30}$	$2.36^{+0.01}_{-0.01}$	$24.62^{+0.38}_{-0.41}$	$7.81^{+0.19}_{-0.19}$	$0.32^{+0.04}_{-0.04}$	$6.61^{+0.07}_{-0.07}$	$2.88^{+0.39}_{-0.38}$	100^{+13}_{-13}	0.89(87)
28	980928	51084.342	$0.476^{+0.034}_{-0.034}$	$107.83^{+32.53}_{-21.88}$	$2.35^{+0.01}_{-0.01}$	$23.56^{+0.41}_{-0.41}$	$7.87^{+0.16}_{-0.17}$	$0.38^{+0.04}_{-0.04}$	$6.58^{+0.07}_{-0.07}$	$2.79^{+0.39}_{-0.40}$	98^{+14}_{-14}	0.78(87)
29	980929	51085.270	$0.630^{+0.036}_{-0.041}$	$55.52^{+10.18}_{-6.99}$	$2.54^{+0.01}_{-0.01}$	$36.81^{+1.33}_{-1.28}$	$7.80^{+0.20}_{-0.19}$	$0.51^{+0.07}_{-0.07}$	$6.52^{+0.09}_{-0.09}$	$2.42^{+0.60}_{-0.65}$	75^{+18}_{-20}	0.79(87)
30	980929	51085.920	$0.510^{+0.031}_{-0.032}$	$93.88^{+22.24}_{-15.95}$	$2.36^{+0.01}_{-0.01}$	$23.53^{+0.50}_{-0.50}$	$7.87^{+0.16}_{-0.16}$	$0.46^{+0.05}_{-0.05}$	$6.56^{+0.07}_{-0.07}$	$2.71^{+0.43}_{-0.43}$	97^{+15}_{-15}	0.64(87)
31	980929	51085.991	$0.568^{+0.041}_{-0.042}$	$69.44^{+17.41}_{-12.04}$	$2.41^{+0.01}_{-0.01}$	$26.53^{+0.90}_{-0.95}$	$7.81^{+0.22}_{-0.21}$	$0.51^{+0.07}_{-0.07}$	$6.50^{+0.09}_{-0.09}$	$2.51^{+0.60}_{-0.60}$	84^{+20}_{-20}	0.87(87)
32	980930	51086.889	$0.564^{+0.032}_{-0.034}$	$72.43^{+14.24}_{-10.46}$	$2.44^{+0.01}_{-0.01}$	$28.14^{+0.71}_{-0.71}$	$7.81^{+0.17}_{-0.16}$	$0.48^{+0.05}_{-0.05}$	$6.52^{+0.08}_{-0.08}$	$2.45^{+0.49}_{-0.49}$	84^{+16}_{-17}	0.64(87)
33	981001	51087.723	$0.556^{+0.032}_{-0.034}$	$74.79^{+15.23}_{-11.05}$	$2.43^{+0.01}_{-0.01}$	$27.04^{+0.66}_{-0.67}$	$7.78^{+0.16}_{-0.15}$	$0.51^{+0.05}_{-0.05}$	$6.53^{+0.09}_{-0.08}$	$2.27^{+0.47}_{-0.48}$	79^{+16}_{-16}	0.55(87)
34	981002	51088.007	$0.550^{+0.040}_{-0.042}$	$73.51^{+19.83}_{-13.50}$	$2.39^{+0.01}_{-0.01}$	$24.51^{+0.69}_{-0.71}$	$7.86^{+0.20}_{-0.19}$	$0.49^{+0.06}_{-0.06}$	$6.54^{+0.10}_{-0.09}$	$2.39^{+0.54}_{-0.55}$	87^{+19}_{-19}	0.46(87)
35	981003	51089.008	$0.533^{+0.033}_{-0.034}$	$78.57^{+18.09}_{-12.83}$	$2.36^{+0.01}_{-0.01}$	$22.05^{+0.51}_{-0.51}$	$7.89^{+0.16}_{-0.15}$	$0.51^{+0.05}_{-0.05}$	$6.55^{+0.08}_{-0.08}$	$2.29^{+0.42}_{-0.43}$	87^{+16}_{-16}	0.56(87)
36	981004	51090.143	$0.638^{+0.030}_{-0.033}$	$53.00^{+7.56}_{-5.59}$	$2.45^{+0.01}_{-0.01}$	$26.91^{+0.92}_{-0.86}$	$7.94^{+0.17}_{-0.17}$	$0.58^{+0.06}_{-0.06}$	$6.47^{+0.08}_{-0.09}$	$2.31^{+0.48}_{-0.53}$	81^{+17}_{-18}	0.57(87)
37	981004	51090.704	$0.572^{+0.030}_{-0.031}$	$72.10^{+12.31}_{-9.38}$	$2.44^{+0.01}_{-0.01}$	$25.82^{+0.73}_{-0.73}$	$7.82^{+0.16}_{-0.15}$	$0.58^{+0.06}_{-0.06}$	$6.49^{+0.09}_{-0.09}$	$2.04^{+0.48}_{-0.49}$	74^{+17}_{-17}	0.74(87)
38	981005	51091.743	$0.742^{+0.023}_{-0.025}$	$42.81^{+3.16}_{-2.63}$	$2.58^{+0.01}_{-0.01}$	$38.44^{+1.64}_{-1.46}$	$8.10^{+0.17}_{-0.18}$	$0.61^{+0.07}_{-0.07}$	$6.48^{+0.10}_{-0.11}$	$2.36^{+0.50}_{-0.56}$	72^{+15}_{-17}	0.56(87)
39	981007	51093.143	$0.863^{+0.018}_{-0.019}$	$31.66^{+1.40}_{-1.29}$	$2.60^{+0.01}_{-0.01}$	$41.28^{+1.75}_{-1.58}$	$8.40^{+0.18}_{-0.18}$	$0.52^{+0.07}_{-0.06}$	$6.64^{+0.10}_{-0.11}$	$2.35^{+0.44}_{-0.47}$	71^{+13}_{-14}	0.44(87)
40	981008	51094.143	$0.669^{+0.026}_{-0.029}$	$47.93^{+5.29}_{-4.16}$	$2.45^{+0.01}_{-0.01}$	$24.97^{+0.91}_{-0.85}$	$7.96^{+0.16}_{-0.16}$	$0.63^{+0.07}_{-0.06}$	$6.48^{+0.09}_{-0.10}$	$1.96^{+0.44}_{-0.48}$	74^{+16}_{-18}	0.55(87)
41	981008	51094.572	$0.721^{+0.022}_{-0.024}$	$43.50^{+3.34}_{-2.76}$	$2.51^{+0.01}_{-0.01}$	$28.75^{+1.14}_{-1.03}$	$8.09^{+0.16}_{-0.17}$	$0.63^{+0.07}_{-0.06}$	$6.49^{+0.09}_{-0.10}$	$2.20^{+0.43}_{-0.48}$	79^{+15}_{-17}	0.62(87)
42	981009	51095.609	$0.670^{+0.024}_{-0.026}$	$48.90^{+4.84}_{-3.92}$	$2.45^{+0.01}_{-0.01}$	$24.34^{+0.89}_{-0.84}$	$8.02^{+0.15}_{-0.15}$	$0.69^{+0.06}_{-0.06}$	$6.44^{+0.10}_{-0.11}$	$1.85^{+0.43}_{-0.46}$	71^{+16}_{-17}	0.70(87)
43	981010	51096.572	$0.736^{+0.022}_{-0.024}$	$41.28^{+2.97}_{-2.48}$	$2.52^{+0.01}_{-0.01}$	$28.54^{+1.22}_{-1.10}$	$8.11^{+0.17}_{-0.17}$	$0.65^{+0.07}_{-0.07}$	$6.53^{+0.10}_{-0.11}$	$2.00^{+0.42}_{-0.47}$	75^{+16}_{-17}	0.50(87)
44	981011	51097.572	$0.683^{+0.022}_{-0.023}$	$47.40^{+4.02}_{-3.33}$	$2.46^{+0.01}_{-0.01}$	$23.49^{+0.87}_{-0.82}$	$8.09^{+0.16}_{-0.16}$	$0.64^{+0.06}_{-0.06}$	$6.45^{+0.09}_{-0.10}$	$1.97^{+0.39}_{-0.42}$	80^{+15}_{-17}	0.68(87)
45	981011	51097.809	$0.649^{+0.026}_{-0.028}$	$50.39^{+5.80}_{-4.55}$	$2.40^{+0.01}_{-0.01}$	$19.74^{+0.76}_{-0.73}$	$8.00^{+0.15}_{-0.15}$	$0.74^{+0.07}_{-0.06}$	$6.43^{+0.10}_{-0.11}$	$1.61^{+0.41}_{-0.45}$	68^{+17}_{-19}	0.61(87)

TABLE 2—*Continued*

Observation Number	Date (UT)	MJD[a]	T_{in} (keV)	$R^{*\,b}_{in}$ (km)	Photon Index	Power-Law[c] Norm.	Fe Edge[d] (keV)	τ_{Fe}[d]	E_{line}[e] (keV)	$N_{line} \times 100$[e,f]	Line Equivalent Width (eV)	χ^2_ν (dof)
46	981012	51098.275	$0.741^{+0.021}_{-0.023}$	$38.41^{+2.65}_{-2.27}$	$2.45^{+0.01}_{-0.01}$	$22.55^{+0.93}_{-0.86}$	$8.28^{+0.16}_{-0.17}$	$0.67^{+0.06}_{-0.06}$	$6.49^{+0.10}_{-0.11}$	$1.85^{+0.36}_{-0.39}$	76^{+14}_{-16}	0.48(87)
47	981013	51099.215	$0.735^{+0.022}_{-0.023}$	$38.69^{+2.75}_{-2.37}$	$2.44^{+0.01}_{-0.01}$	$21.22^{+0.91}_{-0.85}$	$8.20^{+0.16}_{-0.16}$	$0.71^{+0.07}_{-0.06}$	$6.46^{+0.10}_{-0.11}$	$1.87^{+0.37}_{-0.40}$	78^{+15}_{-16}	0.70(87)
48	981013	51099.608	$0.710^{+0.021}_{-0.022}$	$42.65^{+3.15}_{-2.69}$	$2.44^{+0.01}_{-0.01}$	$21.33^{+0.83}_{-0.78}$	$8.19^{+0.16}_{-0.16}$	$0.69^{+0.06}_{-0.06}$	$6.47^{+0.09}_{-0.10}$	$1.83^{+0.36}_{-0.39}$	78^{+15}_{-16}	0.57(87)
49	981014	51100.287	$0.822^{+0.015}_{-0.016}$	$34.62^{+1.42}_{-1.30}$	$2.52^{+0.01}_{-0.01}$	$26.63^{+1.13}_{-1.02}$	$8.51^{+0.16}_{-0.16}$	$0.65^{+0.06}_{-0.06}$	$6.63^{+0.10}_{-0.11}$	$1.98^{+0.33}_{-0.35}$	80^{+13}_{-14}	0.48(87)
50	981015	51101.607	$0.821^{+0.015}_{-0.016}$	$35.56^{+1.42}_{-1.31}$	$2.53^{+0.01}_{-0.01}$	$27.03^{+1.16}_{-1.10}$	$8.51^{+0.15}_{-0.15}$	$0.71^{+0.06}_{-0.06}$	$6.59^{+0.12}_{-0.12}$	$1.80^{+0.33}_{-0.35}$	71^{+13}_{-14}	0.60(87)
51	981015	51101.941	$0.830^{+0.015}_{-0.015}$	$34.08^{+1.30}_{-1.20}$	$2.51^{+0.01}_{-0.01}$	$25.23^{+1.05}_{-0.97}$	$8.53^{+0.14}_{-0.14}$	$0.71^{+0.06}_{-0.06}$	$6.67^{+0.10}_{-0.11}$	$1.81^{+0.31}_{-0.33}$	77^{+13}_{-14}	0.58(87)
52	981020	51106.953	$0.969^{+0.010}_{-0.010}$	$30.54^{+0.74}_{-0.72}$	$2.60^{+0.02}_{-0.02}$	$31.19^{+1.73}_{-1.62}$	$8.88^{+0.13}_{-0.13}$	$0.87^{+0.07}_{-0.07}$	$6.86^{+0.14}_{-0.14}$	$1.73^{+0.34}_{-0.35}$	66^{+13}_{-13}	0.82(87)
53	981022	51108.076	$0.977^{+0.010}_{-0.010}$	$28.59^{+0.61}_{-0.60}$	$2.57^{+0.01}_{-0.01}$	$28.04^{+1.26}_{-1.21}$	$9.01^{+0.13}_{-0.12}$	$0.77^{+0.06}_{-0.06}$	$7.01^{+0.11}_{-0.12}$	$1.74^{+0.28}_{-0.29}$	74^{+12}_{-12}	0.44(87)
54	981023	51109.737	$0.927^{+0.010}_{-0.010}$	$32.50^{+0.77}_{-0.76}$	$2.61^{+0.02}_{-0.02}$	$27.24^{+1.63}_{-1.53}$	$8.81^{+0.14}_{-0.13}$	$0.91^{+0.08}_{-0.08}$	$6.93^{+0.15}_{-0.16}$	$1.31^{+0.31}_{-0.32}$	61^{+14}_{-15}	0.82(87)
55	981024	51110.270	$0.922^{+0.008}_{-0.008}$	$34.75^{+0.63}_{-0.61}$	$2.60^{+0.02}_{-0.02}$	$22.43^{+1.26}_{-1.15}$	$8.87^{+0.12}_{-0.11}$	$1.00^{+0.07}_{-0.07}$	$7.02^{+0.11}_{-0.12}$	$1.42^{+0.24}_{-0.25}$	79^{+13}_{-14}	0.74(87)
56	981025	51111.602	$0.901^{+0.009}_{-0.009}$	$35.11^{+0.71}_{-0.70}$	$2.55^{+0.02}_{-0.02}$	$19.94^{+1.22}_{-1.15}$	$8.93^{+0.15}_{-0.14}$	$0.90^{+0.07}_{-0.07}$	$6.97^{+0.11}_{-0.12}$	$1.49^{+0.25}_{-0.26}$	84^{+14}_{-14}	0.80(87)
57	981026	51112.802	$0.885^{+0.008}_{-0.009}$	$35.96^{+0.73}_{-0.70}$	$2.51^{+0.02}_{-0.02}$	$17.48^{+0.89}_{-0.86}$	$8.90^{+0.12}_{-0.11}$	$1.00^{+0.06}_{-0.06}$	$6.98^{+0.12}_{-0.12}$	$1.26^{+0.22}_{-0.23}$	77^{+13}_{-13}	0.56(87)
58	981027	51113.668	$0.870^{+0.008}_{-0.008}$	$36.92^{+0.73}_{-0.70}$	$2.54^{+0.02}_{-0.02}$	$15.60^{+0.91}_{-0.85}$	$8.85^{+0.11}_{-0.11}$	$1.18^{+0.07}_{-0.07}$	$6.87^{+0.11}_{-0.11}$	$1.28^{+0.20}_{-0.21}$	87^{+13}_{-14}	0.64(87)
59	981029	51115.280	$0.837^{+0.006}_{-0.006}$	$39.17^{+0.67}_{-0.65}$	$2.47^{+0.02}_{-0.02}$	$8.38^{+0.50}_{-0.48}$	$8.84^{+0.10}_{-0.10}$	$1.38^{+0.07}_{-0.07}$	$6.83^{+0.10}_{-0.11}$	$0.91^{+0.13}_{-0.14}$	93^{+13}_{-14}	0.83(87)
60	981031	51117.351	$0.814^{+0.004}_{-0.004}$	$45.26^{+0.60}_{-0.57}$	$2.22^{+0.04}_{-0.04}$	$1.55^{+0.17}_{-0.15}$	$8.61^{+0.12}_{-0.12}$	$1.81^{+0.12}_{-0.12}$	$6.66^{+0.13}_{-0.14}$	$0.48^{+0.08}_{-0.08}$	91^{+14}_{-14}	1.50(87)
61	981102	51119.003	$0.778^{+0.004}_{-0.004}$	$46.95^{+0.67}_{-0.65}$	$2.27^{+0.04}_{-0.04}$	$1.50^{+0.17}_{-0.15}$	$8.38^{+0.12}_{-0.12}$	$1.95^{+0.14}_{-0.14}$	$6.63^{+0.14}_{-0.16}$	$0.37^{+0.06}_{-0.07}$	86^{+15}_{-17}	1.01(87)
62	981104	51121.003	$0.760^{+0.003}_{-0.003}$	$46.41^{+0.57}_{-0.55}$	$2.35^{+0.06}_{-0.06}$	$0.62^{+0.11}_{-0.09}$	$8.48^{+0.12}_{-0.12}$	$2.80^{+0.18}_{-0.19}$	$6.47^{+0.14}_{-0.14}$	$0.26^{+0.05}_{-0.04}$	90^{+16}_{-15}	1.25(87)
63	981107	51124.727	$0.721^{+0.004}_{-0.004}$	$47.34^{+0.67}_{-0.65}$	$2.20^{+0.05}_{-0.05}$	$0.63^{+0.09}_{-0.08}$	$8.42^{+0.13}_{-0.13}$	$2.20^{+0.17}_{-0.17}$	$6.63^{+0.11}_{-0.13}$	$0.24^{+0.04}_{-0.04}$	115^{+20}_{-21}	0.94(87)
64	981109	51126.595	$0.706^{+0.004}_{-0.004}$	$46.90^{+0.73}_{-0.71}$	$2.31^{+0.02}_{-0.02}$	$1.59^{+0.10}_{-0.09}$	$8.63^{+0.08}_{-0.08}$	$1.81^{+0.07}_{-0.07}$	$6.62^{+0.11}_{-0.12}$	$0.27^{+0.04}_{-0.04}$	95^{+14}_{-15}	0.91(87)
65	981111	51128.564	$0.682^{+0.004}_{-0.004}$	$48.74^{+0.87}_{-0.82}$	$2.19^{+0.04}_{-0.04}$	$0.79^{+0.08}_{-0.07}$	$8.35^{+0.13}_{-0.12}$	$1.87^{+0.11}_{-0.12}$	$6.34^{+0.18}_{-0.20}$	$0.18^{+0.04}_{-0.04}$	76^{+18}_{-18}	0.98(87)
66	981113	51130.457	$0.671^{+0.004}_{-0.004}$	$48.27^{+0.76}_{-0.75}$	$2.16^{+0.03}_{-0.03}$	$0.72^{+0.05}_{-0.05}$	$8.45^{+0.10}_{-0.10}$	$1.82^{+0.09}_{-0.09}$	$6.45^{+0.12}_{-0.13}$	$0.18^{+0.03}_{-0.03}$	94^{+16}_{-17}	1.20(87)
67	981115	51132.479	$0.659^{+0.005}_{-0.005}$	$47.53^{+0.92}_{-0.96}$	$2.18^{+0.05}_{-0.05}$	$0.63^{+0.08}_{-0.07}$	$8.40^{+0.19}_{-0.18}$	$1.64^{+0.14}_{-0.14}$	$6.60^{+0.13}_{-0.16}$	$0.15^{+0.04}_{-0.04}$	106^{+27}_{-28}	2.89(87)
68	981117	51134.436	$0.643^{+0.003}_{-0.004}$	$48.27^{+0.81}_{-0.76}$	$2.17^{+0.04}_{-0.04}$	$0.38^{+0.04}_{-0.04}$	$8.35^{+0.12}_{-0.12}$	$2.08^{+0.12}_{-0.12}$	$6.42^{+0.14}_{-0.16}$	$0.12^{+0.02}_{-0.02}$	104^{+19}_{-20}	1.94(87)
69	981119	51136.777	$0.613^{+0.003}_{-0.003}$	$51.12^{+0.74}_{-0.73}$	$2.23^{+0.04}_{-0.03}$	$0.42^{+0.04}_{-0.03}$	$8.11^{+0.10}_{-0.10}$	$2.08^{+0.10}_{-0.11}$	$5.96^{+0.18}_{-0.10}$	$0.09^{+0.02}_{-0.02}$	65^{+14}_{-15}	1.33(87)
70	981120	51137.923	$0.620^{+0.005}_{-0.005}$	$46.77^{+1.10}_{-1.05}$	$2.24^{+0.02}_{-0.03}$	$0.98^{+0.06}_{-0.06}$	$8.54^{+0.09}_{-0.10}$	$1.64^{+0.08}_{-0.08}$	$6.61^{+0.13}_{-0.14}$	$0.13^{+0.03}_{-0.03}$	77^{+19}_{-20}	1.56(87)
71	981122	51139.991	$0.614^{+0.006}_{-0.006}$	$43.72^{+1.22}_{-1.17}$	$2.19^{+0.03}_{-0.03}$	$1.00^{+0.06}_{-0.06}$	$8.56^{+0.09}_{-0.09}$	$1.66^{+0.08}_{-0.09}$	$6.33^{+0.16}_{-0.19}$	$0.14^{+0.04}_{-0.04}$	68^{+18}_{-18}	0.99(87)
72	981123	51140.706	$0.603^{+0.005}_{-0.005}$	$45.00^{+1.17}_{-1.13}$	$2.24^{+0.02}_{-0.02}$	$0.98^{+0.05}_{-0.05}$	$8.48^{+0.08}_{-0.08}$	$1.66^{+0.04}_{-0.08}$	$6.45^{+0.17}_{-0.20}$	$0.09^{+0.03}_{-0.03}$	55^{+18}_{-18}	0.89(87)
73	981126	51143.800	$0.570^{+0.014}_{-0.017}$	$49.20^{+5.25}_{-3.41}$	$2.37^{+0.08}_{-0.08}$	$1.22^{+0.20}_{-0.18}$	$8.35^{+0.30}_{-0.83}$	$1.01^{+0.34}_{-0.35}$	$7.07^{+1.08}_{-0.98}$	$0.06^{+0.08}_{-0.06}$	49^{+64}_{-49}	1.09(87)
74	981128	51145.476	$0.575^{+0.004}_{-0.004}$	$50.04^{+1.04}_{-0.98}$	$2.04^{+0.04}_{-0.04}$	$0.22^{+0.02}_{-0.02}$	$8.52^{+0.14}_{-0.14}$	$1.68^{+0.13}_{-0.07}$	$6.29^{+0.11}_{-0.13}$	$0.09^{+0.02}_{-0.02}$	132^{+23}_{-24}	1.33(87)
75	981130	51147.335	$0.583^{+0.004}_{-0.004}$	$46.51^{+1.12}_{-1.09}$	$2.21^{+0.02}_{-0.02}$	$0.67^{+0.04}_{-0.04}$	$8.43^{+0.08}_{-0.08}$	$1.60^{+0.08}_{-0.08}$	$6.18^{+0.23}_{-0.27}$	$0.06^{+0.02}_{-0.02}$	44^{+17}_{-16}	1.32(87)
76	981203	51150.073	$0.596^{+0.004}_{-0.004}$	$47.76^{+0.95}_{-0.92}$	$2.05^{+0.04}_{-0.04}$	$0.29^{+0.03}_{-0.02}$	$8.38^{+0.12}_{-0.12}$	$1.73^{+0.06}_{-0.06}$	$6.48^{+0.12}_{-0.14}$	$0.08^{+0.02}_{-0.02}$	104^{+24}_{-25}	1.76(87)
77	981205	51152.080	$0.617^{+0.003}_{-0.004}$	$49.29^{+0.86}_{-0.82}$	$2.24^{+0.07}_{-0.07}$	$0.26^{+0.05}_{-0.04}$	$8.19^{+0.15}_{-0.07}$	$2.59^{+0.20}_{-0.20}$	$6.23^{+0.21}_{-0.26}$	$0.06^{+0.02}_{-0.02}$	78^{+24}_{-26}	0.99(87)
78	981205	51152.866	$0.643^{+0.003}_{-0.003}$	$46.49^{+0.65}_{-0.64}$	$2.23^{+0.09}_{-0.09}$	$0.17^{+0.04}_{-0.03}$	$8.48^{+0.11}_{-0.11}$	$3.39^{+0.24}_{-0.24}$	$6.15^{+0.12}_{-0.13}$	$0.11^{+0.02}_{-0.02}$	119^{+19}_{-19}	1.55(86)
79	981207	51154.016	$0.659^{+0.003}_{-0.003}$	$47.79^{+0.74}_{-0.69}$	$2.20^{+0.11}_{-0.11}$	$0.20^{+0.05}_{-0.04}$	$8.43^{+0.12}_{-0.12}$	$4.09^{+0.32}_{-0.32}$	$6.10^{+0.16}_{-0.17}$	$0.12^{+0.03}_{-0.03}$	102^{+23}_{-21}	0.91(87)
80	981208	51155.067	$0.685^{+0.003}_{-0.003}$	$46.72^{+0.60}_{-0.58}$	$2.49^{+0.12}_{-0.12}$	$0.31^{+0.10}_{-0.07}$	$8.40^{+0.12}_{-0.12}$	$4.02^{+0.32}_{-0.32}$	$6.20^{+0.13}_{-0.13}$	$0.14^{+0.03}_{-0.03}$	100^{+19}_{-18}	1.94(87)
81	981210	51157.493	$0.752^{+0.004}_{-0.004}$	$44.44^{+0.62}_{-0.59}$	$2.69^{+0.17}_{-0.17}$	$0.58^{+0.29}_{-0.19}$	$8.73^{+0.12}_{-0.12}$	$4.89^{+0.41}_{-0.41}$	$6.35^{+0.20}_{-0.19}$	$0.17^{+0.05}_{-0.05}$	72^{+21}_{-19}	1.09(87)
82	981213	51160.276	$0.823^{+0.003}_{-0.003}$	$42.17^{+0.55}_{-0.65}$	$3.57^{+0.19}_{-0.20}$	$5.21^{+2.91}_{-1.99}$	$8.63^{+0.19}_{-0.19}$	$3.93^{+0.49}_{-0.55}$	$6.61^{+0.38}_{-0.43}$	$0.13^{+0.07}_{-0.06}$	36^{+19}_{-16}	2.09(87)
83	981215	51162.202	$0.867^{+0.003}_{-0.003}$	$42.93^{+0.52}_{-0.57}$	$3.59^{+0.22}_{-0.26}$	$5.04^{+3.38}_{-2.36}$	$8.82^{+0.16}_{-0.15}$	$5.79^{+0.60}_{-0.63}$	$6.72^{+0.25}_{-0.27}$	$0.25^{+0.08}_{-0.07}$	48^{+16}_{-14}	2.15(87)
84	981216	51163.205	$0.891^{+0.003}_{-0.005}$	$41.45^{+0.84}_{-0.43}$	$4.08^{+0.14}_{-0.16}$	$20.53^{+4.30}_{-5.68}$	$8.31^{+0.16}_{-0.10}$	$6.20^{+0.44}_{-0.62}$	6.5(fixed)	$0.00^{+0.12}_{-0.00}$	0^{+16}_{-0}	1.36(88)
85	981217	51164.205	$0.915^{+0.005}_{-0.005}$	$42.15^{+0.85}_{-0.86}$	$4.14^{+0.16}_{-0.18}$	$23.43^{+8.83}_{-7.59}$	$8.55^{+0.21}_{-0.21}$	$5.57^{+0.74}_{-0.91}$	$6.75^{+0.40}_{-0.50}$	$0.21^{+0.13}_{-0.14}$	27^{+17}_{-17}	1.19(87)
86	981218	51165.590	$0.947^{+0.003}_{-0.003}$	$42.47^{+0.50}_{-0.63}$	$3.53^{+0.15}_{-0.17}$	$8.65^{+4.66}_{-3.33}$	$8.59^{+0.16}_{-0.16}$	$5.83^{+0.59}_{-0.63}$	$7.01^{+0.31}_{-0.81}$	$0.25^{+0.14}_{-0.16}$	30^{+17}_{-19}	1.41(87)
87	981219	51166.011	$0.955^{+0.003}_{-0.003}$	$42.38^{+0.46}_{-0.53}$	$3.60^{+0.14}_{-0.16}$	$9.74^{+4.39}_{-3.44}$	$8.72^{+0.07}_{-0.14}$	$5.82^{+0.50}_{-0.56}$	$7.01^{+0.29}_{-0.45}$	$0.25^{+0.12}_{-0.13}$	29^{+14}_{-15}	1.41(87)
88	981220	51167.418	$0.980^{+0.004}_{-0.003}$	$42.33^{+0.65}_{-0.74}$	$3.81^{+0.16}_{-0.19}$	$16.74^{+8.58}_{-6.54}$	$8.83^{+0.15}_{-0.16}$	$7.35^{+0.66}_{-0.80}$	$6.93^{+0.51}_{-0.84}$	$0.26^{+0.23}_{-0.17}$	23^{+20}_{-15}	1.42(87)
89	981221	51168.010	$0.995^{+0.002}_{-0.003}$	$40.69^{+0.39}_{-0.39}$	$3.85^{+0.09}_{-0.10}$	$19.85^{+5.10}_{-4.42}$	$8.48^{+0.14}_{-0.12}$	$5.86^{+0.40}_{-0.43}$	6.5(fixed)	$0.04^{+0.19}_{-0.04}$	2^{+11}_{-2}	2.22(88)
90	981222	51169.009	$1.009^{+0.003}_{-0.002}$	$40.61^{+0.40}_{-0.42}$	$3.81^{+0.07}_{-0.08}$	$26.63^{+5.73}_{-5.14}$	$8.58^{+0.11}_{-0.12}$	$5.79^{+0.33}_{-0.32}$	6.5(fixed)	$0.35^{+0.25}_{-0.25}$	18^{+12}_{-12}	1.89(87)

TABLE 2—*Continued*

Observation Number	Date (UT)	MJD[a]	T_{in} (keV)	R^{*}_{in}[b] (km)	Photon Index	Power-Law[c] Norm.	Fe Edge[d] (keV)	τ_{Fe}[d]	E_{line}[e] (keV)	$N_{line} \times 100$[e,f]	Line Equivalent Width (eV)	χ^2_ν (dof)
91	981223	51170.520	$1.020^{+0.003}_{-0.003}$	$41.29^{+0.50}_{-0.56}$	$3.65^{+0.10}_{-0.12}$	$17.61^{+5.81}_{-4.93}$	$8.82^{+0.15}_{-0.16}$	$5.07^{+0.55}_{-0.58}$	$7.31^{+0.22}_{-0.28}$	$0.41^{+0.17}_{-0.19}$	37^{+15}_{-17}	1.18(87)
92	981225	51172.065	$1.042^{+0.002}_{-0.003}$	$39.36^{+0.35}_{-0.36}$	$3.85^{+0.06}_{-0.07}$	$31.57^{+5.59}_{-5.10}$	$8.62^{+0.11}_{-0.11}$	$5.63^{+0.32}_{-0.31}$	6.5(fixed)	$0.15^{+0.24}_{-0.15}$	6^{+10}_{-6}	2.98(88)
93	981226	51172.990	$1.036^{+0.003}_{-0.003}$	$40.49^{+0.50}_{-0.52}$	$3.86^{+0.07}_{-0.08}$	$31.16^{+6.72}_{-6.28}$	$8.87^{+0.14}_{-0.14}$	$4.49^{+0.45}_{-0.46}$	$7.32^{+0.19}_{-0.23}$	$0.48^{+0.17}_{-0.18}$	40^{+13}_{-14}	1.78(83)
94	981227	51173.990	$1.037^{+0.003}_{-0.003}$	$40.38^{+0.53}_{-0.57}$	$3.77^{+0.07}_{-0.08}$	$30.68^{+7.02}_{-6.22}$	$8.75^{+0.13}_{-0.13}$	$4.74^{+0.39}_{-0.41}$	$6.97^{+0.35}_{-0.60}$	$0.42^{+0.20}_{-0.21}$	25^{+12}_{-12}	1.62(86)
95	981227	51174.722	$1.045^{+0.003}_{-0.003}$	$40.40^{+0.45}_{-0.48}$	$3.80^{+0.06}_{-0.07}$	$33.07^{+6.35}_{-5.81}$	$8.93^{+0.12}_{-0.12}$	$4.55^{+0.35}_{-0.36}$	$7.23^{+0.19}_{-0.24}$	$0.53^{+0.18}_{-0.18}$	38^{+12}_{-13}	1.35(87)
96	981228	51175.879	$1.048^{+0.003}_{-0.002}$	$40.48^{+0.48}_{-0.51}$	$3.61^{+0.06}_{-0.07}$	$25.13^{+5.53}_{-5.08}$	$8.81^{+0.13}_{-0.14}$	$4.06^{+0.35}_{-0.36}$	$7.20^{+0.21}_{-0.28}$	$0.53^{+0.20}_{-0.21}$	35^{+13}_{-14}	1.51(87)
97	981229	51176.847	$1.051^{+0.003}_{-0.003}$	$40.26^{+0.50}_{-0.53}$	$3.62^{+0.06}_{-0.07}$	$27.02^{+5.86}_{-5.35}$	$8.85^{+0.12}_{-0.12}$	$4.50^{+0.34}_{-0.35}$	$7.19^{+0.28}_{-0.47}$	$0.41^{+0.20}_{-0.21}$	27^{+13}_{-14}	1.43(87)
98	981230	51177.846	$1.056^{+0.004}_{-0.003}$	$39.95^{+0.56}_{-0.59}$	$3.70^{+0.06}_{-0.07}$	$34.57^{+6.88}_{-6.29}$	$8.77^{+0.13}_{-0.13}$	$4.24^{+0.36}_{-0.37}$	$7.10^{+0.29}_{-0.48}$	$0.48^{+0.22}_{-0.23}$	28^{+13}_{-14}	1.45(87)
99	981231	51178.846	$1.064^{+0.002}_{-0.003}$	$39.10^{+0.37}_{-0.38}$	$3.75^{+0.05}_{-0.05}$	$40.70^{+5.49}_{-5.22}$	$8.56^{+0.10}_{-0.11}$	$4.34^{+0.23}_{-0.23}$	6.5(fixed)	$0.27^{+0.29}_{-0.27}$	9^{+10}_{-9}	1.94(88)
100	990101	51179.919	$1.042^{+0.003}_{-0.003}$	$42.08^{+0.37}_{-0.39}$	$3.11^{+0.06}_{-0.06}$	$16.72^{+3.05}_{-2.70}$	$8.76^{+0.09}_{-0.09}$	$3.51^{+0.19}_{-0.20}$	$6.85^{+0.20}_{-0.22}$	$0.96^{+0.27}_{-0.27}$	43^{+12}_{-12}	1.72(87)
101	990102	51180.845	$1.038^{+0.004}_{-0.004}$	$43.39^{+0.36}_{-0.36}$	$2.72^{+0.04}_{-0.04}$	$12.79^{+1.79}_{-1.61}$	$8.76^{+0.09}_{-0.09}$	$2.43^{+0.15}_{-0.16}$	$6.87^{+0.14}_{-0.15}$	$1.57^{+0.31}_{-0.31}$	63^{+12}_{-12}	1.00(87)
102	990104	51182.337	$1.080^{+0.003}_{-0.002}$	$38.34^{+0.36}_{-0.37}$	$3.87^{+0.05}_{-0.05}$	$48.21^{+6.30}_{-6.07}$	$8.66^{+0.11}_{-0.11}$	$4.61^{+0.26}_{-0.26}$	6.5(fixed)	$0.23^{+0.30}_{-0.23}$	7^{+10}_{-7}	1.55(87)
103	990105	51183.540	$1.083^{+0.003}_{-0.002}$	$38.48^{+0.37}_{-0.37}$	$3.86^{+0.05}_{-0.05}$	$48.06^{+6.54}_{-6.12}$	$8.67^{+0.13}_{-0.13}$	$4.02^{+0.27}_{-0.26}$	6.5(fixed)	$0.16^{+0.30}_{-0.16}$	5^{+10}_{-5}	1.20(88)
104	990106	51184.711	$1.088^{+0.002}_{-0.002}$	$38.06^{+0.27}_{-0.28}$	$3.89^{+0.04}_{-0.04}$	$51.07^{+5.08}_{-4.71}$	$8.69^{+0.08}_{-0.09}$	$4.52^{+0.20}_{-0.20}$	6.5(fixed)	$0.13^{+0.21}_{-0.13}$	4^{+6}_{-4}	1.70(79)
105	990107	51185.126	$1.066^{+0.003}_{-0.003}$	$40.69^{+0.53}_{-0.58}$	$3.51^{+0.08}_{-0.10}$	$23.76^{+6.36}_{-5.67}$	$9.08^{+0.14}_{-0.15}$	$4.32^{+0.32}_{-0.33}$	$7.33^{+0.20}_{-0.26}$	$0.58^{+0.22}_{-0.24}$	37^{+14}_{-15}	1.44(86)
106	990107	51185.846	$1.097^{+0.002}_{-0.002}$	$37.24^{+0.33}_{-0.35}$	$4.03^{+0.04}_{-0.05}$	$57.12^{+7.37}_{-6.85}$	$8.65^{+0.11}_{-0.11}$	$4.25^{+0.29}_{-0.28}$	6.5(fixed)	$0.00^{+0.20}_{-0.00}$	0^{+6}_{-0}	1.96(74)
107	990109	51187.126	$1.096^{+0.003}_{-0.003}$	$37.56^{+0.37}_{-0.38}$	$3.96^{+0.07}_{-0.07}$	$49.58^{+7.84}_{-7.28}$	$8.91^{+0.11}_{-0.11}$	$4.52^{+0.38}_{-0.31}$	6.5(fixed)	$0.00^{+0.23}_{-0.00}$	0^{+7}_{-0}	1.93(62)
108	990110	51188.194	$1.097^{+0.003}_{-0.003}$	$37.35^{+0.37}_{-0.37}$	$4.13^{+0.06}_{-0.06}$	$66.74^{+8.93}_{-8.49}$	$8.81^{+0.12}_{-0.13}$	$3.91^{+0.32}_{-0.34}$	6.5(fixed)	$0.00^{+0.17}_{-0.00}$	0^{+5}_{-0}	1.31(62)
109	990110	51188.731	$1.106^{+0.002}_{-0.003}$	$36.59^{+0.32}_{-0.33}$	$4.52^{+0.05}_{-0.05}$	$110.50^{+11.73}_{-11.16}$	$8.75^{+0.22}_{-0.22}$	$2.65^{+0.48}_{-0.50}$	6.5(fixed)	$0.00^{+0.08}_{-0.00}$	0^{+2}_{-0}	1.00(88)
110	990112	51190.054	$1.105^{+0.002}_{-0.003}$	$37.01^{+0.28}_{-0.28}$	$4.27^{+0.05}_{-0.06}$	$76.10^{+7.94}_{-7.72}$	$8.88^{+0.13}_{-0.14}$	$3.86^{+0.39}_{-0.41}$	6.5(fixed)	$0.00^{+0.06}_{-0.00}$	0^{+1}_{-0}	1.53(88)
111	990113	51191.485	$1.120^{+0.002}_{-0.002}$	$36.06^{+0.31}_{-0.32}$	$4.46^{+0.04}_{-0.04}$	$101.30^{+10.26}_{-9.98}$	$8.54^{+0.22}_{-0.20}$	$2.23^{+0.44}_{-0.45}$	6.5(fixed)	$0.00^{+0.08}_{-0.00}$	0^{+2}_{-0}	1.49(88)
112	990114	51192.187	$1.115^{+0.002}_{-0.003}$	$36.57^{+0.34}_{-0.33}$	$4.12^{+0.04}_{-0.04}$	$73.25^{+7.89}_{-8.04}$	$8.72^{+0.12}_{-0.12}$	$3.78^{+0.29}_{-0.31}$	6.5(fixed)	$0.00^{+0.13}_{-0.00}$	0^{+4}_{-0}	1.53(75)
113	990114	51192.593	$1.112^{+0.002}_{-0.003}$	$36.35^{+0.34}_{-0.33}$	$4.33^{+0.05}_{-0.05}$	$95.48^{+10.14}_{-9.94}$	$8.89^{+0.19}_{-0.20}$	$2.72^{+0.38}_{-0.41}$	6.5(fixed)	$0.00^{+0.09}_{-0.00}$	0^{+2}_{-0}	0.86(88)
114	990116	51194.500	$1.125^{+0.004}_{-0.002}$	$36.03^{+0.20}_{-0.53}$	$4.25^{+0.06}_{-0.03}$	$86.47^{+14.40}_{-5.80}$	$8.74^{+0.13}_{-0.21}$	$3.01^{+0.50}_{-0.30}$	6.5(fixed)	$0.00^{+0.12}_{-0.00}$	0^{+3}_{-0}	1.11(88)
115	990118	51196.051	$1.121^{+0.002}_{-0.003}$	$36.46^{+0.33}_{-0.34}$	$4.15^{+0.04}_{-0.04}$	$80.63^{+8.53}_{-7.93}$	$8.69^{+0.12}_{-0.13}$	$3.44^{+0.30}_{-0.29}$	6.5(fixed)	$0.00^{+0.14}_{-0.00}$	0^{+4}_{-0}	2.33(87)
116	990118	51196.522	$1.119^{+0.002}_{-0.002}$	$36.29^{+0.35}_{-0.30}$	$4.52^{+0.05}_{-0.05}$	$119.90^{+10.81}_{-12.37}$	$8.69^{+0.25}_{-0.24}$	$2.16^{+0.46}_{-0.51}$	6.5(fixed)	$0.00^{+0.07}_{-0.00}$	0^{+2}_{-0}	1.40(88)
117	990120	51198.051	$1.115^{+0.002}_{-0.002}$	$37.05^{+0.35}_{-0.35}$	$3.98^{+0.04}_{-0.04}$	$65.52^{+7.34}_{-7.37}$	$8.71^{+0.11}_{-0.11}$	$3.80^{+0.25}_{-0.26}$	6.5(fixed)	$0.00^{+0.25}_{-0.00}$	0^{+7}_{-0}	1.76(79)
118	990122	51200.383	$1.065^{+0.005}_{-0.004}$	$42.15^{+0.44}_{-0.46}$	$2.83^{+0.05}_{-0.05}$	$19.01^{+2.99}_{-2.79}$	$8.89^{+0.11}_{-0.10}$	$2.36^{+0.17}_{-0.18}$	$6.93^{+0.19}_{-0.20}$	$1.69^{+0.42}_{-0.42}$	61^{+15}_{-15}	0.56(87)
119	990123	51201.783	$1.066^{+0.004}_{-0.005}$	$41.92^{+0.38}_{-0.39}$	$2.65^{+0.03}_{-0.04}$	$19.45^{+2.06}_{-1.95}$	$8.86^{+0.09}_{-0.09}$	$1.82^{+0.12}_{-0.12}$	$6.84^{+0.14}_{-0.14}$	$2.29^{+0.40}_{-0.41}$	69^{+12}_{-12}	1.13(87)
120	990125	51203.249	$1.110^{+0.004}_{-0.004}$	$38.11^{+0.51}_{-0.57}$	$3.79^{+0.04}_{-0.05}$	$54.11^{+8.08}_{-7.37}$	$8.89^{+0.16}_{-0.17}$	$2.90^{+0.37}_{-0.34}$	$7.45^{+0.25}_{-0.31}$	$0.54^{+0.24}_{-0.26}$	31^{+13}_{-15}	0.99(87)
121	990126	51204.248	$1.126^{+0.003}_{-0.003}$	$36.47^{+0.45}_{-0.46}$	$4.02^{+0.05}_{-0.05}$	$77.35^{+9.96}_{-9.52}$	$8.58^{+0.16}_{-0.15}$	$3.62^{+0.34}_{-0.35}$	6.5(fixed)	$0.00^{+0.32}_{-0.00}$	0^{+9}_{-0}	0.84(88)
122	990127	51205.850	$1.122^{+0.002}_{-0.003}$	$36.87^{+0.36}_{-0.37}$	$3.97^{+0.04}_{-0.04}$	$72.68^{+7.95}_{-7.23}$	$8.65^{+0.12}_{-0.10}$	$3.79^{+0.25}_{-0.25}$	6.5(fixed)	$0.00^{+0.32}_{-0.00}$	0^{+9}_{-0}	1.68(87)
123	990128	51206.781	$1.128^{+0.003}_{-0.002}$	$36.17^{+0.33}_{-0.35}$	$4.21^{+0.04}_{-0.04}$	$89.98^{+9.25}_{-8.56}$	$8.65^{+0.14}_{-0.15}$	$3.08^{+0.34}_{-0.33}$	6.5(fixed)	$0.00^{+0.10}_{-0.00}$	0^{+3}_{-0}	1.68(87)
124	990130	51208.179	$1.088^{+0.003}_{-0.003}$	$40.12^{+0.42}_{-0.45}$	$3.28^{+0.05}_{-0.05}$	$28.88^{+4.11}_{-3.81}$	$8.85^{+0.11}_{-0.11}$	$2.88^{+0.19}_{-0.20}$	$7.15^{+0.14}_{-0.17}$	$0.97^{+0.24}_{-0.25}$	43^{+10}_{-11}	1.25(87)
125	990130	51208.845	$1.101^{+0.004}_{-0.003}$	$38.78^{+0.49}_{-0.53}$	$3.72^{+0.05}_{-0.05}$	$45.86^{+7.21}_{-6.66}$	$9.05^{+0.15}_{-0.16}$	$3.09^{+0.31}_{-0.31}$	$7.47^{+0.19}_{-0.22}$	$0.63^{+0.22}_{-0.24}$	38^{+13}_{-14}	1.32(86)
126	990131	51209.711	$1.112^{+0.002}_{-0.002}$	$37.49^{+0.35}_{-0.36}$	$3.87^{+0.04}_{-0.04}$	$57.41^{+7.02}_{-6.49}$	$8.73^{+0.11}_{-0.10}$	$3.80^{+0.23}_{-0.24}$	6.5(fixed)	$0.00^{+0.29}_{-0.00}$	0^{+8}_{-0}	1.33(87)
127	990202	51211.709	$1.107^{+0.002}_{-0.003}$	$37.48^{+0.36}_{-0.36}$	$3.91^{+0.04}_{-0.05}$	$59.08^{+7.11}_{-6.81}$	$8.73^{+0.12}_{-0.10}$	$4.15^{+0.24}_{-0.13}$	6.5(fixed)	$0.00^{+0.31}_{-0.00}$	0^{+9}_{-0}	1.23(88)
128	990203	51212.775	$1.105^{+0.002}_{-0.003}$	$37.58^{+0.36}_{-0.36}$	$3.87^{+0.04}_{-0.04}$	$57.16^{+6.66}_{-6.50}$	$8.66^{+0.10}_{-0.10}$	$3.81^{+0.22}_{-0.23}$	6.5(fixed)	$0.00^{+0.16}_{-0.00}$	0^{+4}_{-0}	1.07(88)
129	990204	51213.774	$1.090^{+0.003}_{-0.003}$	$39.19^{+0.51}_{-0.55}$	$3.70^{+0.05}_{-0.06}$	$40.42^{+7.00}_{-6.55}$	$8.94^{+0.15}_{-0.15}$	$3.31^{+0.35}_{-0.34}$	$7.44^{+0.21}_{-0.25}$	$0.58^{+0.22}_{-0.24}$	36^{+13}_{-15}	1.16(87)
130	990205	51214.975	$1.066^{+0.003}_{-0.003}$	$41.51^{+0.37}_{-0.39}$	$2.95^{+0.05}_{-0.05}$	$17.95^{+2.81}_{-2.65}$	$8.87^{+0.10}_{-0.09}$	$2.73^{+0.17}_{-0.18}$	$7.01^{+0.18}_{-0.19}$	$1.22^{+0.30}_{-0.30}$	51^{+12}_{-12}	0.81(87)
131	990206	51215.839	$1.059^{+0.003}_{-0.003}$	$41.94^{+0.34}_{-0.35}$	$2.97^{+0.04}_{-0.05}$	$17.19^{+2.53}_{-2.38}$	$8.91^{+0.09}_{-0.09}$	$2.76^{+0.16}_{-0.17}$	$6.99^{+0.17}_{-0.19}$	$1.19^{+0.28}_{-0.28}$	51^{+12}_{-12}	1.00(87)
132	990207	51216.838	$1.077^{+0.004}_{-0.003}$	$39.60^{+0.53}_{-0.55}$	$3.58^{+0.05}_{-0.05}$	$38.74^{+6.30}_{-5.91}$	$8.80^{+0.12}_{-0.12}$	$3.52^{+0.27}_{-0.28}$	$7.11^{+0.25}_{-0.33}$	$0.65^{+0.26}_{-0.27}$	32^{+12}_{-13}	1.07(87)
133	990208	51217.704	$1.098^{+0.002}_{-0.003}$	$37.75^{+0.36}_{-0.36}$	$3.92^{+0.04}_{-0.04}$	$57.68^{+6.84}_{-6.63}$	$8.66^{+0.12}_{-0.12}$	$4.21^{+0.27}_{-0.27}$	6.5(fixed)	$0.16^{+0.30}_{-0.16}$	4^{+9}_{-4}	1.29(88)
134	990210	51219.053	$1.083^{+0.003}_{-0.002}$	$39.15^{+0.36}_{-0.38}$	$3.78^{+0.04}_{-0.05}$	$39.35^{+5.13}_{-4.92}$	$9.04^{+0.12}_{-0.12}$	$3.56^{+0.27}_{-0.28}$	$7.42^{+0.14}_{-0.16}$	$0.55^{+0.15}_{-0.15}$	37^{+9}_{-10}	2.53(81)
135	990211	51220.508	$1.071^{+0.005}_{-0.004}$	$40.06^{+0.64}_{-0.72}$	$3.66^{+0.07}_{-0.08}$	$35.29^{+8.62}_{-7.66}$	$8.98^{+0.17}_{-0.18}$	$3.86^{+0.42}_{-0.41}$	$7.34^{+0.25}_{-0.34}$	$0.60^{+0.27}_{-0.30}$	38^{+17}_{-19}	0.61(86)

TABLE 2—*Continued*

Observation Number	Date (UT)	MJD[a]	T_{in} (keV)	R^{*}_{in}[b] (km)	Photon Index	Power-Law[c] Norm.	Fe Edge[d] (keV)	τ_{Fe}[d]	E_{line}[e] (keV)	$N_{line} \times 100$[e,f]	Line Equivalent Width (eV)	χ^2_ν (dof)
136	990211	51220.836	$1.078^{+0.004}_{-0.004}$	$39.33^{+0.61}_{-0.67}$	$3.62^{+0.07}_{-0.08}$	$33.35^{+7.85}_{-7.03}$	$8.94^{+0.17}_{-0.18}$	$3.60^{+0.39}_{-0.38}$	$7.30^{+0.26}_{-0.38}$	$0.56^{+0.27}_{-0.30}$	34^{+16}_{-18}	0.75(86)
137	990212	51221.567	$1.093^{+0.003}_{-0.002}$	$37.45^{+0.36}_{-0.37}$	$4.00^{+0.05}_{-0.05}$	$58.63^{+7.53}_{-7.10}$	$8.72^{+0.12}_{-0.10}$	$4.70^{+0.28}_{-0.28}$	6.5(fixed)	$0.00^{+0.26}_{-0.00}$	0^{+8}_{-0}	1.11(87)
138	990214	51223.766	$1.089^{+0.002}_{-0.002}$	$37.35^{+0.33}_{-0.35}$	$4.05^{+0.04}_{-0.04}$	$62.71^{+7.24}_{-7.00}$	$8.68^{+0.12}_{-0.10}$	$4.56^{+0.26}_{-0.28}$	6.5(fixed)	$0.03^{+0.28}_{-0.03}$	1^{+9}_{-1}	1.29(87)
139	990215	51224.699	$1.086^{+0.002}_{-0.002}$	$37.33^{+0.38}_{-0.33}$	$4.06^{+0.05}_{-0.05}$	$59.55^{+7.57}_{-7.14}$	$8.71^{+0.12}_{-0.09}$	$4.78^{+0.26}_{-0.32}$	6.5(fixed)	$0.00^{+0.23}_{-0.00}$	0^{+7}_{-0}	1.38(87)
140	990217	51226.296	$1.085^{+0.002}_{-0.003}$	$37.62^{+0.44}_{-0.41}$	$3.98^{+0.06}_{-0.06}$	$50.92^{+8.52}_{-7.72}$	$8.61^{+0.14}_{-0.12}$	$4.56^{+0.33}_{-0.39}$	6.5(fixed)	$0.00^{+0.30}_{-0.00}$	0^{+10}_{-0}	0.91(88)
141	990218	51227.837	$1.080^{+0.002}_{-0.003}$	$37.50^{+0.35}_{-0.34}$	$4.06^{+0.05}_{-0.05}$	$57.43^{+7.14}_{-6.90}$	$8.69^{+0.11}_{-0.09}$	$4.87^{+0.27}_{-0.31}$	6.5(fixed)	$0.01^{+0.26}_{-0.01}$	0^{+9}_{-0}	1.84(87)
142	990219	51228.696	$1.076^{+0.002}_{-0.002}$	$37.61^{+0.33}_{-0.35}$	$4.01^{+0.04}_{-0.05}$	$54.04^{+6.83}_{-6.53}$	$8.60^{+0.12}_{-0.09}$	$4.83^{+0.27}_{-0.31}$	6.5(fixed)	$0.03^{+0.27}_{-0.03}$	1^{+9}_{-1}	1.83(87)
143	990221	51230.424	$1.051^{+0.003}_{-0.003}$	$40.33^{+0.48}_{-0.55}$	$3.74^{+0.07}_{-0.07}$	$29.34^{+6.55}_{-5.84}$	$8.94^{+0.15}_{-0.15}$	$3.96^{+0.41}_{-0.40}$	$7.45^{+0.15}_{-0.17}$	$0.60^{+0.17}_{-0.19}$	49^{+14}_{-16}	0.99(87)
144	990222	51231.293	$1.037^{+0.003}_{-0.003}$	$41.58^{+0.47}_{-0.47}$	$3.36^{+0.06}_{-0.06}$	$25.35^{+4.49}_{-4.22}$	$8.67^{+0.09}_{-0.09}$	$4.20^{+0.20}_{-0.22}$	$6.61^{+0.31}_{-0.30}$	$0.68^{+0.31}_{-0.30}$	27^{+12}_{-11}	0.93(87)
145	990222	51231.422	$1.032^{+0.002}_{-0.003}$	$42.34^{+0.41}_{-0.44}$	$3.23^{+0.06}_{-0.07}$	$16.94^{+3.57}_{-3.22}$	$8.83^{+0.10}_{-0.10}$	$3.84^{+0.23}_{-0.25}$	$7.07^{+0.17}_{-0.20}$	$0.84^{+0.22}_{-0.23}$	50^{+13}_{-13}	0.92(87)
146	990223	51232.252	$1.017^{+0.005}_{-0.004}$	$43.66^{+0.40}_{-0.40}$	$2.58^{+0.04}_{-0.04}$	$11.40^{+1.47}_{-1.33}$	$8.67^{+0.10}_{-0.09}$	$2.08^{+0.15}_{-0.15}$	$6.87^{+0.13}_{-0.13}$	$1.66^{+0.31}_{-0.32}$	71^{+13}_{-13}	0.73(87)
147	990223	51232.860	$1.007^{+0.005}_{-0.005}$	$44.80^{+0.44}_{-0.44}$	$2.55^{+0.04}_{-0.04}$	$12.37^{+1.48}_{-1.34}$	$8.76^{+0.10}_{-0.10}$	$1.89^{+0.13}_{-0.14}$	$6.82^{+0.12}_{-0.12}$	$1.99^{+0.33}_{-0.33}$	79^{+13}_{-13}	0.85(87)
148	990224	51233.835	$1.020^{+0.004}_{-0.005}$	$43.71^{+0.40}_{-0.40}$	$2.47^{+0.04}_{-0.04}$	$9.16^{+1.06}_{-0.99}$	$8.77^{+0.09}_{-0.09}$	$1.92^{+0.14}_{-0.14}$	$6.86^{+0.14}_{-0.14}$	$1.64^{+0.30}_{-0.30}$	68^{+12}_{-12}	0.94(86)
149	990226	51235.199	$1.009^{+0.005}_{-0.005}$	$44.18^{+0.43}_{-0.42}$	$2.47^{+0.03}_{-0.03}$	$10.47^{+1.00}_{-0.94}$	$8.80^{+0.09}_{-0.09}$	$1.69^{+0.12}_{-0.12}$	$6.88^{+0.11}_{-0.11}$	$2.00^{+0.30}_{-0.29}$	84^{+12}_{-12}	0.64(86)
150	990228	51237.619	$1.005^{+0.003}_{-0.002}$	$43.38^{+0.36}_{-0.37}$	$3.04^{+0.05}_{-0.06}$	$12.71^{+2.27}_{-2.06}$	$8.65^{+0.08}_{-0.08}$	$3.66^{+0.19}_{-0.20}$	$6.81^{+0.17}_{-0.18}$	$0.97^{+0.24}_{-0.24}$	52^{+12}_{-12}	1.11(87)
151	990302	51239.081	$1.001^{+0.004}_{-0.005}$	$43.95^{+0.39}_{-0.38}$	$2.48^{+0.04}_{-0.04}$	$6.41^{+0.83}_{-0.76}$	$8.76^{+0.09}_{-0.08}$	$2.28^{+0.15}_{-0.16}$	$6.90^{+0.13}_{-0.13}$	$1.38^{+0.24}_{-0.24}$	73^{+12}_{-12}	0.91(86)
152	990303	51240.063	$0.999^{+0.005}_{-0.004}$	$44.27^{+0.41}_{-0.41}$	$2.48^{+0.04}_{-0.04}$	$7.42^{+0.91}_{-0.85}$	$8.82^{+0.10}_{-0.09}$	$2.01^{+0.14}_{-0.15}$	$6.88^{+0.11}_{-0.11}$	$1.72^{+0.26}_{-0.26}$	85^{+12}_{-12}	0.85(86)
153	990304	51241.828	$0.981^{+0.006}_{-0.006}$	$40.35^{+0.51}_{-0.50}$	$2.65^{+0.02}_{-0.02}$	$24.06^{+1.49}_{-1.45}$	$8.96^{+0.10}_{-0.09}$	$1.22^{+0.08}_{-0.08}$	$6.96^{+0.10}_{-0.11}$	$1.99^{+0.29}_{-0.29}$	85^{+12}_{-12}	0.55(86)
154	993005	51242.507	$0.965^{+0.006}_{-0.006}$	$40.18^{+0.56}_{-0.55}$	$2.65^{+0.02}_{-0.02}$	$25.53^{+1.64}_{-1.57}$	$9.04^{+0.12}_{-0.11}$	$1.12^{+0.07}_{-0.08}$	$7.00^{+0.10}_{-0.10}$	$2.17^{+0.28}_{-0.29}$	97^{+12}_{-12}	0.73(87)
155	990307	51244.496	$1.045^{+0.009}_{-0.008}$	$29.86^{+0.66}_{-0.68}$	$2.70^{+0.02}_{-0.02}$	$44.47^{+2.52}_{-2.34}$	$9.05^{+0.16}_{-0.16}$	$0.68^{+0.07}_{-0.07}$	$7.12^{+0.12}_{-0.13}$	$2.05^{+0.38}_{-0.40}$	69^{+13}_{-13}	0.59(87)
156	990308	51245.353	$1.035^{+0.010}_{-0.011}$	$25.93^{+0.68}_{-0.70}$	$2.65^{+0.02}_{-0.02}$	$43.71^{+2.19}_{-2.04}$	$8.89^{+0.15}_{-0.14}$	$0.66^{+0.07}_{-0.07}$	$7.06^{+0.14}_{-0.15}$	$1.78^{+0.39}_{-0.41}$	59^{+13}_{-13}	0.41(87)
157	990309	51246.414	$0.997^{+0.011}_{-0.011}$	$33.16^{+0.88}_{-0.88}$	$2.71^{+0.02}_{-0.02}$	$40.73^{+2.88}_{-2.68}$	$9.00^{+0.16}_{-0.15}$	$0.91^{+0.09}_{-0.09}$	$6.98^{+0.16}_{-0.17}$	$2.17^{+0.49}_{-0.50}$	77^{+17}_{-17}	0.37(39)[g]
158	990310	51247.979	$1.005^{+0.015}_{-0.015}$	$28.36^{+0.94}_{-0.94}$	$2.61^{+0.02}_{-0.02}$	$37.86^{+2.56}_{-2.35}$	$9.01^{+0.20}_{-0.19}$	$0.70^{+0.09}_{-0.09}$	$7.01^{+0.15}_{-0.16}$	$2.28^{+0.50}_{-0.52}$	78^{+17}_{-18}	0.42(39)[g]
159	990311	51248.091	$1.008^{+0.013}_{-0.014}$	$29.01^{+0.96}_{-0.97}$	$2.65^{+0.03}_{-0.03}$	$39.55^{+3.01}_{-2.70}$	$9.01^{+0.22}_{-0.21}$	$0.69^{+0.10}_{-0.09}$	$7.11^{+0.16}_{-0.18}$	$2.04^{+0.50}_{-0.53}$	74^{+18}_{-19}	0.44(39)[g]
160	990312	51249.400	$0.987^{+0.015}_{-0.016}$	$26.48^{+0.95}_{-0.96}$	$2.63^{+0.02}_{-0.02}$	$38.98^{+2.37}_{-2.20}$	$8.80^{+0.17}_{-0.17}$	$0.72^{+0.08}_{-0.08}$	$6.90^{+0.16}_{-0.17}$	$1.89^{+0.46}_{-0.48}$	65^{+15}_{-16}	0.31(87)
161	990313	51250.693	$0.800^{+0.020}_{-0.021}$	$35.20^{+2.03}_{-1.81}$	$2.46^{+0.02}_{-0.02}$	$18.81^{+1.09}_{-1.02}$	$8.51^{+0.18}_{-0.17}$	$0.83^{+0.09}_{-0.08}$	$6.69^{+0.15}_{-0.17}$	$1.44^{+0.38}_{-0.40}$	75^{+19}_{-21}	0.31(39)[g]
162	990316	51253.225	$0.940^{+0.015}_{-0.016}$	$30.23^{+1.08}_{-1.04}$	$2.57^{+0.03}_{-0.03}$	$28.74^{+2.16}_{-1.99}$	$8.89^{+0.21}_{-0.20}$	$0.79^{+0.09}_{-0.09}$	$6.96^{+0.14}_{-0.16}$	$2.00^{+0.44}_{-0.47}$	86^{+19}_{-20}	0.50(39)[g]
163	990317	51254.092	$0.865^{+0.016}_{-0.016}$	$34.32^{+1.37}_{-1.26}$	$2.45^{+0.02}_{-0.02}$	$19.03^{+1.28}_{-1.19}$	$8.75^{+0.17}_{-0.17}$	$0.89^{+0.09}_{-0.09}$	$6.82^{+0.16}_{-0.18}$	$1.51^{+0.38}_{-0.40}$	76^{+19}_{-20}	0.48(39)[g]
164	990318	51255.091	$0.868^{+0.010}_{-0.010}$	$43.65^{+1.17}_{-1.12}$	$2.53^{+0.03}_{-0.03}$	$10.47^{+1.09}_{-1.09}$	$8.78^{+0.17}_{-0.16}$	$1.39^{+0.13}_{-0.13}$	$6.80^{+0.17}_{-0.18}$	$1.33^{+0.29}_{-0.30}$	105^{+23}_{-23}	0.34(39)[g]
165	990320	51257.362	$0.848^{+0.007}_{-0.007}$	$46.76^{+0.91}_{-0.88}$	$2.40^{+0.06}_{-0.06}$	$4.28^{+0.71}_{-0.61}$	$8.67^{+0.18}_{-0.18}$	$1.81^{+0.19}_{-0.19}$	$6.76^{+0.15}_{-0.17}$	$0.94^{+0.20}_{-0.21}$	109^{+23}_{-24}	0.50(39)[g]
166	990321	51258.088	$0.846^{+0.007}_{-0.007}$	$44.29^{+0.90}_{-0.87}$	$2.52^{+0.04}_{-0.04}$	$7.07^{+0.82}_{-0.73}$	$8.75^{+0.16}_{-0.16}$	$1.45^{+0.14}_{-0.14}$	$6.81^{+0.16}_{-0.17}$	$0.85^{+0.19}_{-0.20}$	92^{+20}_{-21}	0.52(39)[g]
167	990321	51258.496	$0.834^{+0.007}_{-0.008}$	$44.66^{+0.95}_{-0.91}$	$2.53^{+0.04}_{-0.04}$	$7.46^{+0.79}_{-0.71}$	$8.61^{+0.14}_{-0.14}$	$1.54^{+0.13}_{-0.13}$	$6.73^{+0.16}_{-0.17}$	$0.84^{+0.19}_{-0.20}$	88^{+20}_{-21}	0.56(39)[g]
168	990321	51258.975	$0.813^{+0.009}_{-0.009}$	$43.61^{+1.11}_{-1.05}$	$2.50^{+0.03}_{-0.03}$	$8.64^{+0.75}_{-0.69}$	$8.57^{+0.13}_{-0.12}$	$1.53^{+0.11}_{-0.11}$	$6.74^{+0.14}_{-0.16}$	$0.91^{+0.21}_{-0.22}$	91^{+20}_{-21}	0.64(39)[g]
169	990322	51259.252	$0.823^{+0.009}_{-0.009}$	$42.30^{+1.05}_{-1.00}$	$2.46^{+0.04}_{-0.04}$	$7.47^{+0.73}_{-0.67}$	$8.87^{+0.15}_{-0.15}$	$1.37^{+0.11}_{-0.11}$	$6.80^{+0.14}_{-0.14}$	$1.04^{+0.19}_{-0.20}$	112^{+20}_{-21}	1.08(39)[g]
170[h]	990323	51260.552	$0.829^{+0.011}_{-0.011}$	$47.83^{+1.98}_{-1.83}$	$2.31^{+0.05}_{-0.05}$	$2.11^{+0.34}_{-0.28}$	$8.29^{+0.18}_{-0.18}$	$1.72^{+0.22}_{-0.22}$	6.5(fixed)	$0.62^{+0.24}_{-0.23}$	82^{+31}_{-31}	1.18(72)
171	990324	51261.766	$0.807^{+0.011}_{-0.011}$	$49.33^{+2.05}_{-1.92}$	$2.31^{+0.05}_{-0.05}$	$2.01^{+0.31}_{-0.26}$	$8.34^{+0.17}_{-0.18}$	$1.76^{+0.20}_{-0.20}$	6.5(fixed)	$0.72^{+0.21}_{-0.21}$	107^{+30}_{-31}	1.02(72)
172	990326	51263.108	$0.806^{+0.015}_{-0.015}$	$47.97^{+2.88}_{-2.70}$	$2.16^{+0.06}_{-0.06}$	$1.38^{+0.25}_{-0.21}$	$8.65^{+0.22}_{-0.23}$	$1.65^{+0.23}_{-0.23}$	6.5(fixed)	$0.76^{+0.25}_{-0.26}$	124^{+41}_{-42}	0.98(32)[g]
173	990327	51264.748	$0.768^{+0.010}_{-0.009}$	$48.84^{+1.88}_{-1.96}$	$2.27^{+0.04}_{-0.04}$	$1.38^{+0.17}_{-0.15}$	$8.35^{+0.16}_{-0.16}$	$1.75^{+0.17}_{-0.17}$	6.5(fixed)	$0.51^{+0.13}_{-0.14}$	114^{+30}_{-31}	0.93(72)
174	990328	51265.613	$0.759^{+0.010}_{-0.009}$	$48.69^{+2.02}_{-1.92}$	$2.24^{+0.04}_{-0.04}$	$1.41^{+0.16}_{-0.14}$	$8.38^{+0.14}_{-0.15}$	$1.80^{+0.16}_{-0.15}$	6.5(fixed)	$0.48^{+0.13}_{-0.13}$	112^{+30}_{-31}	2.07(72)
175	990329	51266.880	$0.754^{+0.013}_{-0.012}$	$47.10^{+2.68}_{-2.48}$	$2.29^{+0.07}_{-0.06}$	$0.91^{+0.18}_{-0.15}$	$8.48^{+0.23}_{-0.24}$	$1.77^{+0.25}_{-0.24}$	6.5(fixed)	$0.36^{+0.14}_{-0.14}$	113^{+43}_{-43}	0.94(32)[g]
176	990330	51267.612	$0.734^{+0.014}_{-0.014}$	$49.31^{+3.19}_{-3.02}$	$2.35^{+0.06}_{-0.05}$	$1.71^{+0.35}_{-0.25}$	$8.13^{+0.21}_{-0.23}$	$1.94^{+0.28}_{-0.24}$	6.5(fixed)	$0.33^{+0.17}_{-0.20}$	87^{+46}_{-54}	0.69(32)[g]
177	990401	51269.677	$0.717^{+0.009}_{-0.010}$	$48.62^{+2.26}_{-2.08}$	$2.38^{+0.04}_{-0.03}$	$1.82^{+0.18}_{-0.16}$	$8.41^{+0.14}_{-0.14}$	$1.78^{+0.13}_{-0.13}$	6.5(fixed)	$0.38^{+0.10}_{-0.10}$	114^{+30}_{-30}	1.22(72)
178	990402	51270.742	$0.720^{+0.014}_{-0.014}$	$41.60^{+2.64}_{-2.49}$	$2.41^{+0.03}_{-0.03}$	$3.14^{+0.27}_{-0.23}$	$8.51^{+0.14}_{-0.15}$	$1.50^{+0.11}_{-0.11}$	6.5(fixed)	$0.55^{+0.13}_{-0.14}$	124^{+28}_{-30}	1.16(72)
179	990403	51271.408	$0.717^{+0.015}_{-0.015}$	$40.40^{+2.79}_{-2.51}$	$2.38^{+0.03}_{-0.03}$	$2.97^{+0.26}_{-0.23}$	$8.44^{+0.14}_{-0.14}$	$1.62^{+0.12}_{-0.11}$	6.5(fixed)	$0.46^{+0.13}_{-0.13}$	105^{+30}_{-31}	1.26(72)

TABLE 2—*Continued*

Observation Number	Date (UT)	MJD[a]	T_{in} (keV)	R^{*}_{in}[b] (km)	Photon Index	Power-Law[c] Norm.	Fe Edge[d] (keV)	τ_{Fe}[d]	E_{line}[e] (keV)	$N_{line} \times 100$[e,f]	Line Equivalent Width (eV)	χ^2_ν (dof)
180	990405	51273.541	$0.674^{+0.008}_{-0.009}$	$49.96^{+2.32}_{-2.11}$	$2.30^{+0.04}_{-0.04}$	$1.05^{+0.11}_{-0.09}$	$8.46^{+0.13}_{-0.13}$	$1.90^{+0.13}_{-0.12}$	6.5(fixed)	$0.26^{+0.07}_{-0.07}$	123^{+30}_{-32}	1.30(72)
181	990406	51274.471	$0.664^{+0.008}_{-0.008}$	$49.78^{+2.23}_{-2.11}$	$2.24^{+0.05}_{-0.04}$	$0.75^{+0.09}_{-0.08}$	$8.28^{+0.16}_{-0.17}$	$1.78^{+0.16}_{-0.15}$	6.5(fixed)	$0.22^{+0.06}_{-0.07}$	128^{+34}_{-38}	1.29(72)
182	990408	51276.278	$0.644^{+0.012}_{-0.012}$	$50.57^{+3.18}_{-3.14}$	$2.27^{+0.11}_{-0.09}$	$0.46^{+0.16}_{-0.10}$	$8.06^{+0.29}_{-0.32}$	$2.21^{+0.40}_{-0.32}$	6.5(fixed)	$0.13^{+0.07}_{-0.09}$	124^{+66}_{-85}	0.72(32)[g]
183	990409	51277.401	$0.627^{+0.008}_{-0.008}$	$51.28^{+2.42}_{-2.18}$	$2.31^{+0.05}_{-0.05}$	$0.57^{+0.08}_{-0.07}$	$8.27^{+0.16}_{-0.18}$	$1.84^{+0.18}_{-0.17}$	6.5(fixed)	$0.14^{+0.04}_{-0.05}$	125^{+37}_{-42}	1.21(72)
184	990410	51278.686	$0.611^{+0.013}_{-0.018}$	$52.26^{+5.20}_{-3.89}$	$2.32^{+0.15}_{-0.08}$	$0.58^{+0.27}_{-0.11}$	$8.07^{+0.32}_{-0.60}$	$1.68^{+0.27}_{-0.29}$	6.5(fixed)	$0.14^{+0.06}_{-0.14}$	136^{+63}_{-136}	0.93(32)[g]
185	990411	51279.531	$0.558^{+0.019}_{-0.020}$	$66.97^{+9.90}_{-7.90}$	$2.59^{+0.07}_{-0.08}$	$1.00^{+0.20}_{-0.18}$	$7.05^{+0.23}_{-0.21}$	$2.58^{+0.30}_{-0.29}$	6.5(fixed)	$0.00^{+0.02}_{-0.00}$	0^{+17}_{-0}	1.25(31)[g]
186	990412	51280.544	$0.572^{+0.033}_{-0.016}$	$57.55^{+6.40}_{-9.89}$	$2.47^{+0.08}_{-0.23}$	$0.62^{+0.12}_{-0.28}$	$7.55^{+0.78}_{-0.22}$	$2.40^{+0.26}_{-0.71}$	6.5(fixed)	$0.00^{+0.13}_{-0.00}$	0^{+168}_{-0}	1.02(32)[g]
187	990415	51283.224	$0.515^{+0.017}_{-0.017}$	$72.28^{+10.85}_{-8.55}$	$2.42^{+0.08}_{-0.08}$	$0.54^{+0.10}_{-0.09}$	$7.38^{+0.22}_{-0.24}$	$2.31^{+0.29}_{-0.29}$	6.5(fixed)	$0.00^{+0.02}_{-0.00}$	0^{+37}_{-0}	1.08(32)[g]
188	990417	51285.197	$0.476^{+0.017}_{-0.018}$	$85.61^{+15.29}_{-11.84}$	$2.46^{+0.06}_{-0.06}$	$0.54^{+0.08}_{-0.07}$	$7.18^{+0.20}_{-0.21}$	$2.11^{+0.25}_{-0.24}$	6.5(fixed)	$0.00^{+0.01}_{-0.00}$	0^{+25}_{-0}	0.77(32)[g]
189	990418	51286.058	$0.465^{+0.017}_{-0.020}$	$87.61^{+18.47}_{-15.51}$	$2.43^{+0.06}_{-0.05}$	$0.55^{+0.08}_{-0.08}$	$7.31^{+0.28}_{-0.26}$	$1.78^{+0.23}_{-0.24}$	6.5(fixed)	$0.00^{+0.03}_{-0.00}$	0^{+42}_{-0}	1.28(31)[g]
190	990419	51287.257	$0.456^{+0.018}_{-0.022}$	$87.19^{+21.16}_{-13.36}$	$2.43^{+0.07}_{-0.07}$	$0.49^{+0.09}_{-0.06}$	$7.08^{+0.38}_{-0.46}$	$1.36^{+0.22}_{-0.23}$	6.5(fixed)	$0.00^{+0.01}_{-0.00}$	0^{+13}_{-0}	1.50(72)
191	990420	51288.382	$0.412^{+0.016}_{-0.016}$	$125.64^{+25.76}_{-20.65}$	$2.55^{+0.06}_{-0.07}$	$0.48^{+0.07}_{-0.06}$	$6.53^{+0.27}_{-0.27}$	$1.65^{+0.29}_{-0.29}$	6.5(fixed)	$0.00^{+0.01}_{-0.00}$	0^{+35}_{-0}	1.05(72)
192	990421	51289.146	$0.429^{+0.036}_{-0.032}$	$95.60^{+42.15}_{-28.38}$	$2.46^{+0.05}_{-0.06}$	$0.82^{+0.09}_{-0.09}$	$7.81^{+0.23}_{-0.24}$	$1.45^{+0.24}_{-0.23}$	6.5(fixed)	$0.00^{+0.02}_{-0.00}$	0^{+24}_{-0}	1.07(32)[g]
193	990422	51290.984	$0.333^{+0.068}_{-0.034}$	$259.29^{+429.11}_{-159.97}$	$2.49^{+0.03}_{-0.06}$	$0.99^{+0.10}_{-0.12}$	$7.46^{+0.30}_{-0.32}$	$1.17^{+0.26}_{-0.27}$	6.5(fixed)	$0.00^{+0.03}_{-0.00}$	0^{+27}_{-0}	0.47(32)[g]
194	990423	51291.183	$0.390^{+0.041}_{-0.034}$	$124.83^{+73.35}_{-46.35}$	$2.43^{+0.04}_{-0.04}$	$0.69^{+0.06}_{-0.06}$	$7.52^{+0.24}_{-0.23}$	$1.47^{+0.18}_{-0.18}$	6.5(fixed)	$0.00^{+0.02}_{-0.00}$	0^{+27}_{-0}	1.33(31)[g]
195	990424	51292.451	$0.370^{+0.018}_{-0.021}$	$151.45^{+55.51}_{-34.57}$	$2.52^{+0.07}_{-0.07}$	$0.28^{+0.04}_{-0.04}$	$6.88^{+0.28}_{-0.20}$	$1.54^{+0.32}_{-0.25}$	6.5(fixed)	$0.00^{+0.02}_{-0.00}$	0^{+80}_{-0}	0.63(32)[g]
196	990425	51293.450	$0.350^{+0.034}_{-0.026}$	$189.54^{+101.67}_{-73.63}$	$2.51^{+0.03}_{-0.05}$	$0.44^{+0.05}_{-0.02}$	$7.41^{+0.34}_{-0.34}$	$1.04^{+0.25}_{-0.20}$	6.5(fixed)	$0.00^{+0.02}_{-0.00}$	0^{+54}_{-0}	0.87(32)[g]
197	990427	51295.520	$0.415^{+0.032}_{-0.033}$	$69.78^{+33.71}_{-19.89}$	$2.25^{+0.09}_{-0.09}$	$0.12^{+0.03}_{-0.02}$	$7.53^{+0.37}_{-0.31}$	$1.51^{+0.55}_{-0.55}$	6.5(fixed)	$0.01^{+0.02}_{-0.01}$	74^{+113}_{-74}	0.64(32)[g]
198	990429	51297.376	$0.386^{+0.025}_{-0.027}$	$83.65^{+36.66}_{-23.30}$	$2.48^{+0.16}_{-0.17}$	$0.10^{+0.04}_{-0.03}$	$7.44^{+0.40}_{-0.41}$	$2.21^{+0.74}_{-0.81}$	6.5(fixed)	$0.00^{+0.01}_{-0.00}$	0^{+109}_{-0}	0.51(32)[g]
199	990430	51298.052	$0.403^{+0.016}_{-0.033}$	$64.25^{+20.91}_{-18.61}$	$2.51^{+0.20}_{-0.21}$	$0.07^{+0.02}_{-0.02}$	$7.62^{+0.61}_{-0.64}$	$1.98^{+1.18}_{-0.59}$	6.5(fixed)	$0.01^{+0.01}_{-0.01}$	188^{+189}_{-188}	0.58(32)[g]
200	990501	51299.344	$0.344^{+0.021}_{-0.020}$	$121.51^{+47.08}_{-32.71}$	$2.64^{+0.17}_{-0.17}$	$0.07^{+0.02}_{-0.02}$	$6.70^{+0.26}_{-0.32}$	$3.07^{+0.83}_{-0.86}$	6.5(fixed)	$0.00^{+0.01}_{-0.00}$	0^{+113}_{-0}	0.78(72)
201	990502	51300.458	...	...	...	...	...	...	...	...	...	...
202	990504	51302.459	...	...	...	...	...	...	...	...	...	...
203	990505	51303.391	...	...	...	...	...	...	...	...	...	...
204	990507	51305.124	...	...	...	...	...	...	...	...	...	...
205	990509	51307.322	$0.394^{+0.212}_{-0.113}$	$27.96^{+179.54}_{-3.85}$	$2.02^{+0.05}_{-0.05}$	$0.09^{+0.00}_{-0.01}$	$7.31^{+0.38}_{-0.30}$	$1.20^{+0.21}_{-0.34}$	6.5(fixed)	$0.00^{+0.02}_{-0.00}$	0^{+84}_{-0}	0.40(32)[g]
206	990511	51309.720	$0.281^{+0.132}_{-0.035}$	$187.28^{+594.24}_{-33.18}$	$1.91^{+0.05}_{-0.03}$	$0.06^{+0.00}_{-0.00}$	$6.22^{+0.67}_{-0.91}$	$1.04^{+0.37}_{-0.33}$	6.5(fixed)	$0.02^{+0.02}_{-0.02}$	104^{+126}_{-104}	0.62(32)[g]
207	990513	51311.519	$0.553^{+0.171}_{-0.192}$	$6.94^{+9.15}_{-3.58}$	$1.69^{+0.15}_{-0.18}$	$0.02^{+0.01}_{-0.01}$	$7.46^{+0.71}_{-0.44}$	$1.95^{+1.11}_{-1.13}$	6.5(fixed)	$0.01^{+0.02}_{-0.01}$	150^{+229}_{-150}	0.48(32)[g]
208	990515	51313.317	...	...	$2.27^{+0.05}_{-0.05}$	$0.05^{+0.00}_{-0.00}$	...	...	...	...	...	0.91(77)
209	990520	51318.768	...	...	...	...	...	...	...	...	...	...

NOTE.—Fixed $N_H = 2.0 \times 10^{22}$ cm^{-2}.

[a] Start of observation. MJD = JD − 2,400,000.5.

[b] $R^{*}_{in} = R_{in}(\cos i)^{1/2}/(D/6\ \mathrm{kpc})$, where i is the inclination angle and D is the distance to the source in kpc.

[c] Photons s^{-1} cm^{-2} keV^{-1} at 1 keV.

[d] Fixed width of 7 keV using "smedge" model in XSPEC.

[e] Gaussian with fixed FWHM = 1.2 keV (σ = 0.5 keV).

[f] Photons s^{-1} cm^{-2}.

[g] PCU 0 only.

[h] Start of PCA Gain Epoch 4.

TABLE 3

UNABSORBED 2–20 keV FLUX FOR XTE J1550−564

Observation Number	Date (UT)	MJD[a]	Total (10^{-7} ergs s^{-1} cm^{-2})	Disk (10^{-7} ergs s^{-1} cm^{-2})	Power Law (10^{-7} ergs s^{-1} cm^{-2})	Disk/Total
1	980907	51063.697	$0.109^{+0.010}_{-0.009}$	$0.008^{+0.004}_{-0.003}$	$0.100^{+0.009}_{-0.008}$	$0.08^{+0.04}_{-0.03}$
2	980908	51064.006	$0.141^{+0.012}_{-0.010}$	$0.010^{+0.005}_{-0.004}$	$0.131^{+0.011}_{-0.009}$	$0.07^{+0.05}_{-0.03}$
3	980909	51065.068	$0.257^{+0.016}_{-0.011}$	$0.009^{+0.013}_{-0.006}$	$0.247^{+0.009}_{-0.009}$	$0.04^{+0.05}_{-0.03}$
4	980909	51065.342	$0.258^{+0.016}_{-0.011}$	$0.008^{+0.014}_{-0.006}$	$0.248^{+0.008}_{-0.009}$	$0.03^{+0.06}_{-0.03}$
5	980910	51066.067	$0.328^{+0.048}_{-0.009}$	$0.010^{+0.047}_{-0.007}$	$0.316^{+0.007}_{-0.007}$	$0.03^{+0.15}_{-0.02}$
6	980910	51066.345	$0.353^{+0.056}_{-0.012}$	$0.011^{+0.055}_{-0.010}$	$0.339^{+0.007}_{-0.007}$	$0.03^{+0.16}_{-0.03}$
7	980911	51067.271	$0.438^{+0.037}_{-0.017}$	$0.022^{+0.037}_{-0.015}$	$0.412^{+0.008}_{-0.008}$	$0.05^{+0.09}_{-0.04}$
8	980912	51068.345	$0.504^{+0.035}_{-0.022}$	$0.037^{+0.033}_{-0.019}$	$0.464^{+0.011}_{-0.011}$	$0.07^{+0.07}_{-0.04}$
9	980913	51069.275	$0.582^{+0.037}_{-0.028}$	$0.054^{+0.032}_{-0.022}$	$0.525^{+0.018}_{-0.018}$	$0.09^{+0.06}_{-0.04}$
10	980914	51070.131	$0.581^{+0.039}_{-0.028}$	$0.053^{+0.035}_{-0.023}$	$0.525^{+0.018}_{-0.017}$	$0.09^{+0.07}_{-0.04}$
11	980914	51070.274	$0.582^{+0.039}_{-0.028}$	$0.050^{+0.034}_{-0.022}$	$0.528^{+0.017}_{-0.016}$	$0.09^{+0.07}_{-0.04}$
12	980915	51071.200	$0.645^{+0.042}_{-0.033}$	$0.060^{+0.036}_{-0.025}$	$0.581^{+0.022}_{-0.022}$	$0.09^{+0.06}_{-0.04}$
13	980915	51071.996	$0.545^{+0.038}_{-0.024}$	$0.046^{+0.036}_{-0.022}$	$0.495^{+0.013}_{-0.010}$	$0.08^{+0.07}_{-0.04}$
14	980916	51072.345	$0.672^{+0.044}_{-0.035}$	$0.060^{+0.034}_{-0.024}$	$0.608^{+0.028}_{-0.026}$	$0.09^{+0.06}_{-0.04}$
15	980918	51074.140	$0.882^{+0.059}_{-0.054}$	$0.088^{+0.024}_{-0.023}$	$0.790^{+0.054}_{-0.048}$	$0.10^{+0.04}_{-0.03}$
16	980919	51075.987	$2.503^{+0.117}_{-0.113}$	$0.251^{+0.064}_{-0.059}$	$2.240^{+0.098}_{-0.096}$	$0.10^{+0.03}_{-0.03}$
17	980920	51076.802	$1.092^{+0.072}_{-0.067}$	$0.104^{+0.024}_{-0.024}$	$0.984^{+0.068}_{-0.062}$	$0.10^{+0.03}_{-0.03}$
18	980920	51076.953	$1.277^{+0.096}_{-0.090}$	$0.060^{+0.036}_{-0.036}$	$1.212^{+0.089}_{-0.083}$	$0.05^{+0.03}_{-0.03}$
19	980921	51077.143	$1.396^{+0.104}_{-0.093}$	$0.086^{+0.062}_{-0.049}$	$1.306^{+0.083}_{-0.079}$	$0.06^{+0.05}_{-0.04}$
20	980921	51077.211	$1.205^{+0.078}_{-0.072}$	$0.079^{+0.030}_{-0.032}$	$1.122^{+0.072}_{-0.065}$	$0.07^{+0.03}_{-0.03}$
21	980921	51077.869	$0.931^{+0.065}_{-0.058}$	$0.097^{+0.024}_{-0.024}$	$0.830^{+0.061}_{-0.053}$	$0.10^{+0.03}_{-0.03}$
22	980922	51078.132	$0.817^{+0.057}_{-0.051}$	$0.083^{+0.028}_{-0.025}$	$0.731^{+0.049}_{-0.044}$	$0.10^{+0.04}_{-0.04}$
23	980923	51079.794	$0.661^{+0.045}_{-0.037}$	$0.074^{+0.036}_{-0.026}$	$0.584^{+0.028}_{-0.025}$	$0.11^{+0.06}_{-0.04}$
24	980924	51080.078	$0.646^{+0.044}_{-0.034}$	$0.064^{+0.036}_{-0.025}$	$0.578^{+0.025}_{-0.024}$	$0.10^{+0.06}_{-0.04}$
25	980925	51081.062	$0.550^{+0.037}_{-0.026}$	$0.047^{+0.034}_{-0.022}$	$0.500^{+0.015}_{-0.015}$	$0.09^{+0.07}_{-0.04}$
26	980926	51082.002	$0.536^{+0.036}_{-0.025}$	$0.044^{+0.033}_{-0.021}$	$0.490^{+0.014}_{-0.013}$	$0.08^{+0.07}_{-0.04}$
27	980927	51083.002	$0.520^{+0.035}_{-0.024}$	$0.042^{+0.033}_{-0.020}$	$0.474^{+0.013}_{-0.013}$	$0.08^{+0.07}_{-0.04}$
28	980928	51084.342	$0.505^{+0.034}_{-0.024}$	$0.042^{+0.031}_{-0.019}$	$0.461^{+0.014}_{-0.014}$	$0.08^{+0.07}_{-0.04}$
29	980929	51085.270	$0.599^{+0.044}_{-0.037}$	$0.067^{+0.031}_{-0.023}$	$0.529^{+0.031}_{-0.029}$	$0.11^{+0.06}_{-0.04}$
30	980929	51085.920	$0.504^{+0.033}_{-0.026}$	$0.050^{+0.029}_{-0.020}$	$0.451^{+0.016}_{-0.016}$	$0.10^{+0.07}_{-0.04}$
31	980929	51085.991	$0.529^{+0.045}_{-0.036}$	$0.055^{+0.035}_{-0.024}$	$0.471^{+0.028}_{-0.027}$	$0.10^{+0.08}_{-0.05}$
32	980930	51086.889	$0.530^{+0.034}_{-0.028}$	$0.057^{+0.028}_{-0.021}$	$0.470^{+0.020}_{-0.019}$	$0.11^{+0.06}_{-0.04}$
33	981001	51087.723	$0.519^{+0.034}_{-0.027}$	$0.056^{+0.028}_{-0.020}$	$0.461^{+0.018}_{-0.018}$	$0.11^{+0.06}_{-0.04}$
34	981002	51088.007	$0.497^{+0.040}_{-0.031}$	$0.050^{+0.034}_{-0.023}$	$0.444^{+0.021}_{-0.021}$	$0.10^{+0.08}_{-0.05}$
35	981003	51089.008	$0.472^{+0.032}_{-0.025}$	$0.047^{+0.027}_{-0.019}$	$0.423^{+0.016}_{-0.016}$	$0.10^{+0.07}_{-0.04}$
36	981004	51090.143	$0.514^{+0.034}_{-0.030}$	$0.065^{+0.023}_{-0.019}$	$0.446^{+0.025}_{-0.023}$	$0.13^{+0.06}_{-0.04}$
37	981004	51090.704	$0.500^{+0.034}_{-0.028}$	$0.062^{+0.026}_{-0.020}$	$0.436^{+0.021}_{-0.020}$	$0.12^{+0.06}_{-0.05}$
38	981005	51091.743	$0.619^{+0.040}_{-0.036}$	$0.102^{+0.020}_{-0.019}$	$0.515^{+0.035}_{-0.031}$	$0.17^{+0.04}_{-0.04}$
39	981007	51093.143	$0.667^{+0.039}_{-0.036}$	$0.127^{+0.016}_{-0.015}$	$0.537^{+0.036}_{-0.033}$	$0.19^{+0.04}_{-0.03}$
40	981008	51094.143	$0.483^{+0.031}_{-0.028}$	$0.070^{+0.020}_{-0.017}$	$0.410^{+0.024}_{-0.022}$	$0.15^{+0.05}_{-0.04}$
41	981008	51094.572	$0.524^{+0.032}_{-0.030}$	$0.089^{+0.018}_{-0.016}$	$0.432^{+0.027}_{-0.025}$	$0.17^{+0.05}_{-0.04}$
42	981009	51095.609	$0.477^{+0.030}_{-0.028}$	$0.074^{+0.019}_{-0.016}$	$0.400^{+0.024}_{-0.023}$	$0.16^{+0.05}_{-0.04}$
43	981010	51096.572	$0.514^{+0.033}_{-0.031}$	$0.091^{+0.017}_{-0.016}$	$0.421^{+0.028}_{-0.026}$	$0.18^{+0.05}_{-0.04}$
44	981011	51097.572	$0.459^{+0.029}_{-0.026}$	$0.078^{+0.017}_{-0.015}$	$0.379^{+0.023}_{-0.022}$	$0.17^{+0.05}_{-0.04}$
45	981011	51097.809	$0.422^{+0.030}_{-0.027}$	$0.065^{+0.019}_{-0.016}$	$0.355^{+0.023}_{-0.021}$	$0.16^{+0.06}_{-0.05}$
46	981012	51098.275	$0.455^{+0.029}_{-0.027}$	$0.081^{+0.015}_{-0.014}$	$0.372^{+0.025}_{-0.023}$	$0.18^{+0.05}_{-0.04}$
47	981013	51099.215	$0.438^{+0.029}_{-0.027}$	$0.079^{+0.015}_{-0.014}$	$0.357^{+0.025}_{-0.023}$	$0.18^{+0.05}_{-0.04}$
48	981013	51099.608	$0.436^{+0.027}_{-0.025}$	$0.079^{+0.015}_{-0.014}$	$0.355^{+0.023}_{-0.021}$	$0.18^{+0.05}_{-0.04}$
49	981014	51100.287	$0.512^{+0.030}_{-0.027}$	$0.117^{+0.013}_{-0.013}$	$0.393^{+0.027}_{-0.024}$	$0.23^{+0.04}_{-0.04}$
50	981015	51101.607	$0.515^{+0.030}_{-0.028}$	$0.123^{+0.013}_{-0.013}$	$0.390^{+0.027}_{-0.025}$	$0.24^{+0.04}_{-0.04}$
51	981015	51101.941	$0.497^{+0.028}_{-0.026}$	$0.120^{+0.013}_{-0.012}$	$0.376^{+0.025}_{-0.023}$	$0.24^{+0.04}_{-0.04}$
52	981020	51106.953	$0.622^{+0.039}_{-0.036}$	$0.216^{+0.014}_{-0.014}$	$0.404^{+0.036}_{-0.033}$	$0.35^{+0.06}_{-0.04}$
53	981022	51108.076	$0.583^{+0.030}_{-0.028}$	$0.198^{+0.012}_{-0.011}$	$0.383^{+0.028}_{-0.025}$	$0.34^{+0.04}_{-0.04}$
54	981023	51109.737	$0.544^{+0.036}_{-0.033}$	$0.195^{+0.013}_{-0.012}$	$0.347^{+0.034}_{-0.031}$	$0.36^{+0.05}_{-0.04}$
55	981024	51110.270	$0.505^{+0.028}_{-0.025}$	$0.217^{+0.011}_{-0.011}$	$0.287^{+0.025}_{-0.023}$	$0.43^{+0.05}_{-0.04}$
56	981025	51111.602	$0.477^{+0.030}_{-0.028}$	$0.197^{+0.011}_{-0.011}$	$0.278^{+0.028}_{-0.025}$	$0.41^{+0.05}_{-0.05}$
57	981026	51112.802	$0.448^{+0.024}_{-0.022}$	$0.187^{+0.010}_{-0.010}$	$0.260^{+0.022}_{-0.020}$	$0.42^{+0.05}_{-0.04}$
58	981027	51113.668	$0.400^{+0.023}_{-0.021}$	$0.181^{+0.010}_{-0.010}$	$0.218^{+0.021}_{-0.019}$	$0.45^{+0.05}_{-0.05}$
59	981029	51115.280	$0.297^{+0.015}_{-0.014}$	$0.166^{+0.008}_{-0.007}$	$0.131^{+0.013}_{-0.012}$	$0.56^{+0.05}_{-0.05}$
60	981031	51117.351	$0.226^{+0.009}_{-0.008}$	$0.190^{+0.006}_{-0.006}$	$0.036^{+0.006}_{-0.006}$	$0.84^{+0.06}_{-0.06}$
61	981102	51119.003	$0.192^{+0.008}_{-0.008}$	$0.160^{+0.006}_{-0.006}$	$0.032^{+0.006}_{-0.005}$	$0.83^{+0.06}_{-0.06}$
62	981104	51121.003	$0.149^{+0.005}_{-0.005}$	$0.137^{+0.004}_{-0.004}$	$0.011^{+0.003}_{-0.003}$	$0.92^{+0.06}_{-0.06}$
63	981107	51124.727	$0.122^{+0.005}_{-0.005}$	$0.106^{+0.004}_{-0.004}$	$0.015^{+0.004}_{-0.003}$	$0.87^{+0.07}_{-0.06}$
64	981109	51126.595	$0.124^{+0.005}_{-0.005}$	$0.092^{+0.004}_{-0.003}$	$0.032^{+0.003}_{-0.003}$	$0.74^{+0.06}_{-0.05}$

TABLE 3—*Continued*

Observation Number	Date (UT)	MJD[a]	Total (10^{-7} ergs s^{-1} cm^{-2})	Disk (10^{-7} ergs s^{-1} cm^{-2})	Power Law (10^{-7} ergs s^{-1} cm^{-2})	Disk/Total
65	981111	51128.564	$0.101^{+0.005}_{-0.004}$	$0.081^{+0.003}_{-0.003}$	$0.020^{+0.003}_{-0.003}$	$0.81^{+0.07}_{-0.07}$
66	981113	51130.457	$0.091^{+0.004}_{-0.003}$	$0.073^{+0.003}_{-0.003}$	$0.019^{+0.002}_{-0.002}$	$0.80^{+0.06}_{-0.06}$
67	981115	51132.479	$0.079^{+0.005}_{-0.004}$	$0.063^{+0.003}_{-0.003}$	$0.016^{+0.003}_{-0.003}$	$0.80^{+0.09}_{-0.08}$
68	981117	51134.436	$0.067^{+0.003}_{-0.003}$	$0.057^{+0.002}_{-0.002}$	$0.010^{+0.002}_{-0.002}$	$0.85^{+0.07}_{-0.07}$
69	981119	51136.777	$0.057^{+0.002}_{-0.002}$	$0.048^{+0.002}_{-0.002}$	$0.009^{+0.001}_{-0.001}$	$0.83^{+0.06}_{-0.06}$
70	981120	51137.923	$0.065^{+0.003}_{-0.003}$	$0.043^{+0.002}_{-0.002}$	$0.022^{+0.002}_{-0.002}$	$0.66^{+0.07}_{-0.07}$
71	981122	51139.991	$0.060^{+0.004}_{-0.003}$	$0.035^{+0.002}_{-0.002}$	$0.025^{+0.003}_{-0.003}$	$0.59^{+0.08}_{-0.07}$
72	981123	51140.706	$0.056^{+0.003}_{-0.003}$	$0.034^{+0.002}_{-0.002}$	$0.022^{+0.002}_{-0.002}$	$0.60^{+0.07}_{-0.07}$
73	981126	51143.800	$0.051^{+0.010}_{-0.007}$	$0.028^{+0.007}_{-0.004}$	$0.023^{+0.008}_{-0.006}$	$0.55^{+0.25}_{-0.16}$
74	981128	51145.476	$0.038^{+0.002}_{-0.002}$	$0.031^{+0.002}_{-0.001}$	$0.007^{+0.001}_{-0.001}$	$0.81^{+0.08}_{-0.08}$
75	981130	51147.335	$0.045^{+0.002}_{-0.002}$	$0.029^{+0.002}_{-0.002}$	$0.016^{+0.002}_{-0.001}$	$0.65^{+0.07}_{-0.06}$
76	981203	51150.073	$0.045^{+0.002}_{-0.002}$	$0.035^{+0.002}_{-0.002}$	$0.009^{+0.001}_{-0.001}$	$0.79^{+0.08}_{-0.07}$
77	981205	51152.080	$0.052^{+0.003}_{-0.002}$	$0.046^{+0.002}_{-0.002}$	$0.006^{+0.002}_{-0.001}$	$0.89^{+0.08}_{-0.08}$
78	981205	51152.866	$0.057^{+0.002}_{-0.002}$	$0.053^{+0.002}_{-0.002}$	$0.004^{+0.002}_{-0.001}$	$0.93^{+0.07}_{-0.07}$
79	981207	51154.016	$0.069^{+0.003}_{-0.003}$	$0.064^{+0.002}_{-0.002}$	$0.004^{+0.002}_{-0.002}$	$0.93^{+0.07}_{-0.08}$
80	981208	51155.067	$0.082^{+0.004}_{-0.003}$	$0.077^{+0.002}_{-0.002}$	$0.004^{+0.003}_{-0.002}$	$0.94^{+0.06}_{-0.07}$
81	981210	51157.493	$0.124^{+0.007}_{-0.005}$	$0.118^{+0.004}_{-0.004}$	$0.006^{+0.006}_{-0.003}$	$0.95^{+0.07}_{-0.08}$
82	981213	51160.276	$0.192^{+0.018}_{-0.011}$	$0.175^{+0.005}_{-0.006}$	$0.017^{+0.017}_{-0.009}$	$0.91^{+0.08}_{-0.11}$
83	981215	51162.202	$0.256^{+0.022}_{-0.012}$	$0.240^{+0.007}_{-0.007}$	$0.016^{+0.021}_{-0.009}$	$0.94^{+0.07}_{-0.10}$
84	981216	51163.205	$0.293^{+0.020}_{-0.016}$	$0.257^{+0.011}_{-0.008}$	$0.036^{+0.016}_{-0.014}$	$0.88^{+0.09}_{-0.08}$
85	981217	51164.205	$0.345^{+0.030}_{-0.022}$	$0.306^{+0.014}_{-0.014}$	$0.039^{+0.027}_{-0.017}$	$0.89^{+0.10}_{-0.11}$
86	981218	51165.590	$0.401^{+0.028}_{-0.018}$	$0.372^{+0.010}_{-0.012}$	$0.029^{+0.026}_{-0.014}$	$0.93^{+0.07}_{-0.09}$
87	981219	51166.011	$0.418^{+0.025}_{-0.017}$	$0.387^{+0.009}_{-0.010}$	$0.030^{+0.024}_{-0.014}$	$0.93^{+0.06}_{-0.08}$
88	981220	51167.418	$0.480^{+0.039}_{-0.026}$	$0.439^{+0.015}_{-0.016}$	$0.040^{+0.036}_{-0.020}$	$0.92^{+0.09}_{-0.10}$
89	981221	51168.010	$0.485^{+0.021}_{-0.017}$	$0.439^{+0.009}_{-0.009}$	$0.046^{+0.019}_{-0.014}$	$0.90^{+0.05}_{-0.06}$
90	981222	51169.009	$0.534^{+0.024}_{-0.020}$	$0.470^{+0.010}_{-0.011}$	$0.064^{+0.022}_{-0.017}$	$0.88^{+0.05}_{-0.06}$
91	981223	51170.520	$0.565^{+0.031}_{-0.024}$	$0.513^{+0.014}_{-0.015}$	$0.052^{+0.028}_{-0.019}$	$0.91^{+0.07}_{-0.07}$
92	981225	51172.065	$0.592^{+0.023}_{-0.019}$	$0.519^{+0.010}_{-0.011}$	$0.073^{+0.020}_{-0.016}$	$0.88^{+0.05}_{-0.05}$
93	981226	51172.990	$0.605^{+0.028}_{-0.024}$	$0.533^{+0.014}_{-0.015}$	$0.071^{+0.024}_{-0.019}$	$0.88^{+0.06}_{-0.06}$
94	981227	51173.990	$0.612^{+0.032}_{-0.026}$	$0.533^{+0.016}_{-0.016}$	$0.078^{+0.027}_{-0.021}$	$0.87^{+0.07}_{-0.07}$
95	981227	51174.722	$0.637^{+0.028}_{-0.024}$	$0.555^{+0.014}_{-0.014}$	$0.082^{+0.024}_{-0.019}$	$0.87^{+0.06}_{-0.06}$
96	981228	51175.879	$0.643^{+0.031}_{-0.026}$	$0.565^{+0.015}_{-0.015}$	$0.078^{+0.027}_{-0.021}$	$0.88^{+0.06}_{-0.06}$
97	981229	51176.847	$0.650^{+0.032}_{-0.027}$	$0.566^{+0.015}_{-0.016}$	$0.083^{+0.028}_{-0.021}$	$0.87^{+0.06}_{-0.06}$
98	981230	51177.846	$0.668^{+0.034}_{-0.029}$	$0.571^{+0.018}_{-0.018}$	$0.096^{+0.029}_{-0.023}$	$0.86^{+0.07}_{-0.07}$
99	981231	51178.846	$0.675^{+0.025}_{-0.022}$	$0.568^{+0.012}_{-0.012}$	$0.106^{+0.022}_{-0.019}$	$0.84^{+0.05}_{-0.05}$
100	990101	51179.919	$0.693^{+0.031}_{-0.025}$	$0.593^{+0.013}_{-0.012}$	$0.099^{+0.028}_{-0.022}$	$0.86^{+0.05}_{-0.05}$
101	990102	51180.845	$0.753^{+0.032}_{-0.028}$	$0.618^{+0.014}_{-0.014}$	$0.133^{+0.029}_{-0.024}$	$0.82^{+0.05}_{-0.05}$
102	990104	51182.337	$0.698^{+0.025}_{-0.022}$	$0.589^{+0.012}_{-0.012}$	$0.109^{+0.022}_{-0.019}$	$0.84^{+0.05}_{-0.05}$
103	990105	51183.540	$0.712^{+0.026}_{-0.023}$	$0.601^{+0.013}_{-0.013}$	$0.110^{+0.023}_{-0.019}$	$0.85^{+0.05}_{-0.05}$
104	990106	51184.711	$0.715^{+0.019}_{-0.018}$	$0.602^{+0.010}_{-0.010}$	$0.113^{+0.017}_{-0.015}$	$0.84^{+0.04}_{-0.04}$
105	990107	51185.126	$0.705^{+0.041}_{-0.033}$	$0.621^{+0.018}_{-0.019}$	$0.083^{+0.036}_{-0.026}$	$0.88^{+0.07}_{-0.07}$
106	990107	51185.846	$0.707^{+0.024}_{-0.021}$	$0.600^{+0.012}_{-0.012}$	$0.107^{+0.020}_{-0.018}$	$0.85^{+0.04}_{-0.04}$
107	990109	51187.126	$0.708^{+0.029}_{-0.025}$	$0.607^{+0.014}_{-0.014}$	$0.101^{+0.026}_{-0.021}$	$0.86^{+0.05}_{-0.05}$
108	990110	51188.194	$0.716^{+0.028}_{-0.025}$	$0.603^{+0.013}_{-0.014}$	$0.113^{+0.025}_{-0.021}$	$0.84^{+0.05}_{-0.05}$
109	990110	51188.731	$0.725^{+0.024}_{-0.022}$	$0.603^{+0.011}_{-0.013}$	$0.122^{+0.021}_{-0.019}$	$0.83^{+0.04}_{-0.04}$
110	990112	51190.054	$0.723^{+0.022}_{-0.020}$	$0.614^{+0.010}_{-0.011}$	$0.109^{+0.019}_{-0.017}$	$0.85^{+0.04}_{-0.04}$
111	990113	51191.485	$0.742^{+0.022}_{-0.020}$	$0.623^{+0.012}_{-0.012}$	$0.119^{+0.018}_{-0.016}$	$0.84^{+0.04}_{-0.04}$
112	990114	51192.187	$0.752^{+0.024}_{-0.023}$	$0.627^{+0.013}_{-0.013}$	$0.125^{+0.021}_{-0.019}$	$0.83^{+0.04}_{-0.04}$
113	990114	51192.593	$0.740^{+0.026}_{-0.024}$	$0.611^{+0.012}_{-0.013}$	$0.128^{+0.022}_{-0.020}$	$0.83^{+0.05}_{-0.05}$
114	990116	51194.500	$0.763^{+0.029}_{-0.025}$	$0.636^{+0.011}_{-0.019}$	$0.128^{+0.027}_{-0.016}$	$0.83^{+0.04}_{-0.05}$
115	990118	51196.051	$0.773^{+0.024}_{-0.022}$	$0.640^{+0.012}_{-0.013}$	$0.133^{+0.021}_{-0.018}$	$0.83^{+0.04}_{-0.04}$
116	990118	51196.522	$0.760^{+0.024}_{-0.023}$	$0.628^{+0.013}_{-0.012}$	$0.131^{+0.021}_{-0.019}$	$0.83^{+0.04}_{-0.04}$
117	990120	51198.051	$0.774^{+0.026}_{-0.024}$	$0.644^{+0.014}_{-0.013}$	$0.130^{+0.022}_{-0.020}$	$0.83^{+0.04}_{-0.04}$
118	990122	51200.383	$0.835^{+0.047}_{-0.039}$	$0.663^{+0.019}_{-0.018}$	$0.170^{+0.043}_{-0.035}$	$0.80^{+0.06}_{-0.06}$
119	990123	51201.783	$0.888^{+0.042}_{-0.037}$	$0.659^{+0.016}_{-0.017}$	$0.226^{+0.038}_{-0.033}$	$0.74^{+0.05}_{-0.05}$
120	990125	51203.249	$0.802^{+0.035}_{-0.033}$	$0.666^{+0.020}_{-0.022}$	$0.135^{+0.029}_{-0.024}$	$0.83^{+0.06}_{-0.06}$
121	990126	51204.248	$0.802^{+0.034}_{-0.031}$	$0.654^{+0.018}_{-0.018}$	$0.148^{+0.029}_{-0.025}$	$0.82^{+0.06}_{-0.05}$
122	990127	51205.850	$0.804^{+0.027}_{-0.025}$	$0.657^{+0.014}_{-0.015}$	$0.146^{+0.023}_{-0.020}$	$0.82^{+0.04}_{-0.04}$
123	990128	51206.781	$0.788^{+0.025}_{-0.023}$	$0.649^{+0.013}_{-0.014}$	$0.139^{+0.021}_{-0.019}$	$0.82^{+0.04}_{-0.04}$
124	990130	51208.179	$0.807^{+0.034}_{-0.030}$	$0.669^{+0.016}_{-0.016}$	$0.137^{+0.030}_{-0.025}$	$0.83^{+0.05}_{-0.05}$
125	990130	51208.845	$0.788^{+0.035}_{-0.031}$	$0.663^{+0.019}_{-0.019}$	$0.125^{+0.029}_{-0.024}$	$0.84^{+0.06}_{-0.06}$
126	990131	51209.711	$0.781^{+0.028}_{-0.025}$	$0.650^{+0.014}_{-0.014}$	$0.131^{+0.024}_{-0.020}$	$0.83^{+0.05}_{-0.05}$
127	990202	51211.709	$0.763^{+0.027}_{-0.024}$	$0.636^{+0.013}_{-0.013}$	$0.127^{+0.023}_{-0.020}$	$0.83^{+0.05}_{-0.05}$
128	990203	51212.775	$0.763^{+0.026}_{-0.024}$	$0.633^{+0.013}_{-0.013}$	$0.130^{+0.023}_{-0.020}$	$0.83^{+0.05}_{-0.05}$
129	990204	51213.774	$0.757^{+0.035}_{-0.031}$	$0.644^{+0.018}_{-0.020}$	$0.113^{+0.029}_{-0.024}$	$0.85^{+0.06}_{-0.06}$

TABLE 3—*Continued*

Observation Number	Date (UT)	MJD[a]	Total (10^{-7} ergs s^{-1} cm^{-2})	Disk (10^{-7} ergs s^{-1} cm^{-2})	Power Law (10^{-7} ergs s^{-1} cm^{-2})	Disk/Total
130	990205	51214.975	$0.781^{+0.036}_{-0.031}$	$0.646^{+0.014}_{-0.014}$	$0.133^{+0.033}_{-0.027}$	$0.83^{+0.05}_{-0.05}$
131	990206	51215.839	$0.764^{+0.031}_{-0.027}$	$0.639^{+0.013}_{-0.013}$	$0.124^{+0.028}_{-0.024}$	$0.84^{+0.05}_{-0.05}$
132	990207	51216.838	$0.745^{+0.036}_{-0.032}$	$0.619^{+0.019}_{-0.018}$	$0.126^{+0.031}_{-0.026}$	$0.83^{+0.06}_{-0.06}$
133	990208	51217.704	$0.743^{+0.026}_{-0.024}$	$0.619^{+0.013}_{-0.013}$	$0.124^{+0.022}_{-0.019}$	$0.83^{+0.05}_{-0.05}$
134	990210	51219.053	$0.722^{+0.024}_{-0.021}$	$0.622^{+0.013}_{-0.013}$	$0.099^{+0.020}_{-0.017}$	$0.86^{+0.05}_{-0.04}$
135	990211	51220.508	$0.720^{+0.045}_{-0.038}$	$0.616^{+0.023}_{-0.023}$	$0.103^{+0.039}_{-0.029}$	$0.86^{+0.08}_{-0.08}$
136	990211	51220.836	$0.717^{+0.042}_{-0.036}$	$0.614^{+0.021}_{-0.023}$	$0.102^{+0.037}_{-0.028}$	$0.86^{+0.08}_{-0.08}$
137	990212	51221.567	$0.710^{+0.026}_{-0.023}$	$0.596^{+0.013}_{-0.013}$	$0.114^{+0.022}_{-0.019}$	$0.84^{+0.05}_{-0.05}$
138	990214	51223.766	$0.698^{+0.023}_{-0.021}$	$0.582^{+0.012}_{-0.012}$	$0.116^{+0.020}_{-0.018}$	$0.83^{+0.04}_{-0.04}$
139	990215	51224.699	$0.682^{+0.024}_{-0.021}$	$0.574^{+0.013}_{-0.011}$	$0.108^{+0.021}_{-0.018}$	$0.84^{+0.05}_{-0.05}$
140	990217	51226.296	$0.682^{+0.029}_{-0.026}$	$0.580^{+0.014}_{-0.015}$	$0.102^{+0.026}_{-0.021}$	$0.85^{+0.05}_{-0.06}$
141	990218	51227.837	$0.667^{+0.023}_{-0.021}$	$0.563^{+0.011}_{-0.012}$	$0.104^{+0.020}_{-0.017}$	$0.84^{+0.05}_{-0.05}$
142	990219	51228.696	$0.659^{+0.023}_{-0.021}$	$0.556^{+0.011}_{-0.012}$	$0.103^{+0.020}_{-0.017}$	$0.84^{+0.04}_{-0.05}$
143	990221	51230.424	$0.647^{+0.030}_{-0.026}$	$0.569^{+0.015}_{-0.017}$	$0.078^{+0.026}_{-0.020}$	$0.88^{+0.06}_{-0.06}$
144	990222	51231.293	$0.672^{+0.033}_{-0.028}$	$0.565^{+0.014}_{-0.014}$	$0.107^{+0.030}_{-0.024}$	$0.84^{+0.06}_{-0.06}$
145	990222	51231.422	$0.658^{+0.031}_{-0.026}$	$0.572^{+0.012}_{-0.014}$	$0.085^{+0.028}_{-0.022}$	$0.87^{+0.05}_{-0.06}$
146	990223	51232.252	$0.714^{+0.034}_{-0.029}$	$0.565^{+0.015}_{-0.014}$	$0.148^{+0.031}_{-0.025}$	$0.79^{+0.05}_{-0.05}$
147	990223	51232.860	$0.736^{+0.036}_{-0.031}$	$0.566^{+0.016}_{-0.016}$	$0.168^{+0.033}_{-0.027}$	$0.77^{+0.06}_{-0.06}$
148	990224	51233.835	$0.718^{+0.030}_{-0.027}$	$0.575^{+0.014}_{-0.015}$	$0.142^{+0.026}_{-0.023}$	$0.80^{+0.05}_{-0.05}$
149	990226	51235.199	$0.722^{+0.030}_{-0.026}$	$0.556^{+0.016}_{-0.014}$	$0.164^{+0.025}_{-0.022}$	$0.77^{+0.05}_{-0.05}$
150	990228	51237.619	$0.609^{+0.026}_{-0.021}$	$0.525^{+0.011}_{-0.010}$	$0.083^{+0.023}_{-0.018}$	$0.86^{+0.05}_{-0.05}$
151	990302	51239.081	$0.626^{+0.024}_{-0.021}$	$0.528^{+0.012}_{-0.014}$	$0.097^{+0.020}_{-0.017}$	$0.84^{+0.05}_{-0.05}$
152	990303	51240.063	$0.646^{+0.026}_{-0.023}$	$0.531^{+0.014}_{-0.014}$	$0.113^{+0.022}_{-0.019}$	$0.82^{+0.05}_{-0.05}$
153	990304	51241.828	$0.688^{+0.031}_{-0.029}$	$0.401^{+0.014}_{-0.013}$	$0.285^{+0.028}_{-0.026}$	$0.58^{+0.05}_{-0.04}$
154	993005	51242.507	$0.670^{+0.034}_{-0.031}$	$0.367^{+0.014}_{-0.014}$	$0.301^{+0.031}_{-0.028}$	$0.55^{+0.05}_{-0.05}$
155	990307	51244.496	$0.798^{+0.047}_{-0.044}$	$0.303^{+0.017}_{-0.016}$	$0.492^{+0.044}_{-0.040}$	$0.38^{+0.04}_{-0.04}$
156	990308	51245.353	$0.743^{+0.044}_{-0.040}$	$0.218^{+0.015}_{-0.015}$	$0.524^{+0.041}_{-0.037}$	$0.29^{+0.04}_{-0.04}$
157	990309	51246.414	$0.742^{+0.054}_{-0.049}$	$0.295^{+0.021}_{-0.021}$	$0.445^{+0.050}_{-0.044}$	$0.40^{+0.06}_{-0.05}$
158	990310	51247.979	$0.710^{+0.056}_{-0.050}$	$0.224^{+0.020}_{-0.020}$	$0.483^{+0.052}_{-0.046}$	$0.32^{+0.05}_{-0.05}$
159	990311	51248.091	$0.717^{+0.061}_{-0.055}$	$0.238^{+0.020}_{-0.021}$	$0.477^{+0.057}_{-0.050}$	$0.33^{+0.06}_{-0.05}$
160	990312	51249.400	$0.666^{+0.049}_{-0.046}$	$0.179^{+0.017}_{-0.017}$	$0.485^{+0.046}_{-0.042}$	$0.27^{+0.05}_{-0.04}$
161	990313	51250.693	$0.411^{+0.033}_{-0.031}$	$0.104^{+0.016}_{-0.015}$	$0.305^{+0.029}_{-0.026}$	$0.25^{+0.06}_{-0.05}$
162	990316	51253.225	$0.573^{+0.050}_{-0.046}$	$0.182^{+0.018}_{-0.017}$	$0.390^{+0.047}_{-0.042}$	$0.32^{+0.06}_{-0.05}$
163	990317	51254.092	$0.464^{+0.038}_{-0.035}$	$0.151^{+0.016}_{-0.016}$	$0.311^{+0.035}_{-0.031}$	$0.32^{+0.06}_{-0.06}$
164	990318	51255.091	$0.399^{+0.031}_{-0.028}$	$0.249^{+0.018}_{-0.017}$	$0.149^{+0.025}_{-0.021}$	$0.62^{+0.09}_{-0.09}$
165	990320	51257.362	$0.328^{+0.025}_{-0.021}$	$0.253^{+0.013}_{-0.013}$	$0.074^{+0.021}_{-0.016}$	$0.77^{+0.09}_{-0.09}$
166	990321	51258.088	$0.327^{+0.023}_{-0.020}$	$0.223^{+0.012}_{-0.012}$	$0.103^{+0.020}_{-0.017}$	$0.68^{+0.08}_{-0.08}$
167	990321	51258.496	$0.317^{+0.022}_{-0.019}$	$0.211^{+0.012}_{-0.011}$	$0.106^{+0.018}_{-0.016}$	$0.66^{+0.08}_{-0.08}$
168	990321	51258.975	$0.305^{+0.022}_{-0.020}$	$0.175^{+0.012}_{-0.011}$	$0.129^{+0.019}_{-0.016}$	$0.57^{+0.08}_{-0.07}$
169	990322	51259.252	$0.296^{+0.023}_{-0.020}$	$0.176^{+0.011}_{-0.011}$	$0.119^{+0.020}_{-0.017}$	$0.59^{+0.09}_{-0.08}$
170[b]	990323	51260.552	$0.277^{+0.026}_{-0.023}$	$0.234^{+0.023}_{-0.022}$	$0.043^{+0.011}_{-0.009}$	$0.84^{+0.17}_{-0.14}$
171	990324	51261.766	$0.256^{+0.024}_{-0.022}$	$0.215^{+0.021}_{-0.020}$	$0.041^{+0.011}_{-0.008}$	$0.84^{+0.17}_{-0.14}$
172	990326	51263.108	$0.238^{+0.031}_{-0.028}$	$0.201^{+0.029}_{-0.027}$	$0.036^{+0.011}_{-0.009}$	$0.85^{+0.25}_{-0.20}$
173	990327	51264.748	$0.191^{+0.016}_{-0.016}$	$0.161^{+0.015}_{-0.015}$	$0.030^{+0.006}_{-0.005}$	$0.84^{+0.16}_{-0.14}$
174	990328	51265.613	$0.181^{+0.016}_{-0.015}$	$0.149^{+0.015}_{-0.014}$	$0.032^{+0.006}_{-0.005}$	$0.82^{+0.16}_{-0.14}$
175	990329	51266.880	$0.154^{+0.019}_{-0.017}$	$0.135^{+0.018}_{-0.016}$	$0.019^{+0.007}_{-0.005}$	$0.88^{+0.24}_{-0.19}$
176	990330	51267.612	$0.160^{+0.022}_{-0.019}$	$0.127^{+0.020}_{-0.018}$	$0.032^{+0.011}_{-0.008}$	$0.80^{+0.25}_{-0.20}$
177	990401	51269.677	$0.141^{+0.013}_{-0.012}$	$0.108^{+0.012}_{-0.011}$	$0.032^{+0.005}_{-0.005}$	$0.77^{+0.16}_{-0.14}$
178	990402	51270.742	$0.136^{+0.015}_{-0.013}$	$0.081^{+0.012}_{-0.011}$	$0.054^{+0.008}_{-0.006}$	$0.60^{+0.17}_{-0.13}$
179	990403	51271.408	$0.129^{+0.015}_{-0.013}$	$0.075^{+0.012}_{-0.011}$	$0.054^{+0.008}_{-0.007}$	$0.58^{+0.17}_{-0.14}$
180	990405	51273.541	$0.102^{+0.009}_{-0.008}$	$0.080^{+0.009}_{-0.008}$	$0.022^{+0.004}_{-0.003}$	$0.79^{+0.16}_{-0.14}$
181	990406	51274.471	$0.090^{+0.008}_{-0.008}$	$0.073^{+0.008}_{-0.007}$	$0.017^{+0.004}_{-0.003}$	$0.81^{+0.17}_{-0.14}$
182	990408	51276.278	$0.072^{+0.011}_{-0.010}$	$0.063^{+0.009}_{-0.009}$	$0.010^{+0.006}_{-0.003}$	$0.87^{+0.28}_{-0.22}$
183	990409	51277.401	$0.067^{+0.007}_{-0.006}$	$0.055^{+0.006}_{-0.005}$	$0.011^{+0.003}_{-0.002}$	$0.83^{+0.18}_{-0.15}$
184	990410	51278.686	$0.060^{+0.014}_{-0.010}$	$0.049^{+0.011}_{-0.009}$	$0.011^{+0.008}_{-0.004}$	$0.81^{+0.38}_{-0.27}$
185	990411	51279.531	$0.058^{+0.017}_{-0.013}$	$0.046^{+0.016}_{-0.012}$	$0.013^{+0.005}_{-0.003}$	$0.79^{+0.56}_{-0.34}$
186	990412	51280.544	$0.049^{+0.015}_{-0.014}$	$0.039^{+0.013}_{-0.013}$	$0.009^{+0.007}_{-0.005}$	$0.81^{+0.70}_{-0.40}$
187	990415	51283.224	$0.041^{+0.012}_{-0.009}$	$0.032^{+0.011}_{-0.008}$	$0.009^{+0.003}_{-0.002}$	$0.78^{+0.55}_{-0.33}$
188	990417	51285.197	$0.035^{+0.011}_{-0.008}$	$0.026^{+0.011}_{-0.008}$	$0.008^{+0.002}_{-0.002}$	$0.76^{+0.64}_{-0.35}$
189	990418	51286.058	$0.032^{+0.012}_{-0.009}$	$0.023^{+0.011}_{-0.008}$	$0.009^{+0.002}_{-0.002}$	$0.72^{+0.75}_{-0.38}$
190	990419	51287.257	$0.028^{+0.012}_{-0.007}$	$0.020^{+0.011}_{-0.007}$	$0.008^{+0.003}_{-0.002}$	$0.71^{+0.79}_{-0.38}$
191	990420	51288.382	$0.026^{+0.010}_{-0.007}$	$0.020^{+0.010}_{-0.007}$	$0.006^{+0.002}_{-0.001}$	$0.76^{+0.76}_{-0.39}$
192	990421	51289.146	$0.029^{+0.018}_{-0.009}$	$0.016^{+0.018}_{-0.009}$	$0.013^{+0.003}_{-0.002}$	$0.54^{+1.18}_{-0.41}$
193	990422	51290.984	$0.031^{+0.096}_{-0.015}$	$0.016^{+0.096}_{-0.015}$	$0.015^{+0.003}_{-0.002}$	$0.51^{+6.57}_{-0.50}$

TABLE 3—*Continued*

Observation Number	Date (UT)	MJD[a]	Total (10^{-7} ergs s^{-1} cm^{-2})	Disk (10^{-7} ergs s^{-1} cm^{-2})	Power Law (10^{-7} ergs s^{-1} cm^{-2})	Disk/Total
194.....	990423	51291.183	$0.025^{+0.021}_{-0.009}$	$0.013^{+0.021}_{-0.009}$	$0.011^{+0.002}_{-0.002}$	$0.53^{+1.68}_{-0.45}$
195.....	990424	51292.451	$0.017^{+0.011}_{-0.006}$	$0.013^{+0.011}_{-0.006}$	$0.004^{+0.001}_{-0.001}$	$0.76^{+1.47}_{-0.52}$
196.....	990425	51293.450	$0.019^{+0.018}_{-0.009}$	$0.013^{+0.018}_{-0.009}$	$0.007^{+0.001}_{-0.001}$	$0.66^{+2.30}_{-0.56}$
197.....	990427	51295.520	$0.009^{+0.008}_{-0.004}$	$0.006^{+0.008}_{-0.004}$	$0.003^{+0.001}_{-0.001}$	$0.71^{+2.04}_{-0.55}$
198.....	990429	51297.376	$0.007^{+0.006}_{-0.003}$	$0.005^{+0.006}_{-0.003}$	$0.001^{+0.001}_{-0.001}$	$0.78^{+2.18}_{-0.60}$
199.....	990430	51298.052	$0.005^{+0.004}_{-0.003}$	$0.004^{+0.003}_{-0.003}$	$0.001^{+0.001}_{-0.000}$	$0.82^{+2.03}_{-0.62}$
200.....	990501	51299.344	$0.005^{+0.004}_{-0.002}$	$0.005^{+0.004}_{-0.002}$	$0.001^{+0.001}_{-0.000}$	$0.84^{+2.13}_{-0.62}$
201.....	990502	51300.458	...	...	...	...
202.....	990504	51302.459	...	...	...	...
203.....	990505	51303.391	...	...	...	...
204.....	990507	51305.124	...	...	...	...
205.....	990509	51307.322	$0.004^{+0.038}_{-0.001}$	$0.001^{+0.038}_{-0.001}$	$0.003^{+0.001}_{-0.001}$	$0.19^{+****}_{-0.19}$
206.....	990511	51309.720	$0.004^{+0.029}_{-0.001}$	$0.002^{+0.029}_{-0.001}$	$0.002^{+0.000}_{-0.000}$	$0.42^{+9.68}_{-0.40}$
207.....	990513	51311.519	$0.002^{+0.002}_{-0.001}$	$0.000^{+0.002}_{-0.001}$	$0.001^{+0.001}_{-0.001}$	$0.29^{+3.71}_{-0.35}$
208.....	990515	51313.317	$0.001^{+0.000}_{-0.000}$	...	$0.001^{+0.000}_{-0.000}$	...
209.....	990520	51318.768	...	...	...	...

[a] Start of observation. MJD = JD − 2,400,000.5.
[b] Start of PCA gain epoch 4.

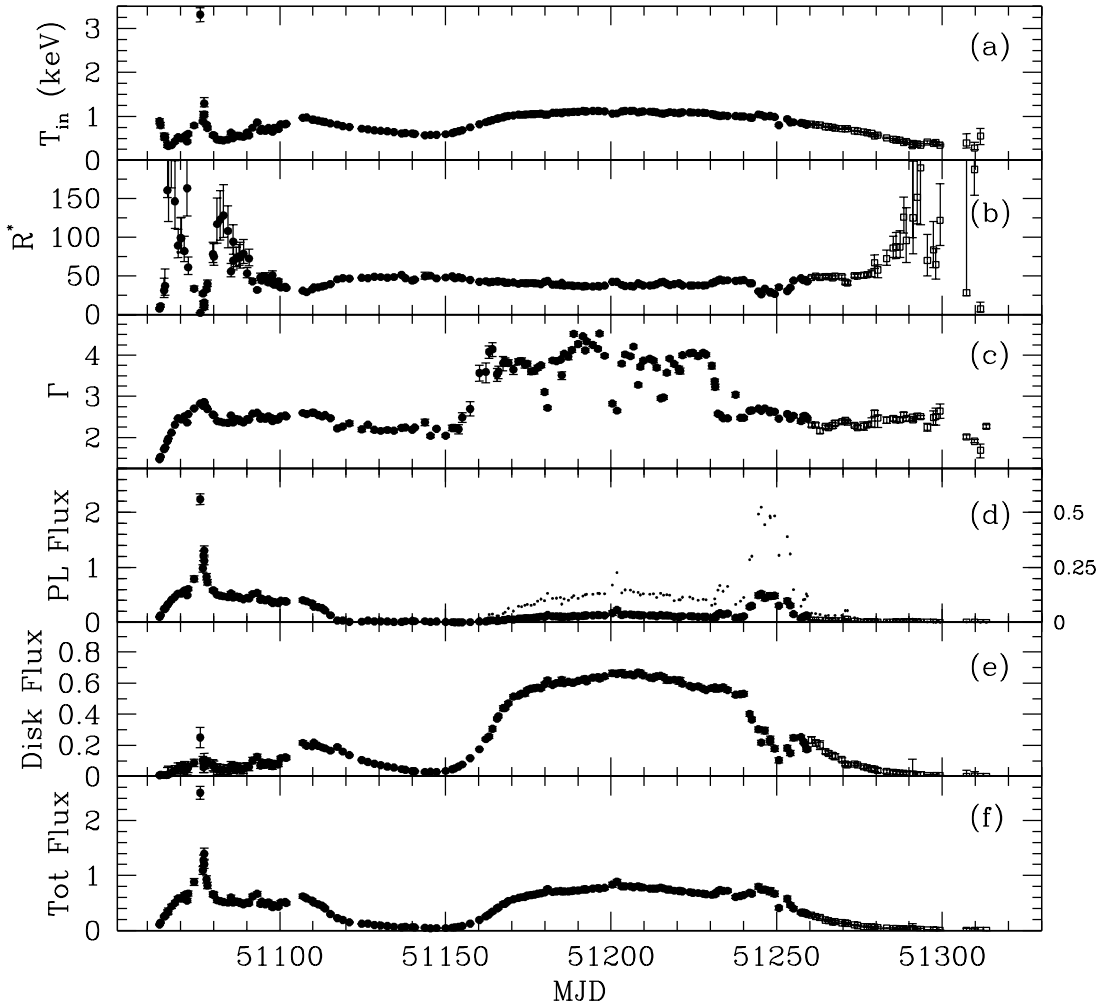

FIG. 4.—Spectral parameters and fluxes for PCA observations of XTE J1550−564. See the text for details on the spectral models and fitting. The quantities plotted here are (*a*) the color temperature of the accretion disk T_{in} in keV, (*b*) the inner disk radius $R^* = R_{in}(\cos i)^{1/2}/(D/6\ \mathrm{kpc})$ in km, where i is the inclination angle and D is the distance to the source in kpc, (*c*) the power-law photon index Γ, the unabsorbed 2–20 keV flux in units of 10^{-7} ergs s^{-1} cm^{-2} for (*d*) the power law, (*e*) the disk, and (*f*) the total. Data points from gain epoch 4, beginning on MJD 51260 (MJD = JD − 2,400,000.5), are plotted using an open square. When error bars are not visible, it is because they are comparable to or smaller than the plotting symbol. The dots plotted without error bars in (*d*) correspond to the right axis and are shown to highlight the behavior of the faint power-law component during the second half of the outburst.

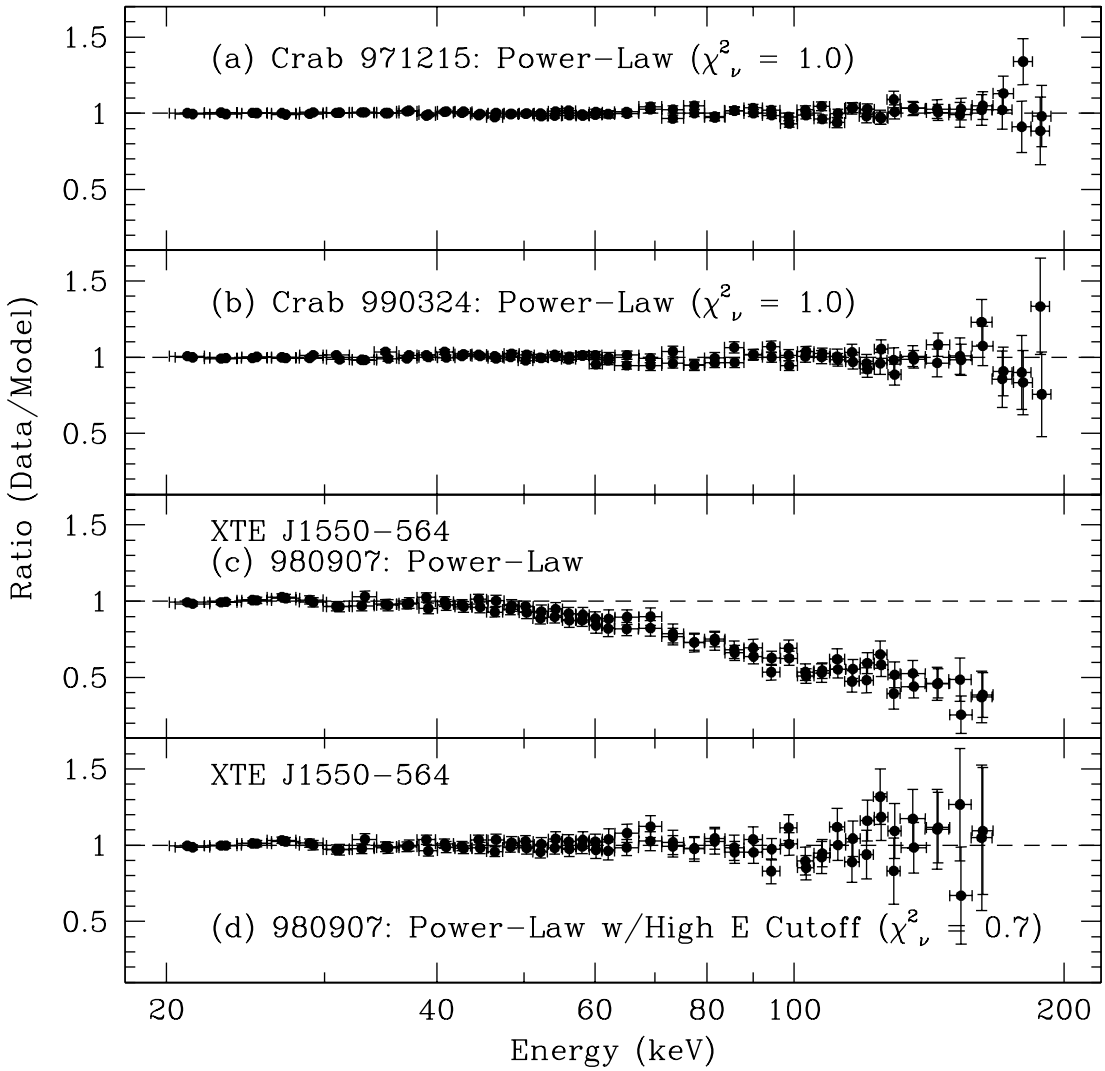

FIG. 5.—Ratio data/model for (*a*) power-law fit to the Crab on 1997 December 15, (*b*) later power-law fit to the Crab on 1999 March 24, (*c*) power-law fit to the first observation of XTE J1550−564 on 1998 September 7, and (*d*) the same observation of XTE J1550−564 fit to a model consisting of a power law with a high-energy cutoff (see eqs. [1a] and [1b]).

source displays strong 0.08–8 Hz QPOs (Cui et al. 1999). A high-energy cutoff is observed in the HEXTE spectrum during the initial rise with $E_{\rm fold} \sim 70$–150 (Fig. 3*a*, Table 4). Following the initial rise, the spectra from MJD 51074 to 51115 remain dominated by the power-law component (Fig. 3*b*), which has photon index $\Gamma \sim 2.4$–2.9 (Fig. 4*c*). The source displays strong 3–13 Hz QPOs during this time, whenever the power law contributes more than 60% of the observed X-ray flux (Remillard et al. 1999a; Sobczak et al. 1999a). This behavior is consistent with the *very high state* of black hole X-ray novae (BHXNe) (see Tanaka & Lewin 1995 and references therein for details on the spectral states of BHXNe). A high-energy cutoff in the power-law tail is observed during a number of very high state observations (Table 4). The peak luminosity (bolometric disk luminosity plus 2–100 keV power-law luminosity) during the flare on MJD 51075 is $L = 1.2 \times 10^{39}(D/6\ {\rm kpc})^2$ ergs s^{-1}, which corresponds to the Eddington luminosity for $M = 9.6\ M_\odot$ at 6 kpc (Sobczak et al. 1999a).

After MJD 51115 (1998 October 29), the source fades rapidly, the power-law component decays and hardens ($\Gamma = 2.0$–2.4), and the disk component begins to dominate the spectrum (see Fig. 3*c*). The source generally shows little temporal variability during this time (Remillard et al. 1999a; Sobczak et al. 1999a). We identify this behavior with the *high/soft state*. However, during this time the source occasionally exhibits QPOs at $\sim$5 Hz and power density spectra that have properties intermediate between the very high and high/soft states or the high/soft and low/hard states (Remillard et al. 1999a; Sobczak et al. 1999a). The *low/hard state* was not observed and the intensity increased dramatically after MJD 51150, marking the start of the second half of the outburst.

During the second half of the outburst (MJD 51150−51230), most of the observed spectra are dominated by the disk component (Fig. 3*d*), which contributes more than 85% of the 2–20 keV flux (Fig. 4*e*), and no QPOs are observed. Figure 4*c* shows that Γ increased sharply at the onset of the second half of the outburst from $\Gamma \sim 2$ to 4. These features are typical of the *high/soft state* of BHXNe. This dichotomy between the power-law–dominated first half and disk-dominated second half of the outburst is shared by GRO J1655−40 and cannot be easily explained by the standard disk instability model.

TABLE 4

HEXTE SPECTRAL PARAMETERS FOR XTE J1550−564

Observation Number	Date (UT)	MJD[a]	$\Gamma_{\rm HEXTE}$	$E_{\rm cut}$ (keV)	$E_{\rm fold}$ (keV)	Best χ^2_ν (dof)	PL χ^2_ν	$E_{\rm max}$ (keV)	20–100 keV Flux[b,c] (10^{-8} ergs s^{-1} cm^{-2})
1	980907	51063.695	$1.56^{+0.02}_{-0.03}$	$44.9^{+2.7}_{-2.7}$	114^{+7}_{-6}	0.65(79)	4.91	170	$1.17^{+0.09}_{-0.09}$
2	980908	51064.008	$1.52^{+0.03}_{-0.04}$	$31.1^{+1.5}_{-1.7}$	80^{+3}_{-4}	1.29(85)	26.92	200	$1.22^{+0.14}_{-0.16}$
3	980909	51065.066	$1.83^{+0.05}_{-0.06}$	$28.5^{+1.5}_{-1.6}$	68^{+3}_{-4}	1.08(79)	20.16	170	$1.43^{+0.22}_{-0.23}$
4	980909	51065.344	$2.00^{+0.04}_{-0.05}$	$31.1^{+1.8}_{-1.9}$	72^{+4}_{-4}	0.95(77)	11.06	160	$1.29^{+0.19}_{-0.20}$
5	980910	51066.066	$2.16^{+0.04}_{-0.05}$	$27.8^{+1.1}_{-1.3}$	75^{+4}_{-5}	1.22(75)	9.42	150	$1.18^{+0.14}_{-0.16}$
6	980910	51066.344	$2.22^{+0.06}_{-0.07}$	$27.5^{+1.9}_{-1.8}$	74^{+6}_{-6}	0.97(77)	8.66	160	$1.14^{+0.22}_{-0.21}$
7	980911	51067.270	$2.35^{+0.04}_{-0.05}$	$26.0^{+1.3}_{-1.2}$	80^{+6}_{-6}	1.16(75)	6.81	150	$1.07^{+0.15}_{-0.15}$
8	980912	51068.344	$2.61^{+0.04}_{-0.05}$	$27.6^{+1.7}_{-1.8}$	116^{+13}_{-12}	1.03(71)	2.98	140	$0.88^{+0.11}_{-0.12}$
9	980913	51069.273	$2.72^{+0.03}_{-0.05}$	$30.9^{+2.5}_{-3.2}$	129^{+14}_{-13}	0.98(69)	2.62	130	$0.78^{+0.09}_{-0.11}$
10	980914	51070.133	$2.70^{+0.03}_{-0.03}$	$29.0^{+1.8}_{-1.6}$	126^{+14}_{-11}	0.94(69)	2.78	130	$0.79^{+0.08}_{-0.08}$
11	980914	51070.273	$2.70^{+0.04}_{-0.04}$	$29.0^{+2.2}_{-2.2}$	127^{+7}_{-13}	0.83(65)	2.47	120	$0.79^{+0.09}_{-0.10}$
12	980915	51071.199	$2.70^{+0.04}_{-0.05}$	$27.8^{+2.3}_{-2.4}$	122^{+15}_{-15}	0.92(65)	2.71	120	$0.77^{+0.11}_{-0.12}$
13	980915	51071.996	$2.69^{+0.05}_{-0.09}$	$31.0^{+3.0}_{-4.8}$	118^{+24}_{-18}	1.20(61)	1.77	110	$0.85^{+0.14}_{-0.21}$
14	980916	51072.344	$2.76^{+0.04}_{-0.05}$	$29.0^{+2.8}_{-2.5}$	147^{+23}_{-18}	1.40(67)	2.35	125	$0.77^{+0.10}_{-0.10}$
15	980918	51074.141	$2.95^{+0.01}_{-0.01}$	...	...	1.30(53)	...	90	$0.81^{+0.04}_{-0.03}$
16	980919	51075.988	$2.96^{+0.01}_{-0.01}$	...	...	1.23(77)	...	150	$2.14^{+0.04}_{-0.04}$
17	980920	51076.801	$2.77^{+0.04}_{-0.04}$	$26.4^{+3.2}_{-2.3}$	216^{+27}_{-33}	1.28(75)	1.94	150	$0.93^{+0.11}_{-0.10}$
18	980920	51076.953	$2.77^{+0.03}_{-0.04}$	$26.7^{+3.1}_{-2.7}$	256^{+68}_{-48}	0.85(75)	1.22	150	$1.03^{+0.11}_{-0.12}$
19	980921	51077.145	$2.79^{+0.02}_{-0.04}$	$29.8^{+4.8}_{-4.9}$	346^{+70}_{-66}	0.67(75)	1.17	150	$1.11^{+0.09}_{-0.12}$
20	980921	51077.211	$2.79^{+0.02}_{-0.02}$	$28.0^{+2.1}_{-2.1}$	260^{+37}_{-30}	1.19(75)	2.26	150	$1.02^{+0.07}_{-0.07}$
21	980921	51077.867	$2.81^{+0.02}_{-0.02}$	$28.0^{+2.0}_{-2.0}$	264^{+39}_{-31}	1.22(75)	2.21	150	$0.84^{+0.05}_{-0.06}$
22	980922	51078.133	$2.82^{+0.03}_{-0.04}$	$29.2^{+2.9}_{-2.5}$	190^{+32}_{-25}	1.04(71)	1.82	140	$0.76^{+0.08}_{-0.08}$
23	980923	51079.793	$2.68^{+0.06}_{-0.07}$	$30.5^{+3.4}_{-3.2}$	101^{+24}_{-16}	1.11(41)	1.67	70	$0.71^{+0.14}_{-0.14}$
24	980924	51080.078	$2.68^{+0.05}_{-0.04}$	$25.9^{+1.7}_{-1.3}$	124^{+22}_{-13}	1.03(75)	2.03	150	$0.75^{+0.12}_{-0.08}$
25	980925	51081.062	$2.63^{+0.04}_{-0.07}$	$27.4^{+1.9}_{-2.3}$	107^{+13}_{-14}	1.33(55)	3.39	100	$0.80^{+0.12}_{-0.15}$
26	980926	51082.004	$2.60^{+0.04}_{-0.04}$	$26.1^{+1.7}_{-1.4}$	108^{+10}_{-9}	1.41(75)	5.82	150	$0.82^{+0.11}_{-0.10}$
27	980927	51083.004	$2.62^{+0.05}_{-0.04}$	$26.4^{+2.3}_{-1.5}$	128^{+20}_{-14}	0.91(75)	2.20	150	$0.84^{+0.13}_{-0.10}$
28	980928	51084.340	$2.49^{+0.05}_{-0.07}$	$26.8^{+1.9}_{-1.8}$	85^{+9}_{-9}	0.77(61)	3.76	110	$0.84^{+0.15}_{-0.16}$
29	980929	51085.270	$2.50^{+0.12}_{-0.32}$	$26.7^{+5.2}_{-6.3}$	87^{+28}_{-35}	1.11(51)	1.54	90	$0.73^{+0.33}_{-0.46}$
30	980929	51085.918	$2.56^{+0.07}_{-0.11}$	$28.3^{+3.3}_{-3.3}$	95^{+18}_{-16}	0.79(55)	1.64	100	$0.79^{+0.20}_{-0.22}$
31	980929	51085.992	$2.82^{+0.03}_{-0.03}$	...	...	1.45(53)	...	90	$0.80^{+0.09}_{-0.08}$
32	980930	51086.891	$2.62^{+0.03}_{-0.05}$	$30.5^{+2.4}_{-3.1}$	132^{+11}_{-12}	1.22(73)	4.17	145	$0.75^{+0.07}_{-0.11}$
33	981001	51087.723	$2.59^{+0.03}_{-0.03}$	$27.0^{+1.6}_{-1.3}$	131^{+13}_{-10}	1.20(71)	4.29	140	$0.75^{+0.08}_{-0.07}$
34	981002	51088.008	$2.59^{+0.03}_{-0.05}$	$29.7^{+2.1}_{-2.7}$	126^{+11}_{-11}	1.24(75)	4.03	150	$0.78^{+0.08}_{-0.11}$
35	981003	51089.008	$2.45^{+0.04}_{-0.07}$	$26.9^{+1.6}_{-1.9}$	93^{+10}_{-11}	1.34(67)	3.24	125	$0.78^{+0.12}_{-0.15}$
36	981004	51090.145	$2.51^{+0.08}_{-0.19}$	$26.0^{+4.5}_{-5.3}$	116^{+29}_{-39}	0.78(55)	1.63	100	$0.74^{+0.21}_{-0.31}$
37	981004	51090.703	$2.43^{+0.07}_{-0.14}$	$25.4^{+2.4}_{-3.0}$	98^{+22}_{-24}	1.02(55)	1.60	100	$0.71^{+0.18}_{-0.24}$
38	981005	51091.742	$2.74^{+0.02}_{-0.02}$	...	...	1.51(53)	...	90	$0.71^{+0.04}_{-0.04}$
39	981007	51093.145	$2.45^{+0.06}_{-0.11}$	$27.6^{+3.6}_{-4.0}$	118^{+26}_{-26}	0.91(55)	1.62	100	$0.72^{+0.16}_{-0.21}$
40	981008	51094.145	$2.31^{+0.07}_{-0.13}$	$24.6^{+1.9}_{-2.6}$	88^{+14}_{-19}	1.18(55)	2.38	100	$0.71^{+0.16}_{-0.23}$
41	981008	51094.570	$2.55^{+0.03}_{-0.04}$	$31.4^{+3.1}_{-3.0}$	159^{+24}_{-19}	1.29(75)	2.12	150	$0.67^{+0.08}_{-0.08}$
42	981009	51095.609	$2.66^{+0.02}_{-0.02}$	...	...	1.58(57)	...	100	$0.69^{+0.04}_{-0.04}$
43	981010	51096.574	$2.63^{+0.01}_{-0.01}$	...	...	1.26(57)	...	100	$0.68^{+0.03}_{-0.03}$
44	981011	51097.570	$2.22^{+0.13}_{-0.23}$	$24.3^{+4.4}_{-5.6}$	86^{+30}_{-28}	0.90(55)	1.29	100	$0.65^{+0.32}_{-0.33}$
45	981011	51097.809	$2.32^{+0.08}_{-0.15}$	$27.5^{+1.6}_{-3.4}$	91^{+25}_{-23}	1.11(41)	1.53	70	$0.66^{+0.18}_{-0.24}$
46	981012	51098.277	$2.58^{+0.02}_{-0.02}$	...	...	1.17(57)	...	100	$0.68^{+0.04}_{-0.04}$
47	981013	51099.215	$2.47^{+0.05}_{-0.06}$	$35.7^{+5.0}_{-5.1}$	131^{+41}_{-25}	0.89(55)	1.18	100	$0.64^{+0.11}_{-0.11}$
48	981013	51099.609	$2.49^{+0.04}_{-0.05}$	$35.4^{+6.8}_{-35.4}$	178^{+41}_{-29}	0.84(71)	1.24	140	$0.64^{+0.10}_{-0.31}$
49	981014	51100.285	$2.40^{+0.07}_{-0.27}$	$29.5^{+8.0}_{-29.4}$	157^{+47}_{-39}	0.87(55)	1.26	100	$0.66^{+0.17}_{-0.19}$
50	981015	51101.605	$2.58^{+0.02}_{-0.02}$	...	...	1.00(57)	...	100	$0.62^{+0.04}_{-0.04}$
51	981015	51101.941	$2.54^{+0.02}_{-0.02}$	...	...	1.53(49)	...	80	$0.65^{+0.04}_{-0.03}$
52	981020	51106.953	$2.48^{+0.03}_{-0.03}$	...	...	0.88(57)	...	100	$0.63^{+0.06}_{-0.05}$
53	981022	51108.074	$2.37^{+0.02}_{-0.03}$	$33.2^{+3.7}_{-3.9}$	237^{+27}_{-25}	1.02(77)	2.46	165	$0.63^{+0.05}_{-0.06}$
54	981023	51109.738	$2.39^{+0.04}_{-0.03}$	...	...	0.76(43)	...	70	$0.58^{+0.07}_{-0.06}$
55	981024	51110.270	$2.38^{+0.02}_{-0.02}$	...	...	1.34(57)	...	100	$0.47^{+0.03}_{-0.03}$
56	981025	51111.602	$2.39^{+0.03}_{-0.03}$	...	...	0.69(43)	...	70	$0.51^{+0.06}_{-0.05}$
57	981026	51112.801	$2.40^{+0.02}_{-0.02}$	...	...	1.22(55)	...	100	$0.49^{+0.03}_{-0.03}$
58	981027	51113.668	$2.41^{+0.05}_{-0.05}$	...	...	1.34(27)	...	50	$0.38^{+0.06}_{-0.05}$
59	981029	51115.281	$2.18^{+0.03}_{-0.03}$	...	...	0.88(49)	...	80	$0.28^{+0.03}_{-0.03}$
60	981031	51117.352	$1.92^{+0.06}_{-0.06}$	...	...	1.42(37)	...	60	$0.13^{+0.03}_{-0.02}$
61	981102	51119.004	$1.90^{+0.06}_{-0.06}$	...	...	0.86(43)	...	70	$0.11^{+0.02}_{-0.02}$
62	981104	51121.004	2.5(fixed)	...	...	...	...	100	<0.030
63	981107	51124.727	2.5(fixed)	...	...	...	...	100	<0.050
64	981109	51126.594	$1.98^{+0.07}_{-0.06}$	...	...	0.63(31)	...	55	$0.10^{+0.02}_{-0.02}$

TABLE 4—*Continued*

Observation Number	Date (UT)	MJD[a]	$\Gamma_{\rm HEXTE}$	$E_{\rm cut}$ (keV)	$E_{\rm fold}$ (keV)	Best χ^2_ν (dof)	PL χ^2_ν	$E_{\rm max}$ (keV)	20–100 keV Flux[b,c] (10^{-8} ergs s^{-1} cm^{-2})
65	981111	51128.562	$1.75^{+0.13}_{-0.12}$	...	...	0.82(27)	...	50	$0.09^{+0.05}_{-0.03}$
66	981113	51130.457	$1.74^{+0.09}_{-0.09}$	...	...	0.97(27)	...	50	$0.09^{+0.03}_{-0.02}$
67	981115	51132.480	2.5(fixed)	...	...	...	...	100	<0.055
68	981117	51134.438	2.5(fixed)	...	...	...	...	100	<0.033
69	981119	51136.777	2.5(fixed)	...	...	...	...	100	<0.032
70	981120	51137.922	2.5(fixed)	...	...	...	...	100	<0.063
71	981122	51139.992	2.5(fixed)	...	...	...	...	100	<0.076
72	981123	51140.707	$2.23^{+0.15}_{-0.19}$	...	...	0.34(27)	...	50	$0.07^{+0.04}_{-0.03}$
73	981126	51143.801	2.5(fixed)	...	...	...	...	100	<0.090
74	981128	51145.477	2.5(fixed)	...	...	...	...	100	<0.028
75	981130	51147.336	2.5(fixed)	...	...	...	...	100	<0.048
76	981203	51150.074	2.5(fixed)	...	...	...	...	100	<0.034
77	981205	51152.078	2.5(fixed)	...	...	...	...	100	<0.018
78	981205	51152.867	2.5(fixed)	...	...	...	...	100	<0.013
79	981207	51154.016	2.5(fixed)	...	...	...	...	100	<0.014
80	981208	51155.066	2.5(fixed)	...	...	...	...	100	<0.012
81	981210	51157.492	2.5(fixed)	...	...	...	...	100	<0.010
82	981213	51160.277	2.5(fixed)	...	...	...	...	100	<0.008
83	981215	51162.203	2.5(fixed)	...	...	...	...	100	<0.006
84	981216	51163.207	2.5(fixed)	...	...	...	...	100	<0.030
85	981217	51164.207	...	...	...	...	...	...	...
86	981218	51165.590	2.5(fixed)	...	...	...	...	100	<0.012
87	981219	51166.012	2.5(fixed)	...	...	...	...	100	<0.013
88	981220	51167.418	...	...	...	...	...	...	...
89	981221	51168.012	2.5(fixed)	...	...	...	...	100	<0.014
90	981222	51169.008	2.5(fixed)	...	...	...	...	100	<0.013
91	981223	51170.520	2.5(fixed)	...	...	...	...	100	<0.015
92	981225	51172.066	2.5(fixed)	...	...	...	...	100	<0.016
93	981226	51172.988	2.5(fixed)	...	...	...	...	100	<0.014
94	981227	51173.988	2.5(fixed)	...	...	...	...	100	<0.018
95	981227	51174.723	2.5(fixed)	...	...	...	...	100	<0.016
96	981228	51175.879	2.5(fixed)	...	...	...	...	100	<0.023
97	981229	51176.848	2.5(fixed)	...	...	...	...	100	<0.025
98	981230	51177.844	2.5(fixed)	...	...	...	...	100	<0.023
99	981231	51178.844	2.5(fixed)	...	...	...	...	100	<0.027
100	990101	51179.918	$2.14^{+0.11}_{-0.10}$	...	...	0.94(27)	...	50	$0.07^{+0.03}_{-0.02}$
101	990102	51180.844	$2.12^{+0.03}_{-0.03}$	...	...	1.25(57)	...	100	$0.20^{+0.02}_{-0.02}$
102	990104	51182.336	2.5(fixed)	...	...	...	...	100	<0.018
103	990105	51183.539	2.5(fixed)	...	...	...	...	100	<0.022
104	990106	51184.711	2.5(fixed)	...	...	...	...	100	<0.017
105	990107	51185.125	2.5(fixed)	...	...	...	...	100	<0.032
106	990107	51185.848	2.5(fixed)	...	...	...	...	100	<0.012
107	990109	51187.125	2.5(fixed)	...	...	...	...	100	<0.008
108	990110	51188.195	2.5(fixed)	...	...	...	...	100	<0.010
109	990110	51188.730	2.5(fixed)	...	...	...	...	100	<0.009
110	990112	51190.055	2.5(fixed)	...	...	...	...	100	<0.013
111	990113	51191.484	2.5(fixed)	...	...	...	...	100	<0.009
112	990114	51192.188	2.5(fixed)	...	...	...	...	100	<0.011
113	990114	51192.594	2.5(fixed)	...	...	...	...	100	<0.018
114	990116	51194.500	2.5(fixed)	...	...	...	...	100	<0.013
115	990118	51196.051	2.5(fixed)	...	...	...	...	100	<0.015
116	990118	51196.523	...	...	...	...	...	...	...
117	990120	51198.051	2.5(fixed)	...	...	...	...	100	<0.019
118	990122	51200.383	2.5(fixed)	...	...	...	...	100	<0.189
119	990123	51201.781	$2.20^{+0.02}_{-0.02}$	...	...	0.91(51)	...	100	$0.38^{+0.03}_{-0.03}$
120	990125	51203.250	2.5(fixed)	...	...	...	...	100	<0.032
121	990126	51204.246	2.5(fixed)	...	...	...	...	100	<0.038
122	990127	51205.852	2.5(fixed)	...	...	...	...	100	<0.025
123	990128	51206.781	2.5(fixed)	...	...	...	...	100	<0.016
124	990130	51208.180	2.5(fixed)	...	...	...	...	100	<0.079
125	990130	51208.844	2.5(fixed)	...	...	...	...	100	<0.029
126	990131	51209.711	2.5(fixed)	...	...	...	...	100	<0.027
127	990202	51211.711	2.5(fixed)	...	...	...	...	100	<0.021
128	990203	51212.773	2.5(fixed)	...	...	...	...	100	<0.026
129	990204	51213.773	2.5(fixed)	...	...	...	...	100	<0.028
130	990205	51214.973	$2.09^{+0.04}_{-0.04}$	...	...	1.22(57)	...	100	$0.14^{+0.02}_{-0.02}$

TABLE 4—*Continued*

Observation Number	Date (UT)	MJD[a]	$\Gamma_{\rm HEXTE}$	$E_{\rm cut}$ (keV)	$E_{\rm fold}$ (keV)	Best χ^2_ν (dof)	PL χ^2_ν	$E_{\rm max}$ (keV)	20–100 keV Flux[b,c] (10^{-8} ergs s^{-1} cm^{-2})
131	990206	51215.840	$2.07^{+0.03}_{-0.03}$	...	...	0.72(63)	...	110	$0.13^{+0.01}_{-0.01}$
132	990207	51216.836	2.5(fixed)	...	...	...	...	100	<0.038
133	990208	51217.703	2.5(fixed)	...	...	...	...	100	<0.020
134	990210	51219.055	2.5(fixed)	...	...	...	...	100	<0.024
135	990211	51220.508	2.5(fixed)	...	...	...	...	100	<0.021
136	990211	51220.836	2.5(fixed)	...	...	...	...	100	<0.031
137	990212	51221.566	2.5(fixed)	...	...	...	...	100	<0.017
138	990214	51223.766	2.5(fixed)	...	...	...	...	100	<0.016
139	990215	51224.699	2.5(fixed)	...	...	...	...	100	<0.014
140	990217	51226.297	2.5(fixed)	...	...	...	...	100	<0.021
141	990218	51227.836	2.5(fixed)	...	...	...	...	100	<0.013
142	990219	51228.695	2.5(fixed)	...	...	...	...	100	<0.013
143	990221	51230.426	2.5(fixed)	...	...	...	...	100	<0.017
144	990222	51231.293	2.5(fixed)	...	...	...	...	100	<0.054
145	990222	51231.422	2.5(fixed)	...	...	...	...	100	<0.045
146	990223	51232.250	$2.07^{+0.04}_{-0.04}$	...	...	0.99(37)	...	60	$0.29^{+0.04}_{-0.04}$
147	990223	51232.859	$2.13^{+0.03}_{-0.03}$	...	...	0.81(57)	...	100	$0.34^{+0.04}_{-0.04}$
148	990224	51233.836	$2.19^{+0.03}_{-0.03}$	...	...	0.91(71)	...	130	$0.30^{+0.03}_{-0.03}$
149	990226	51235.199	$1.94^{+0.14}_{-0.06}$	$22.4^{+18.1}_{-22.4}$	182^{+111}_{-36}	0.90(75)	1.34	150	$0.37^{+0.19}_{-0.06}$
150	990228	51237.617	$1.91^{+0.11}_{-0.10}$	...	...	0.90(27)	...	50	$0.08^{+0.04}_{-0.02}$
151	990302	51239.082	$2.13^{+0.02}_{-0.02}$	...	...	1.03(57)	...	100	$0.20^{+0.02}_{-0.01}$
152	990303	51240.062	$2.16^{+0.03}_{-0.03}$	...	...	0.97(53)	...	90	$0.25^{+0.03}_{-0.02}$
153	990304	51241.828	$2.39^{+0.02}_{-0.02}$	...	...	0.96(67)	...	120	$0.42^{+0.03}_{-0.03}$
154	993005	51242.508	$2.36^{+0.03}_{-0.03}$	...	...	0.84(63)	...	110	$0.45^{+0.04}_{-0.04}$
155	990307	51244.496	$2.56^{+0.02}_{-0.02}$	...	...	0.98(63)	...	110	$0.64^{+0.05}_{-0.05}$
156	990308	51245.352	$2.59^{+0.01}_{-0.01}$	...	...	1.34(67)	...	120	$0.71^{+0.03}_{-0.03}$
157	990309	51246.414	$2.53^{+0.01}_{-0.01}$	...	...	1.42(77)	...	150	$0.56^{+0.02}_{-0.02}$
158	990310	51247.980	$2.58^{+0.01}_{-0.01}$	...	...	0.92(73)	...	140	$0.70^{+0.03}_{-0.03}$
159	990311	51248.090	$2.53^{+0.01}_{-0.02}$	...	...	0.91(67)	...	120	$0.67^{+0.03}_{-0.03}$
160	990312	51249.398	$2.51^{+0.03}_{-0.03}$	...	...	0.79(53)	...	90	$0.71^{+0.07}_{-0.06}$
161	990313	51250.691	$2.30^{+0.04}_{-0.08}$	$33.7^{+4.1}_{-6.7}$	153^{+28}_{-12}	1.19(61)	1.85	110	$0.61^{+0.08}_{-0.14}$
162	990316	51253.227	$2.41^{+0.03}_{-0.03}$	...	...	1.56(53)	...	90	$0.63^{+0.08}_{-0.07}$
163	990317	51254.090	$2.38^{+0.02}_{-0.02}$	...	...	0.93(57)	...	100	$0.63^{+0.04}_{-0.04}$
164	990318	51255.090	$2.25^{+0.02}_{-0.02}$	...	...	1.09(57)	...	100	$0.29^{+0.02}_{-0.02}$
165	990320	51257.363	$1.95^{+0.12}_{-0.11}$	...	...	0.71(27)	...	50	$0.21^{+0.10}_{-0.07}$
166	990321	51258.086	$2.15^{+0.07}_{-0.07}$	...	...	0.56(27)	...	50	$0.21^{+0.06}_{-0.04}$
167	990321	51258.496	$2.06^{+0.05}_{-0.05}$	...	...	1.04(37)	...	60	$0.24^{+0.05}_{-0.04}$
168	990321	51258.977	$2.23^{+0.03}_{-0.03}$	...	...	0.95(67)	...	120	$0.26^{+0.03}_{-0.02}$
169	990322	51259.254	$2.13^{+0.09}_{-0.09}$	...	...	0.98(37)	...	60	$0.28^{+0.10}_{-0.07}$
170	990323	51260.551	$1.84^{+0.07}_{-0.07}$	...	...	1.11(27)	...	50	$0.16^{+0.04}_{-0.03}$
171	990324	51261.766	$1.81^{+0.07}_{-0.07}$	...	...	0.93(37)	...	60	$0.15^{+0.04}_{-0.03}$
172	990326	51263.109	$1.78^{+0.11}_{-0.11}$	...	...	1.19(27)	...	50	$0.15^{+0.06}_{-0.04}$
173	990327	51264.746	$1.95^{+0.06}_{-0.06}$	...	...	0.85(57)	...	100	$0.11^{+0.02}_{-0.02}$
174	990328	51265.613	$1.96^{+0.08}_{-0.08}$	...	...	0.99(27)	...	50	$0.12^{+0.04}_{-0.03}$
175	990329	51266.879	$1.94^{+0.13}_{-0.13}$	...	...	0.85(27)	...	50	$0.07^{+0.04}_{-0.02}$
176	990330	51267.613	$1.77^{+0.08}_{-0.07}$	...	...	1.15(27)	...	50	$0.12^{+0.03}_{-0.03}$
177	990401	51269.676	$1.83^{+0.08}_{-0.08}$	...	...	1.07(27)	...	50	$0.11^{+0.03}_{-0.03}$
178	990402	51270.742	$2.07^{+0.04}_{-0.04}$	...	...	1.10(57)	...	100	$0.15^{+0.02}_{-0.02}$
179	990403	51271.406	$2.01^{+0.06}_{-0.06}$	...	...	0.57(39)	...	70	$0.15^{+0.03}_{-0.03}$
180	990405	51273.539	$1.97^{+0.07}_{-0.07}$	...	...	0.75(43)	...	70	$0.08^{+0.02}_{-0.02}$
181	990406	51274.473	$1.57^{+0.14}_{-0.14}$	...	...	0.67(25)	...	49	$0.08^{+0.05}_{-0.03}$
182	990408	51276.277	2.5(fixed)	...	...	...	...	100	<0.031
183	990409	51277.402	2.5(fixed)	...	...	...	...	100	<0.038
184	990410	51278.688	2.5(fixed)	...	...	...	...	100	<0.041
185	990411	51279.531	2.5(fixed)	...	...	...	...	100	<0.030
186	990412	51280.543	2.5(fixed)	...	...	...	...	100	<0.023
187	990415	51283.223	2.5(fixed)	...	...	...	...	100	<0.030
188	990417	51285.195	2.5(fixed)	...	...	...	...	100	<0.025
189	990418	51286.059	2.5(fixed)	...	...	...	...	100	<0.024
190	990419	51287.258	2.5(fixed)	...	...	...	...	100	<0.037
191	990420	51288.383	2.5(fixed)	...	...	...	...	100	<0.019
192	990421	51289.145	2.5(fixed)	...	...	...	...	100	<0.039
193	990422	51290.984	2.5(fixed)	...	...	...	...	100	<0.049
194	990423	51291.184	2.5(fixed)	...	...	...	...	100	<0.034
195	990424	51292.449	2.5(fixed)	...	...	...	...	100	<0.017

TABLE 4—*Continued*

Observation Number	Date (UT)	MJD[a]	Γ_{HEXTE}	E_{cut} (keV)	E_{fold} (keV)	Best χ^2_ν (dof)	PL χ^2_ν	E_{max} (keV)	20–100 keV Flux[b,c] (10^{-8} ergs s^{-1} cm^{-2})
196.....	990425	51293.449	2.5(fixed)	...	...	...	...	100	<0.020
197.....	990427	51295.520	2.5(fixed)	...	...	...	...	100	<0.013
198.....	990429	51297.375	2.5(fixed)	...	...	...	...	100	<0.007
199.....	990430	51298.051	2.5(fixed)	...	...	...	...	100	<0.005
200.....	990501	51299.344	2.5(fixed)	...	...	...	...	100	<0.003
201.....	990502	51300.457	...	...	...	...	...	...	...
202.....	990504	51302.461	...	...	...	...	...	...	...
203.....	990505	51303.391	...	...	...	...	...	...	...
204.....	990507	51305.125	...	...	...	...	...	...	...
205.....	990509	51307.320	2.5(fixed)	...	...	...	...	100	<0.020
206.....	990511	51309.719	2.5(fixed)	...	...	...	...	100	<0.015
207.....	990513	51311.520	2.5(fixed)	...	...	...	...	100	<0.009
208.....	990515	51313.316	...	...	...	...	...	...	...
209.....	990520	51318.770	...	...	...	...	...	...	...

NOTE.—HEXTE only from 20 − E_{max} keV.
[a] Start of observation. MJD = JD − 2,400,000.5.
[b] Flux is normalized to the HEXTE (Cluster A), which is ~20%–30% lower than the PCA normalization.
[c] Upper limits for the 20–100 keV flux are given at the 3 σ level of confidence.

Also during the second half of the outburst, there are a few instances lasting 2 or 3 days when the power law hardens from $\Gamma \sim 4$ to 2.5 (Fig. 4*c*). During one of these instances (MJD 51201), the power-law flux increases by almost a factor of 2 and the source is also detected in the HEXTE (see Table 4). After MJD 51230 (1999 February 21), the power law hardens considerably (Fig. 4*c*) and there is an intense power-law flare, which begins on MJD 51241 (1999 March 4; see Fig. 4*d*), accompanied by a sharp decline in the disk flux (Fig. 4*e*). QPOs from 5–18 Hz also reappear during this power-law flare. A sample spectrum from this flare is shown in Figure 3*e*. A high-energy cutoff in the power-law component is marginally detected in two HEXTE observations during the second half of the outburst (Table 4). The total flux decreases steadily as the power-law flare fades after MJD 51260 (1999 March 23; see Fig. 4*f*). The spectrum of one of the last few observations resembles the low/hard state and is shown in Figure 3*f*.

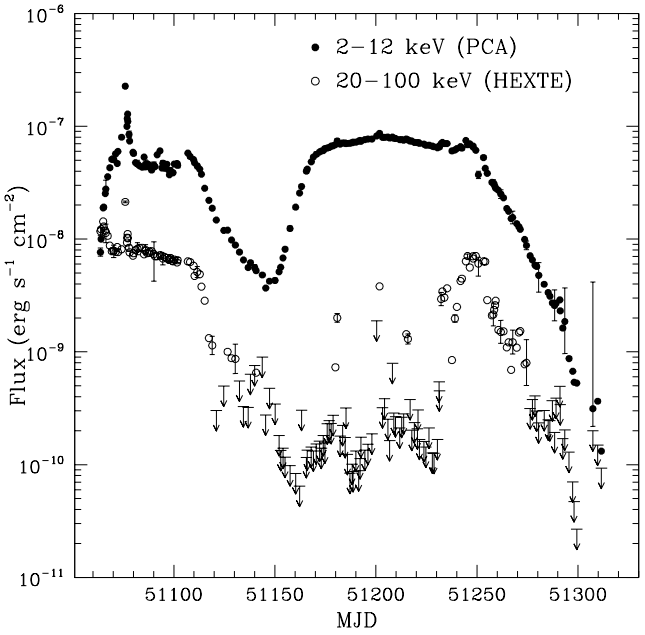

FIG. 6.—Plot of the 2–12 keV PCA flux and the 20–100 keV HEXTE flux vs. time (MJD = JD −2,400,000.5). Representative error bars are plotted for every fifth point. Upper limits for the HEXTE data are plotted at the 3 σ level of confidence (recall that the normalization of the HEXTE instrument is systematically ~20%–30% lower than the PCA).

A comparison of the 2–12 keV (soft) PCA flux and the 20–100 keV (hard) HEXTE flux is shown in Figure 6. During the first few observations, the hard flux exceeds or is approximately equal to the soft flux. Following the initial rise, during the very high state in the first half of the outburst, the soft flux exceeds the hard flux by almost an order of magnitude. During the high/soft state in the second half of the outburst, the source is usually undetectable in the HEXTE, and the upper limits on the hard flux show that the soft flux exceeds the hard flux by more than 2.5 orders of magnitude. This strong dominance of the soft flux over the hard flux is characteristic of the high/soft state. The hard flux increases again during the power-law flare and subsequent decline that mark the end of the outburst. Similar variations in the relative strength of the soft and hard flux between outburst states were also observed for the BHXN Nova Muscae 1991 (Esin, McClintock, & Narayan 1997) and are a good means of differentiating the very high and high/soft states.

From Figure 4*b*, it appears that the inner radius of the disk does not appear to be constant throughout the outburst cycle. From Figure 4*b* and Table 2, we see that the intense 6.8 crab flare on MJD 51075 (1999 September 19) is accompanied by a dramatic decrease of the inner disk radius from 33 to 2 km over one day. Similar behavior was observed for GRO J1655−40 during its 1996–1997 outburst: The observed inner disk radius decreased by almost a factor of 4 during periods of increased power-law emission in the very high state, and it was generally larger in the high/soft state (Sobczak et al. 1999b). Below we discuss both the problems and possible interpretations that are relevant to our spectral results, focussing on the observed variation of the inner disk radius.

4. DISCUSSION

4.1. *The Inner Disk Radius*

The physical radius of the inner disk may vary in XTE J1550−564 and GRO J1655−40—by as much as a factor of 16 in one day in the case of XTE J1550−564.

Another possibility, however, is that the apparent decrease of the inner disk radius observed during intense flares is caused by the failure of the multicolor disk/power-law model at these times. This failure may be caused by one or both of the following effects: (1) *Variations in spectral hardening, which occurs because electron scattering as opposed to free-free absorption dominates the opacity in the inner disk* (Shakura & Sunyaev 1973). This causes the observed (color) temperature of the disk to appear higher than the effective temperature, which decreases the normalization of the multicolor disk model from which the radius is inferred (Ebisawa et al. 1994; Shimura & Takahara 1995). The spectral hardening correction is likely not to be constant in extreme situations, such as the 6.8 crab flare, and any increase in spectral hardening will appear as a decrease in the observed inner disk radius. (2) *The Compton upscattering of soft disk photons, which is likely the origin of the power-law component in BHXNe.* In this case, an increase in power-law emission naturally implies an increase in the Comptonization of soft disk photons. Therefore, the measured normalization of the multicolor disk (from which the radius is derived) represents only a fraction of the intrinsic X-ray emission from the disk because the photons that are upscattered to produce the power-law component are missing. This causes the inferred radius to decrease (Zhang et al. 2000), although a corresponding increase in the mass accretion rate is necessary to explain the associated increase in the apparent disk temperature. Thus, intense flares may cause an apparent decrease in the radius of the inner disk due to increased spectral hardening and/or Compton upscattering of soft disk photons, while the actual physical radius may remain fairly constant.

The above interpretation is bolstered by the constancy of the inner disk radius of XTE J1550−564 when the power law is weak: The observed inner disk radius remains approximately constant at $\sim$40 km (assuming $i = 0°$, $D = 6$ kpc) over 120 days from MJD 51120−51240 when the power law contributes less than 20% of the 2–20 keV flux, even though the disk flux and total flux vary by an order of magnitude. The observed inner disk radius in GRO J1655−40 also remains approximately constant over more than 150 days during the high state, when the power law contributes less than 10% of the flux (Sobczak et al. 1999b). Similar behavior has been observed for several other BHXNe and Galactic black hole candidates, where the observed stable inner disk radius was plausibly identified with the last stable orbit (Tanaka & Lewin 1995). If we hypothesize that the stable value of the radius for XTE J1550−564 is a reasonable measure of the radius of the last stable orbit ($6r_g$, where $r_g = GM/c^2$), then a drop by a factor of 20 (observed between the peak flare and the high/soft state) would imply a decrease from $6r_g$ to $0.3r_g$, which is well within the event horizon of the black hole. This result is independent of the assumed distance and inclination. We thus conclude that the small inner disk radius observed during the 6.8 crab flare is unphysical and that the inner disk radius during the most intense power-law activity cannot be reliably determined from the multicolor disk model. This interpretation is supported by the work of Merloni, Fabian, & Ross (1999), who used a self-consistent model for radiative transfer and vertical temperature structure in a Shakura-Sunyaev disk and found that (1) the multicolor disk model systematically underestimates the inner disk radius when most of the gravitational energy is dissipated in the corona and (2) the multicolor disk model gives stable, acceptable results for high accretion rates ($\gtrsim$10% of the Eddington accretion rate) and/or when a lower fraction of the gravitational energy is dissipated in the corona.

In contrast to the apparent decrease of the inner disk radius observed during the 6.8 crab flare, the radius appears to increase at times near the beginning and end of the outburst cycle (Fig. 4*b*). It is not clear whether these observed increases of the inner disk radius are physical or not; in the following we discuss two possible causes.

The advection-dominated accretion flow (ADAF) model predicts changes in the inner disk radius during the initial rise and the final decline of the outburst. According to the ADAF model, the inner edge of the disk should move inward (from hundreds of gravitational radii) to the last stable orbit during the initial rise, and it should move outward again at the end of the outburst during the transition from the high/soft state to the low/hard state (Esin, McClintock, & Narayan 1997). However, the ADAF model predicts that the radius should move inward on a viscous timescale of several days (Hameury et al. 1998) during the initial rise; instead, about 30 days elapsed between the initial rise and the time when the observed inner disk radius reached an approximately constant value (Fig. 4*b*). On the other hand, the observed increase of the inner disk radius near the end of the outburst from MJD 51279−51293 is in better agreement with the predictions of the ADAF model. The critical mass accretion rate at which the soft-to-hard transition takes place in the ADAF model is approximately $\dot{m}_{\rm crit} \sim 1.3\alpha^2$ (in Eddington units), where α is the standard viscosity coefficient (Esin et al. 1997). The ADAF model predicts that the inner edge of the disk should begin to move outward from the last stable orbit when $\dot{m} \lesssim \dot{m}_{\rm crit}$. We can estimate the mass accretion rate ($\dot{m}$) of XTE J1550−564 in Eddington units by assuming that the 6.8 crab flare corresponds to the Eddington accretion rate and scaling the inferred accretion rate by the total observed flux. The ratio of the total observed flux on MJD 51279, when the observed radius begins to increase, to the total flux during the 6.8 crab flare corresponds to a mass accretion rate $\dot{m} \sim 0.02$ (Table 3). The mass accretion rate at this time corresponds to the critical accretion rate for $\alpha = 0.12$, which is smaller than the value $\alpha = 0.25$ used by Esin et al. (1997) to model the outburst of Nova Muscae 1991 but is still in reasonable agreement with the predictions of the ADAF model.

It is also possible that the observed increase of the inner disk radius at early times is not physical, but rather due to the flattening of the radial temperature profile from the $T \sim r^{3/4}$ assumed in the multicolor disk model. This effect would cause the radius inferred from the multicolor disk model to increase. The flattening of the radial temperature profile in the disk could be caused by irradiation of the disk during the initial rise and following the intense 6.8 crab flare.

4.2. *Black Hole Mass*

We can estimate the mass of the black hole in XTE J1550−564 by equating the observed inner disk radius with the last stable orbit predicted by general relativity. Merloni et al. (1999) find that the multicolor disk model, with appropriate corrections for spectral hardening and relativistic effects, gives stable, acceptable results for

high accretion rates ($\gtrsim 10\%$ of the Eddington accretion rate) and/or when a lower fraction of the gravitational energy is dissipated in the corona. In this case, the actual inner disk radius ($R_{\rm in}$) can be determined from the *stable* observed (color) radius ($r_{\rm in}$) during the high/soft state according to the formula

$$R_{\rm in} = \eta g(i) f^2 r_{\rm in} , \quad (2)$$

where η is the ratio of the inner disk radius to the radius at which the disk emissivity peaks, $g(i)$ is the correction for relativistic effects as a function of inclination, f is the correction for constant spectral hardening ($f = 1.7$; Shimura & Takahara 1995), and $r_{\rm in} = 40$ km $(D/6$ kpc$)(\cos i)^{-1/2}$ for XTE J1550−564 (see above). Both η and $g(i)$ are functions of black hole angular momentum. Assuming a Schwarzschild black hole with $0° \leq i \leq 70°$, for which $\eta = 0.63$ and $g(i) \sim 0.9$ (Zhang, Cui, & Chen 1997; Sobczak et al. 1999a), equation (2) becomes $R_{\rm in} = 66$ km $(D/6$ kpc$)(\cos i)^{-1/2}$. Equating $R_{\rm in}$ with the last stable orbit for a Schwarzschild black hole ($6GM/c^2$), we find

$$M_{\rm BH} = 7.4\ M_\odot (D/6\ {\rm kpc})(\cos i)^{-1/2} . \quad (3)$$

For example, for $i = 60°$ and $D = 6$ kpc, $M_{\rm BH} = 10\ M_\odot$.

5. CONCLUSION

We have analyzed *RXTE* data acquired during observations of the X-ray nova XTE J1550−564. Satisfactory fits to all the PCA data were obtained with a model consisting of a multicolor disk, a power law, and Fe emission and absorption components. XTE J1550−564 is observed in the very high and high/soft canonical outburst states of BHXNe. We distinguished these two states based on the relative flux contribution of the disk and power-law spectral components, the value of the power-law photon index, the presence or absence of QPOs, and the relative strength of the 2–12 keV and 20–100 keV fluxes.

The source exhibited an intense (6.8 crab) flare on MJD 51075, during which the inner disk radius appears to have decreased dramatically from 33 to 2 km (for $i = 0$ and $D = 6$ kpc). However, the apparent decrease of the inner disk radius observed during periods of increased power-law emission may be caused by the failure of the multicolor disk model; the actual physical radius of the inner disk may remain fairly constant. This interpretation is supported by the fact that the observed inner disk radius remains approximately constant over 120 days from MJD 51120−51240, when the power law is weak, even though the disk flux and total flux vary by an order of magnitude. The mass of the black hole inferred by equating the approximately constant inner disk radius observed in the high/soft state with the last stable orbit for a Schwarzschild black hole (see § 4.2) is $M_{\rm BH} = 7.4\ M_\odot (D/6\ {\rm kpc})(\cos i)^{-1/2}$.

The outburst of XTE J1550−564 has many features in common with the most recent outburst of the microquasar GRO J1655−40 (Sobczak et al. 1999b). During the first half of their outbursts, the X-ray spectra of both sources are dominated by the power-law component and both the observed inner disk radius and flux exhibit extreme variability. Following their initial outbursts, the flux from both sources declined, only to be followed by a second outburst. During the second half of their outbursts, the X-ray spectra of both sources are primarily disk-dominated with an approximately constant inner disk radius and slowly varying intensity. Neither of these sources can be described as a "canonical" BHXN.

This work was supported, in part, by NASA grants NAG5-3680 and NAS5-30612. Partial support for J. M. and G. S. was provided by the Smithsonian Institution Scholarly Studies Program. W. C. would like to thank Shuang Nan Zhang and Wan Chen for extensive discussions on spectral modeling and interpretation of the results.

REFERENCES

Campbell-Wilson, D., McIntyre, V., Hunstead, R., & Green, A. 1998, IAU Circ. 7010
Chen, W., Shrader, C. R., & Livio, M. 1997, ApJ, 491, 312
Cui, W., Zhang, S. N., Chen, W., & Morgan, E. H. 1999, ApJ, 512, L43
Ebisawa, K., et al. 1994, PASJ, 46, 375
Esin, A. A., McClintock, J. E., & Narayan, R. 1997, ApJ, 489, 865
Grove, J. E., Johnson, W. N., Kroeger, R. A., McNaron-Brown, K., Skibo, J. G., Hulburt, E. O., & Philips, B. F. 1998, ApJ, 500, 899
Hameury, J.-M., Lasota, J.-P., McClintock, J. E., & Narayan, R. 1998, ApJ, 489, 234
Homan, J., Wijnands, R., & van der Klis, M. 1999, IAU Circ. 7121
Inoue, H. 1991, in Frontiers of X-Ray Astronomy, ed. Y. Tanaka & K. Koyama (Tokyo: Universal Academy Press), 291
Jahoda, K., Swank, J. H., Giles, A. B., Stark, M. J., Strohmayer, T., Zhang, W., & Morgan, E. H. 1996, Proc. SPIE, 2808, 59
Jain, R., Bailyn, C. D., Orosz, J. A., Remillard R. A., & McClintock, J. E. 1999, ApJ, 517, L131
Levine, A. M., Bradt, H., Cui, W., Jernigan, J. G., Morgan, E. H., Remillard, R., Shirey, R. E., & Smith, D. A. 1996, ApJ, 469, 33
Makishima, K., Maejima, Y., Mitsuda, K., Bradt, H. V., Remillard, R. A., Tuohy, I. R., Hoshi, R., & Nakagawa, M. 1986, ApJ, 308, 635
Merloni, A., Fabian, A. C., & Ross, R. R. 1999, MNRAS, 313, 193
Mitsuda, K., et al.. 1984, PASJ, 36, 741
Morgan, E. H., Remillard, R. A., & Greiner, J. 1997, ApJ, 482, 993
Morrison, R., & McCammon, D. 1983, ApJ, 270, 119
Nagase, F. 1989, PASJ, 41, 1
Orosz, J., Bailyn, C., & Jain, R. 1998, IAU Circ. 7009
Remillard, R. A., McClintock, J. E., Sobczak, G. J., Bailyn, C. D., Orosz, J. A., Morgan, E. H., & Levine, A. M. 1999a, ApJ, 517, L127
Remillard, R. A., & Morgan, E. H. 1999, AAS Meeting, 195, 3702
Remillard, R. A., Morgan, E. H., McClintock, J. E., Bailyn, C. D., & Orosz, J. A. 1999b, ApJ, 522, 397
Rothschild, R. E., et al. 1998, ApJ, 496, 538
Shakura, N. I., & Sunyaev, R. A. 1973, A&A, 24, 337
Shimura, T., & Takahara, F. 1995, ApJ, 445, 780
Smith, D. A., & *RXTE*/ASM teams. 1998, IAU Circ. 7008
Sobczak, G. J., McClintock, J. E., Remillard, R. A., Levine, A. M., Morgan, E. H., Bailyn, C. D., & Orosz, J. A. 1999a, ApJ, 517, L121
Sobczak, G. J., McClintock, J. E., Remillard, R. A., Bailyn, C. D., & Orosz, J. A. 1999b, ApJ, 520, 776
Sobczak, G. J., McClintock, J. E., Remillard, R. A., Cui, W., Levine, A. M., Morgan, E. H., Orosz, J. A., & Bailyn, C. D. 2000, ApJ, 531, 537
Tanaka, Y., & Lewin, W. H. G. 1995, in X-Ray Binaries, ed. W. H. G. Lewin, J. van Paradijs, & E. P. J. van den Heuvel (Cambridge: Cambridge Univ. Press), 126
Titarchuk, L. 1994, ApJ, 434, 570
Zhang, S. N., Cui, W., & Chen, W. 1997, ApJ, 482, L155
Zhang, S. N., Cui, W., Chen, W., Yao, Y., Zhang, X., Sun, X., Wu, X., & Xu, H. 2000, Science, 287, 1239